16 Extraosseous Metastases and Local Recurrence

Ali Guermazi, Iman El-Hariry, and Yves Miaux

CONTENTS

A. Guermazi, MD
Senior Radiologist, Scientific Director, Oncology Services, Department of Radiology Services, Synarc Inc., 575 Market Street, 17th Floor, San Francisco, CA 94105, USA
I. El-Hariry, MD, PhD
Senior Director, Oncology Clinical Development and Medical Affairs, Glaxo Smith Kline R&D, Greenford Road, Greenford, Middlesex UB6 0HE, England, UK
Y. Miaux, MD, MSc
Senior Vice President, Radiology Services, Synarc Inc., 575 Market Street, 17th Floor, San Francisco, CA 94105, USA

16.1 Introduction

Renal cell cancer metastasizes in approximately 33% of patients (Flanigan et al. 2003; Russo 2003) and recurs locally in about 5% (Scatarige et al. 2001a). Accurate detection of recurrent disease provides key prognostic information and assists the oncologist in making treatment decisions involving surgery or immunotherapy (Motzer et al. 1996). Common sites of metastases include the lung, mediastinum, bones, brain, and liver. Less common sites include the contralateral kidney, the adrenal gland, pancreas, mesentery, and abdominal wall. Several reports detail the capacity of renal carcinoma to appear almost anywhere in the body (Flanigan et al. 2003; Janzen et al. 2003; Thrasher and Paulson 1993). More than one organ is often involved in the metastatic process (Flanigan et al. 2003). Metastases may be found at diagnosis or at some interval after nephrectomy (Flanigan et al. 2003; Itano et al. 2000). Indeed, approximately 20–50% of patients with renal cell carcinoma (RCC) eventually develop metastatic disease after nephrectomy (Flanigan et al. 2003; Itano et al. 2000; Janzen et al. 2003). A shorter interval between nephrectomy and the development of metastases is associated with a poorer prognosis. Patients with metastatic RCC face a dismal prognosis, with a median survival time of only 6–12 months and a 2-year survival rate of 10–20%. Recent advances in biologic response modifier therapy have given hope to the small percentage of patients who respond to this therapy (Flanigan et al. 2003), and has rekindled interest in cytoreductive nephrectomy as an integral part of the management of these patients (Flanigan and Yonover 2001; Flanigan et al. 2003).

The purpose of this chapter is to illustrate both typical and less typical US, CT, and MR imaging appearances of metastases and local recurrence from renal cancers. The emphasis is on spiral CT, which is considered the ideal modality for conducting postoperative surveillance in patients at risk of

recurrent or metastatic disease (Scatarige et al. 2001a). Of importance for the reader, bone metastases will be discussed in Chap. 17.

16.2 Clinical Features and Pathophysiology

Metastatic dissemination is unpredictable and occurs via lymphatic and hematogenous routes (Scatarige et al. 2001a). Retrograde collateral flow via the lumbar veins into the vertebral plexus of Batson appears to be particularly important in metastasis to the axial skeleton and the meninges (Arkless 1965), as well as to the head and neck (Som et al. 1987). Local recurrence is associated with incomplete resection of the primary tumor, positive surgical margins, and regional lymph node metastasis (Rabinovitch et al. 1994).

The most important determinant in predicting local recurrence or distant metastasis is the surgical stage of RCC. Large tumors that invade locally or propagate as venous tumor thrombus have higher rates of distant metastasis. Other factors that may influence prognosis include regional lymph node metastases, a high Fuhrman grade on histopathology, and spindled (sarcomatoid) tumor architecture (Chae et al. 2005; Janzen et al. 2003; Johnsen and Hellsten 1997; Saidi et al. 1998).

Distant metastases or local recurrence usually occur within the first 6 years after surgery (Rabinovitch et al. 1994; Saidi et al. 1998). Late metastasis is a distinctive clinical aspect of renal cancer, and can be observed in as many as 11% of patients surviving 10 years or more after surgery (Newmark et al. 1994). The most frequent sites for late metastases are lung, pancreas, bone, skeletal muscle, and bowel (Newmark et al. 1994; Saitoh et al. 1982).

Spontaneous regression of metastases from renal cancer is now well documented. This rare event, reported in less than 1% of the patients, may effect one (Guthbjartsson and Gislason 1995) or multiple (Omland and Fossa 1989) locations, but is usually not permanent (Mignon and Mesurolle 2003). Spontaneous regression of metastases is most commonly seen following nephrectomy but has been reported after irradiation of the primary tumor, embolization with or without nephrectomy (Lokich 1997), following infusion of recombinant interleukin-2 (Mizuo et al. 1990), or after radiofrequency ablation of the primary tumor (Sanchez-Ortiz et al. 2003). It most commonly involves pulmonary metastases followed by skeletal, soft tissue, brain, and liver metastases (Guthbjartsson and Gislason, 1995; Hammad et al. 2003; Omland and Fossa 1989). The mechanism is unknown, but the evidence seems to favor an immunologic basis (Guthbjartsson and Gislason 1995; Omland and Fossa 1989).

Local recurrences and distant metastases are usually highly vascular, like the primary tumor; therefore, arterial-phase scanning is essential for maximizing lesion conspicuity. To facilitate detection of vascular liver metastases, the abdomen and pelvis are scanned first, from the diaphragm to the symphysis pubis, during the arterial phase of enhancement. Next, the chest is imaged from the lung apices through the liver and remaining kidney. Because these patients, as well as those with familial renal carcinoma or von Hippel-Lindau disease, are at increased risk for additional renal primary carcinomas, the remaining kidney must be carefully scrutinized on each follow-up CT (Scatarige et al. 2001a). The venous phase is also important since some metastatic nodules or masses are difficult, if not impossible, to discern within the hypervascular cortex at arterial phase, and appear as hypodense nodules at the venous phase (Mignon and Mesurolle 2003). Retroperitoneal anatomy is significantly modified after nephrectomy (Fig. 16.1). Indeed, the small bowel and colon may migrate into the nephrectomy fossa. For CT scanning, a good oral opacification of the bowel is mandatory to differentiate nonopacified bowel from local recurrence (Scatarige et al. 2001a).

Hypervascular metastases are not specific to kidney cancer metastases and may be seen in metastases from thyroid cancer, neuroendocrine tumors, hepatocarcinoma, and pheochromocytoma (Mignon and Mesurolle 2003).

16.3 Thoracic Metastases

16.3.1 Lung and Endobronchus

The reported incidence of lung metastases ranges from 3 to 16% (Janzen et al. 2003). Pulmonary metastases occur in 29–60% of patients with distant disease (Janzen et al. 2003; Motzer et al. 1996). The latency period can be as long as 25 years (Shiono et al. 2004). Most lung metastases are asymptomatic, at least early in their history, indicating the use of chest CT rather than chest radiographs for follow-up

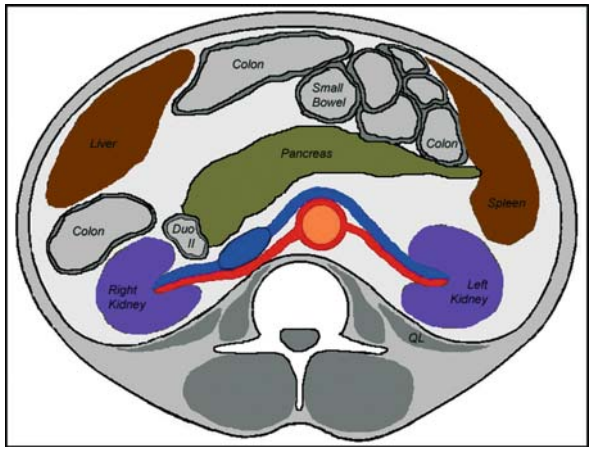

a

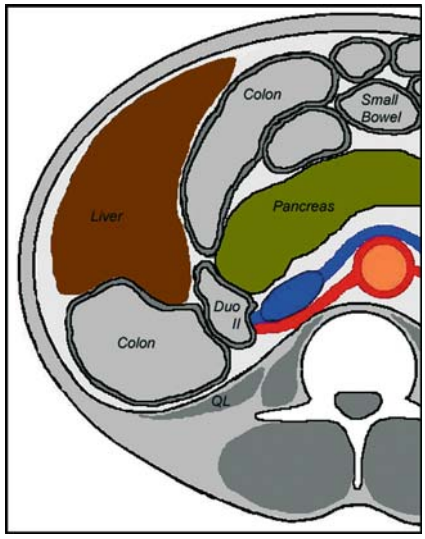

b

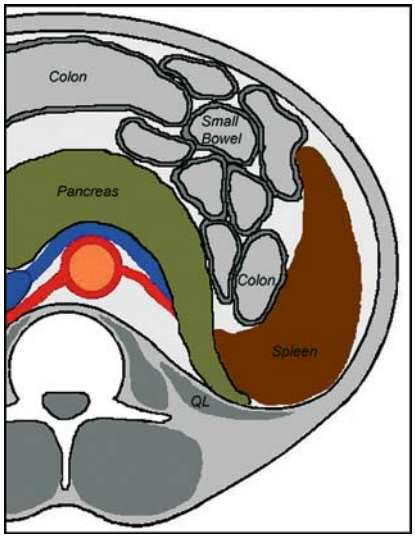

c

Fig. 16.1a-c. Normal and surgically altered retroperitoneum. **a** Normal retroperitoneum. **b** After right nephrectomy, the right colon and right hepatic lobe occupy the renal fossa. Second portion of duodenum and pancreatic head may assume more posterolateral position. **c** After left nephrectomy, pancreatic tail assumes a more posterior position, approaching quadratus lumborum. Spleen shifts posteromedially. Caudal to pancreas, proximal jejunum and descending colon fill left renal fossa. *Duo II* second portion of duodenum, *QL* quadratus lumborum. (Modified from Scatarige et al. 2001)

after nephrectomy, because chest CT is more sensitive and more likely to display metastases earlier (Saidi et al. 1998). The lung is the most common site of single metastases (Johnsen and Hellsten 1997). Also, patients with lung-only metastases have better survival rates compared with patients with metastases at other sites (Flanigan and Yonover 2001; Russo 2003); therefore, an aggressive surgical approach that aims to remove all neoplastic growth is believed to benefit these patients (Janzen et al. 2003; Johnsen and Hellsten 1997), and repeat metastasectomies are warranted (Shiono et al. 2004). Incomplete resection of renal carcinoma pulmonary metastases is associated with a poor prognosis, with a 5-year survival rate of 22.1% compared with 41.5% in patients with complete resection (Shiono et al. 2004). The lung is also the most common site for spontaneous regression of metastases from renal cancer (Lokich 1997; Mizuo et al. 1990; Omland and Fossa 1989; Sanchez-Ortiz et al. 2003).

Computed tomography is considered the state-of-the-art technology for assessing pulmonary involvement (Lim and Carter 1993). Pulmonary metastases appear as one or multiple, well-defined, rounded or oval, solid nodules or masses, of variable size (Fig. 16.2; Badoual et al. 2002; Chae et al. 2005; Mignon and Mesurolle 2003). Small nodules may be missed on radiographs (Fig. 16.3; Lim and Carter 1993). They are usually bilateral and peripherally located, predominantly in the inferior lobes. Numerous pulmonary metastases confined to one lobe have been reported that were initially confused radiologically with lobar pneumonia (Toye et al. 1990). The hypervascularity of renal metastases to the lung is demonstrated with the large masses (Mignon and Mesurolle 2003), and may lead to hemorrhage (Scatarige et al. 2001a). Atypical presentations are the involvement of the interstitial lymphatics leading to a nonspecific carcinomatous lymphangitis (Fig. 16.4; Scatarige et al. 2001a),

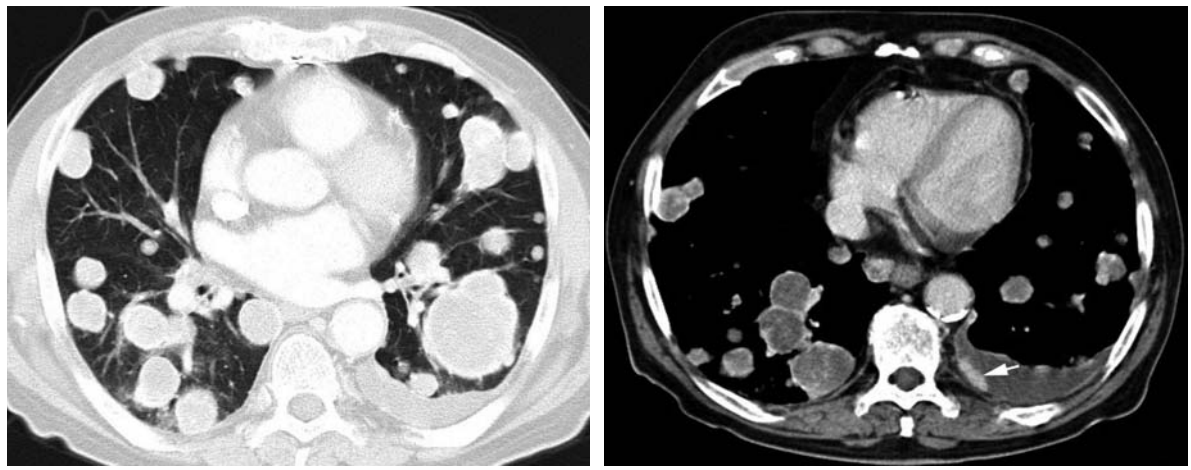

Fig. 16.2a,b. Lung and pleural metastases in a 67-year-old man who underwent nephrectomy for renal cell carcinoma. **a** Axial CT scan shows several bilateral rounded and oval pulmonary nodules of different sizes. **b** Axial contrast-enhanced CT scan of the chest shows that the pulmonary lesions are enhancing peripherally. It also shows a strongly enhanced left pleural-based lesion (*arrow*) associated with left pleural effusion.

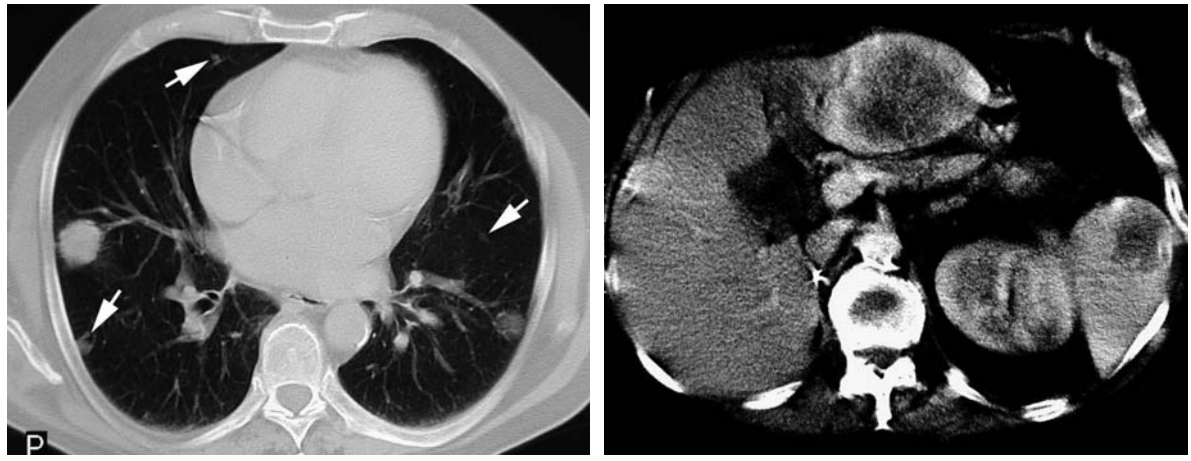

Fig. 16.3a,b. Lung, liver, and spleen metastases in a 66-year-old man who underwent right nephrectomy for renal cell carcinoma. **a** Axial CT scan shows bilateral rounded pulmonary nodules of different sizes. The small peripheral nodules (*arrows*) were not seen on a conventional radiograph. **b** Axial contrast-enhanced CT scan of the abdomen shows large lesions in left hepatic lobe and spleen with peripheral enhancement and central necrosis.

or the coexistence of pulmonary cystic lesions (Fig. 16.5), micronodules, and recurrent pneumothoraces leading to some confusion with Langerhans cell histiocytosis (Essadki et al. 1998). Solitary pulmonary nodules are rare and still challenging since conventional imaging modalities, including radiograph, CT, and MR imaging, cannot reveal the exact nature of the lesion. Histological biopsy is often required to establish a definite diagnosis and may detect benign diseases such as hematoma, fibrosis, hamartoma, calcified nodules (Chang et al. 2003), and intrapulmonary lymph node (Kolosseus et al. 1995). 18F-fluoro-2-deoxyglucose positron emission tomography (FDG-PET) has been shown to be a sensitive, specific, and accurate modality to differentiate radiologically indeterminate solitary pulmonary lesions in patients with RCC (Chang et al. 2003).

Endobronchial metastases can be detected incidentally or on imaging or bronchoscopy in patients presenting with hemoptysis or atelectasis (Barthwal et al. 2003; Merine and Fishman 1988).

16.3.2 Pleura

Metastases to the pleura are considered exceptionally rare (Griniatsos et al. 2003). Metastases to the

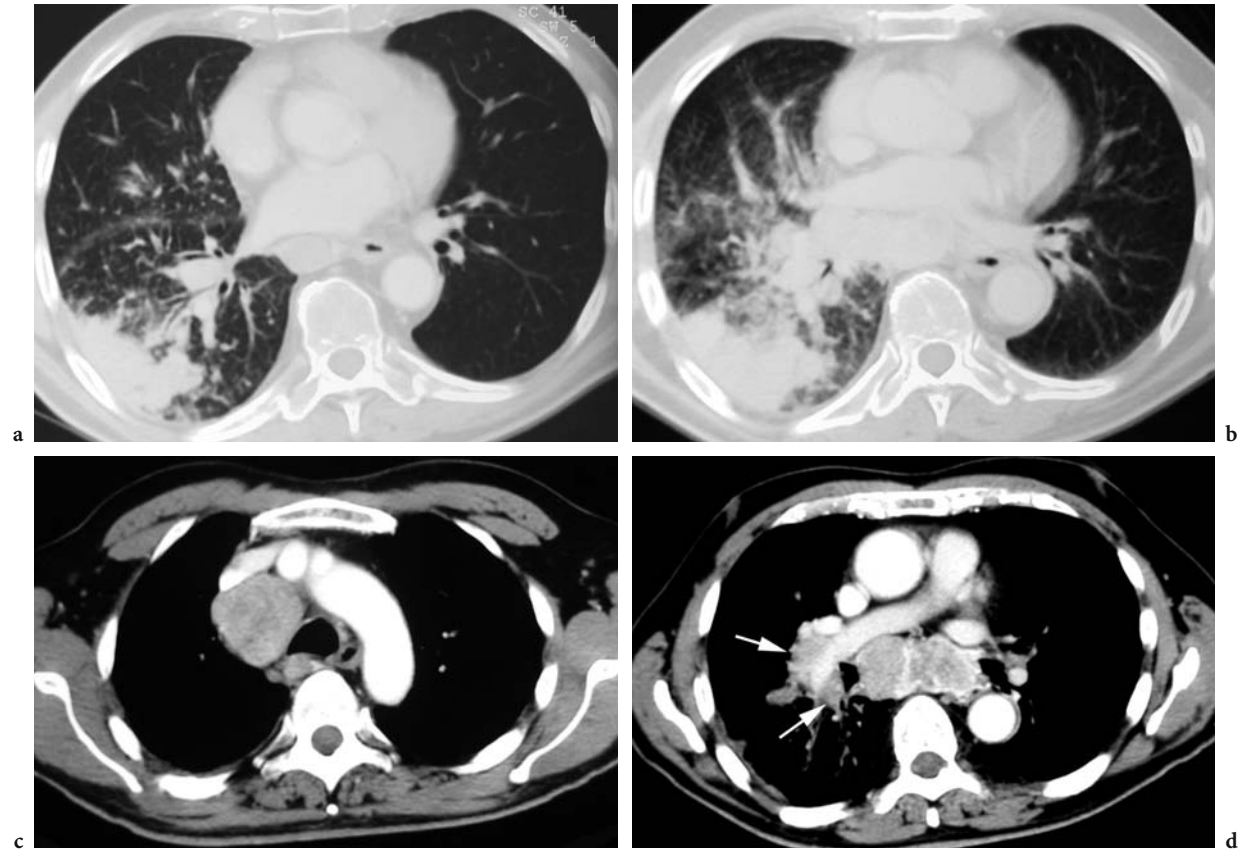

Fig. 16.4a-d. Pulmonary lymphangitic carcinomatosis and mediastinal lymph node metastases in a 48-year-old man who underwent nephrectomy for renal cell carcinoma. **a** Axial CT scan shows right inferior lobe with ill-defined parenchymal consolidation surrounded by thickened nodular, interlobular septa forming polygonal arcades, indicating an interstitial lymphangitic disease. There is also a mild enlargement of the right hilar lymph nodes. **b** Two-month follow-up axial CT scan shows worsening of the pulmonary consolidation, interstitial disease, and right hilar lymph nodes. **c, d** Axial contrast-enhanced CT scans show enhancement at different intensities of enlarged (**c**) right lateral tracheal, (**d**) subcarinal and right hilar (*arrows*) lymph nodes.

pleura are usually associated with lung metastases and spread via arteries (Ohgou et al. 1998). Metastases to the pleura without metastases to the lung are rare. This suggests that the pleural metastases may also spread via Batson's venous plexus (Ohgou et al. 1998). Pleural metastases were thought never to occur without involving other metastatic sites (Saitoh et al. 1982), but a few exclusively pleural metastases in RCC have been reported (Thoroddsen et al. 2002). The prognosis of pleural metastasis is poor and the majority of patients die within 6 months of diagnosis (Griniatsos et al. 2003). Spontaneous regression of pleural metastases has been reported (Lokich 1997; Thoroddsen et al. 2002).

Radiologically, CT is the best modality for the diagnosis of pleural metastases that may be associated with pleural-based solid masses and/or malignant effusion (Lokich 1997). Masses can be solitary or multiple (Fig. 16.6; Griniatsos et al. 2003). When solitary, the mass may be large and associated, or not, with pleural effusion (Fig. 16.7; Griniatsos et al. 2003). In a case report with several pleural metastases, radiography showed abnormal shadows that were suspected as malignant mesothelioma. Computed tomography showed several enhanced pleural nodules (Fig. 16.8) and also hepatic metastases (Ohgou et al. 1998).

16.3.3 Heart and Pericardium

The reported incidence of metastases to the heart and pericardium from RCC is about 4% (Carroll et al. 1994). Clinically, they are usually silent (Carroll et al. 1994; Cheng 2003), although they may present with dyspnea and lower-extremity edema if the right cavities are involved (Carroll

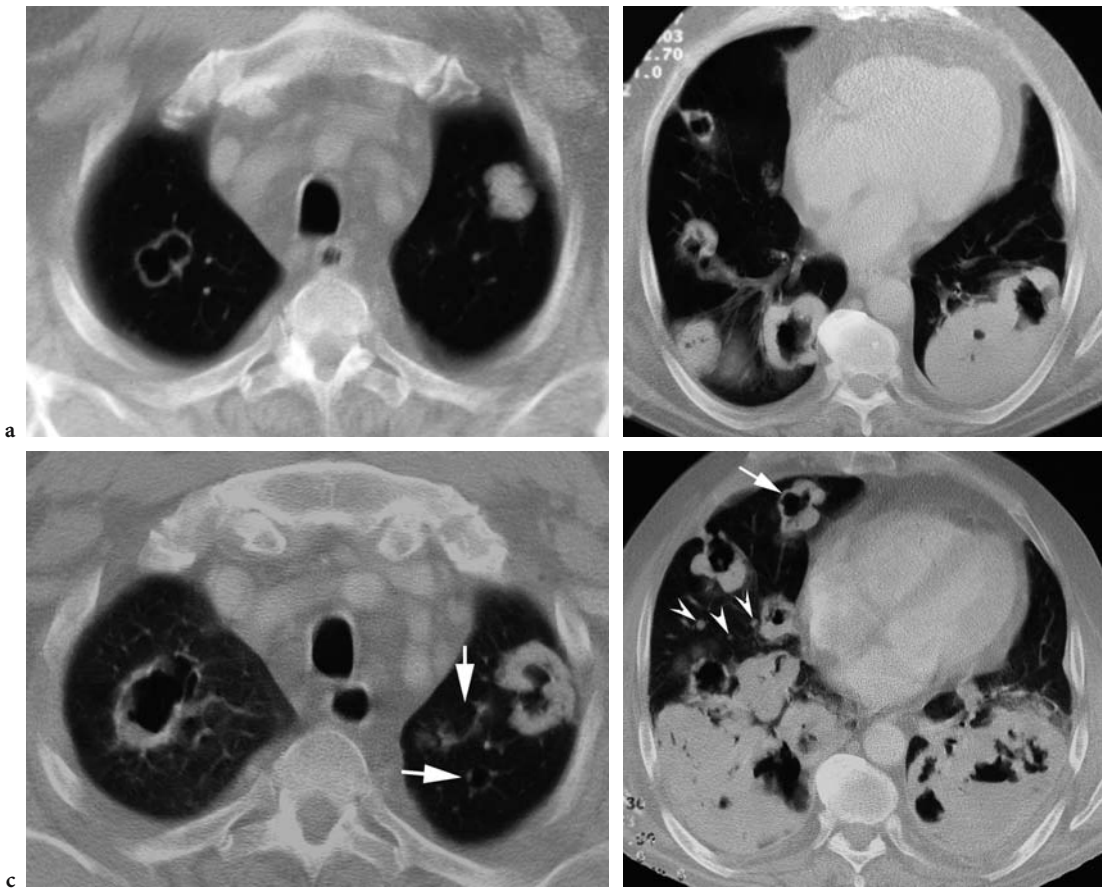

Fig. 16.5a-d. Mixed nodular and cystic lung metastases in a 67-year-old woman who underwent nephrectomy for renal cell carcinoma. **a** Axial CT scan of the upper chest shows a left solid oval pulmonary nodule and a right cystic lung nodule showing a thin and smooth wall. **b** Axial CT scan of the lower chest shows several bilateral excavated lung nodules. The left posterior mass is probably secondary to several confluent nodules. **c, d** Five-month follow-up axial CT scans at the same levels as **a** and **b** show enlargement of both solid and cystic nodular lesions. There are also new solid micronodules (*arrowheads*) and cystic nodules (*arrows*).

et al. 1994; Santo-Tomas et al. 1998), and syncope or signs of pulmonary vascular congestion if the left cavities are involved (Safi et al. 2003). In the majority of cases, RCC invades the inferior vena cava and extends up the vena cava into the right atrium (Fig. 16.9; Allen et al. 1991). Cardiac metastases without extension to the vena cava are extremely rare (Cheng 2003; Safi et al. 2003). In these very few cases, the primary tumor metastasizes to the heart systemically via hematogenous or lymphatic routes (Safi et al. 2003).

It is important to differentiate muscular metastatic lesions to the heart (Mahnken and Tacke 2000) with right cardiac cavities involvement from an inferior vena cava tumoral thrombosis extension (Allen et al. 1991; Carroll et al. 1994; Santo-Tomas et al. 1998).

Transthoracic, or better transesophageal, echocardiography is an important diagnostic tool for superior preoperative images of the tumor and its extensions (Allen et al. 1991). In the case of metastases invading the right ventricular myocardium without caval involvement, echocardiography shows a large mass within the right ventricle that spares the right atrium and inferior vena cava (Carroll et al. 1994; Cheng 2003; Santo-Tomas et al. 1998). Left ventricular involvement may show the same appearance as right involvement, with a large mobile mass infiltrating the left ventricle (Safi et al. 2003). Doppler may show partial or complete obstruction of the flow into the heart or within the cavity or outflow from the cavity (Carroll et al. 1994; Safi et al. 2003). Echocardiography, and less importantly CT, remain the most commonly used diagnostic modalities.

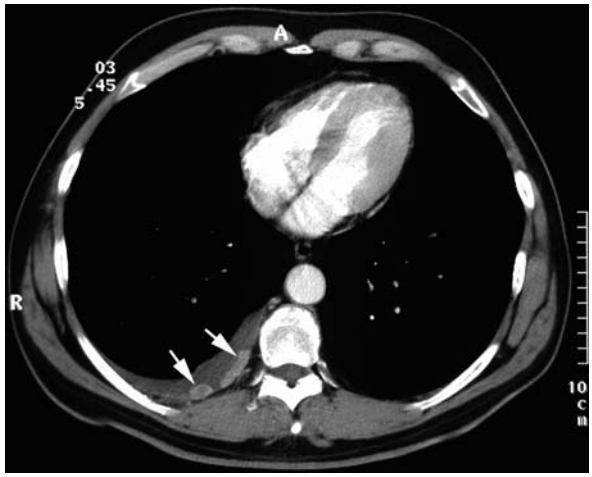

a

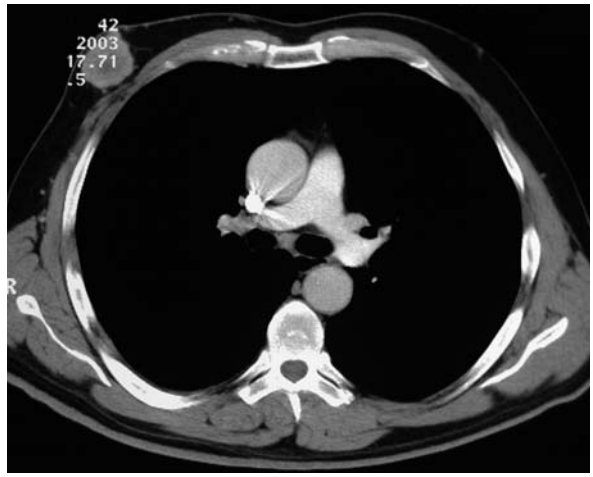

b

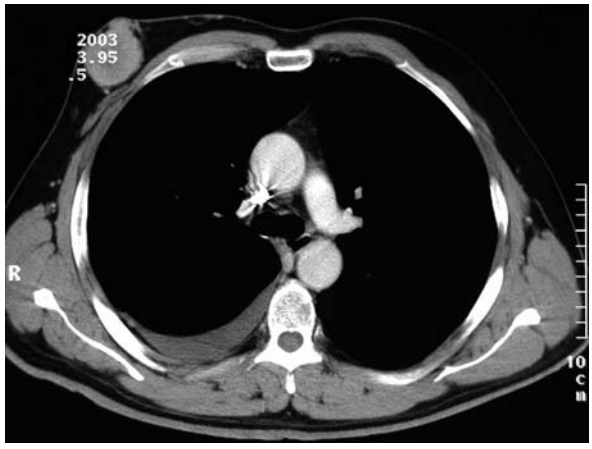

c

Fig. 16.6a-c. Pleural and breast metastases in a 61-year-old man who underwent nephrectomy for renal cell carcinoma. **a** Axial contrast-enhanced CT scan shows two right pleural-based enhancing masses (*arrows*) associated with ipsilateral pleural effusion. **b** Axial contrast-enhanced CT scan cephalad to **a** shows a well-defined moderately enhancing right breast mass with central necrosis. **c** Seven-week follow-up axial contrast-enhanced CT scan at the same level of **b** shows that the breast mass is increasing in size with more obvious cutaneous involvement. The right pleural effusion has also increased in size.

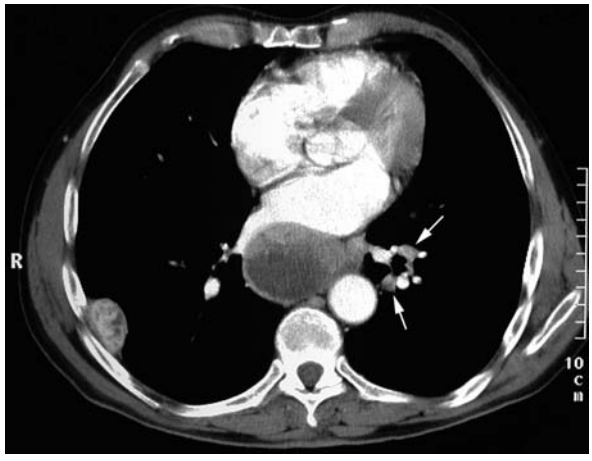

a

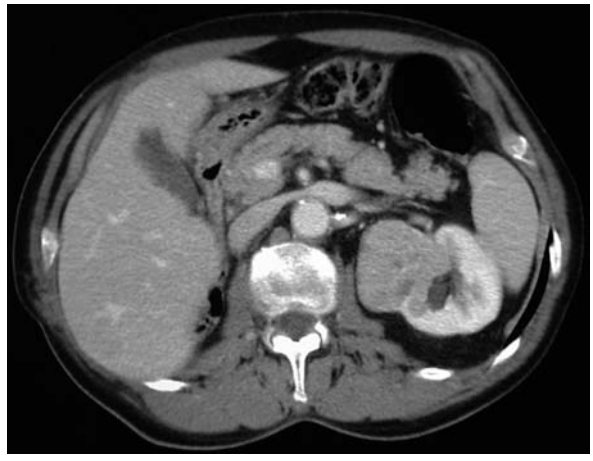

b

Fig. 16.7a,b. Pleural, nodal, and contralateral kidney metastases in a 70-year-old man who underwent right nephrectomy for renal cell carcinoma. **a** Axial contrast-enhanced CT scan shows a single right pleural-based lesion that enhances heterogeneously. There is a large, moderately enhancing subcarinal adenopathy with central necrosis and two small left hilar adenopathies (*arrows*). **b** Axial contrast-enhanced CT scan at the portal venous phase shows a moderately enhancing mass of the left kidney with areas of necrosis.

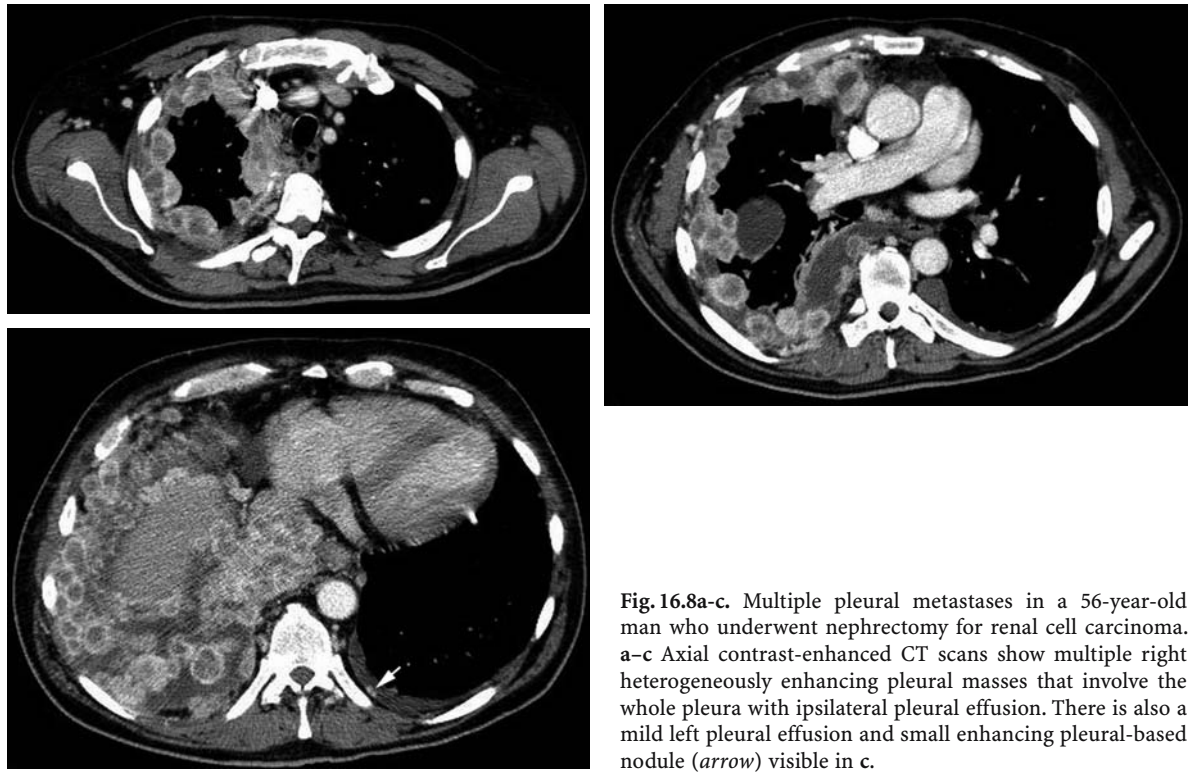

Fig. 16.8a-c. Multiple pleural metastases in a 56-year-old man who underwent nephrectomy for renal cell carcinoma. **a–c** Axial contrast-enhanced CT scans show multiple right heterogeneously enhancing pleural masses that involve the whole pleura with ipsilateral pleural effusion. There is also a mild left pleural effusion and small enhancing pleural-based nodule (*arrow*) visible in **c**.

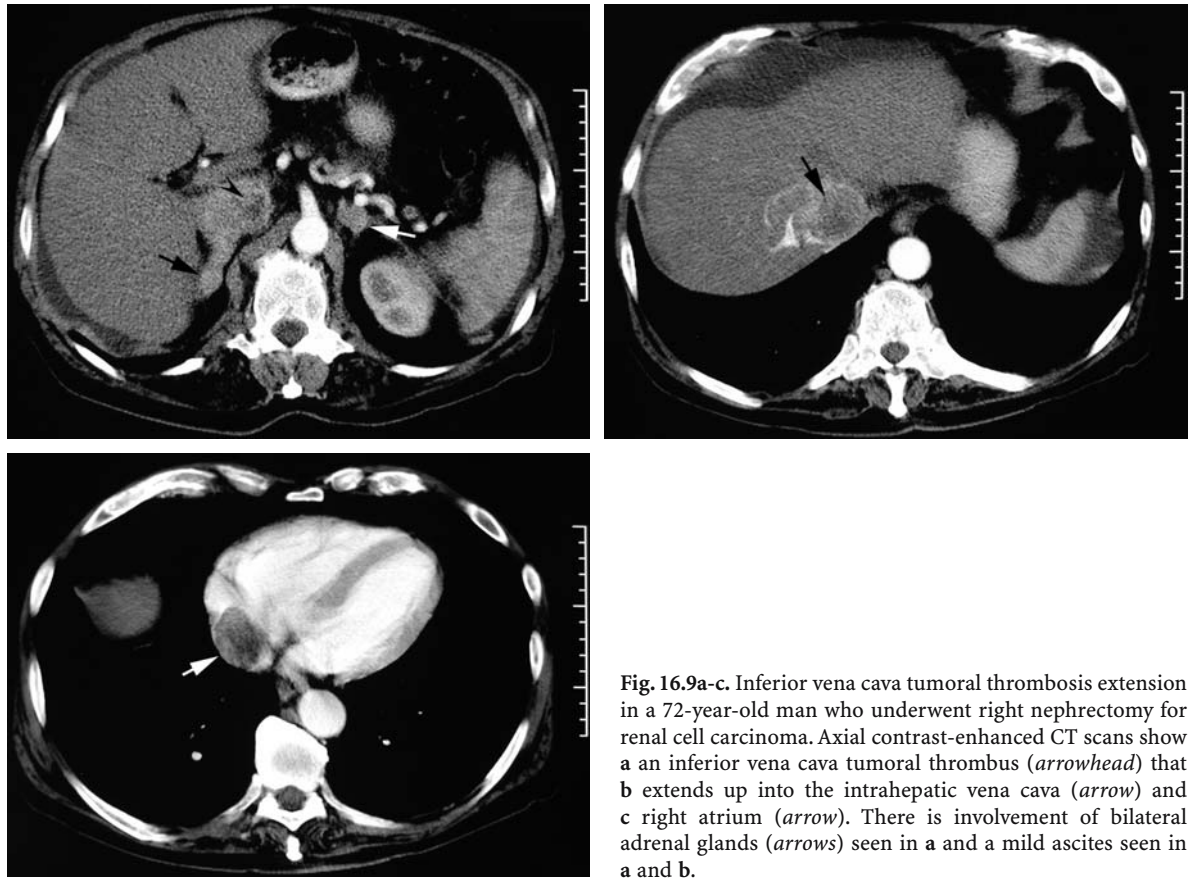

Fig. 16.9a-c. Inferior vena cava tumoral thrombosis extension in a 72-year-old man who underwent right nephrectomy for renal cell carcinoma. Axial contrast-enhanced CT scans show **a** an inferior vena cava tumoral thrombus (*arrowhead*) that **b** extends up into the intrahepatic vena cava (*arrow*) and **c** right atrium (*arrow*). There is involvement of bilateral adrenal glands (*arrows*) seen in **a** and a mild ascites seen in **a** and **b**.

Recently, MR imaging has been shown to be superior to echocardiography not only in demonstrating a global view of cardiac anatomy involvement (i.e., pericardium, myocardium, or cardiac cavities) but also in providing a better preoperative assessment of anatomic relations of cardiac metastatic masses to their surrounding structures (Safi et al. 2003).

16.3.4 Breast

Metastasis to the breast is unusual in RCC. The involvement is usually metachronous (Pursner et al. 1997; Vassalli et al. 2001). The latency period can be as long as 18 years. Clinically, metastases to the breast are asymptomatic with the lesion most commonly solitary and well circumscribed, located superficially in the upper quadrant of the breast (Vassalli et al. 2001). Bilateral involvement has been reported once in a 14-year-old girl (Pursner et al. 1997). Pain, tenderness, or discharge are rare. The overlying skin is rarely dimpled or adherent to the tumor (Vassalli et al. 2001). Pathologically, the tumor may infiltrate in a pattern that mimics ductal carcinoma in situ (Gupta et al. 2001). The prognosis is generally poor since breast involvement can be a signal of rapid widespread dissemination (Gupta et al. 2001; Vassalli et al. 2001).

Mammography and breast ultrasound may show a nodular mass. Because CT is routinely performed for the follow-up evaluation of patients after nephrectomy, it is important to look carefully at breast area since it may show a well-defined breast mass (Figs. 16.6, 16.10; Pursner et al. 1997).

16.4 Abdominal and Pelvic Metastases

16.4.1 Liver

Liver metastases have been reported in 1–7% of cases (Janzen et al. 2003). Metastasis to the liver seems to be associated with a particularly poor prognosis (Flanigan et al. 2001; Raptopoulos et al. 2001)

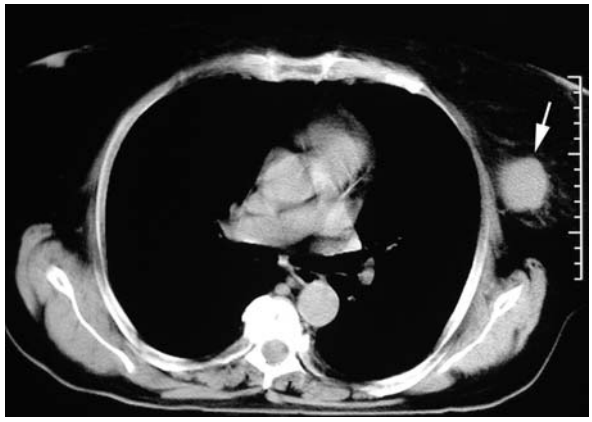

a

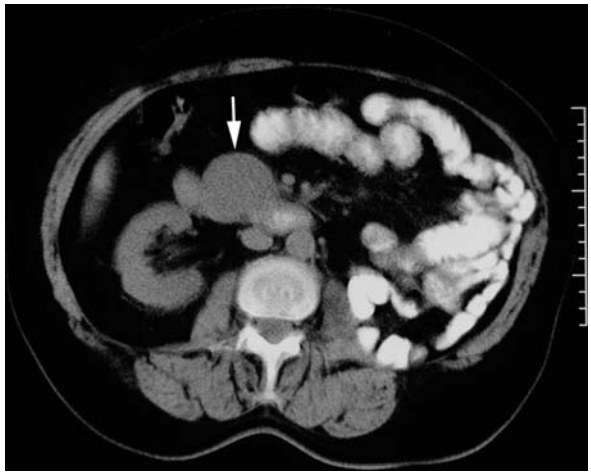

b

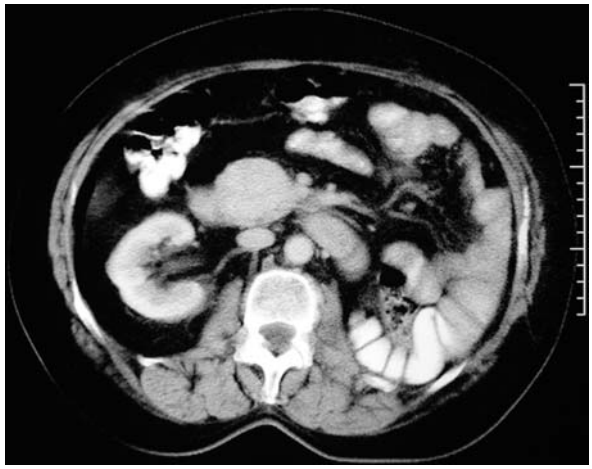

c

Fig. 16.10a-c. Breast and duodenal metastases in a 69-year-old woman who underwent left nephrectomy for renal cell carcinoma. **a** Axial contrast-enhanced CT scan of the chest shows a well-defined enhancing mass of the left breast (*arrow*) with infiltration of adjacent tissue. **b** Axial unenhanced CT scan of the abdomen discloses a rounded mass in the wall of the third duodenum (*arrow*) which enhances strongly and homogeneously (**c**) after contrast injection.

because of its association with widely disseminated disease (Janzen et al. 2003). Solitary metastasis to the liver is reported to occur in 5.4% of all cases with metastasis, but improved survival with surgery is anecdotal (Janzen et al. 2003; Saitoh et al. 1982). Spontaneous regression of liver metastases from renal cancer has been reported (Ritchie et al. 1988; Wyczolkowski et al. 2001).

On ultrasound (US), liver metastases from RCC are usually hypoechoic (Chae et al. 2005). On CT, they are suggestive when highly vascular, like the primary tumor (Fig. 16.11). Because the hypervascular hepatic lesion may become isodense or nearly isodense on contrast-enhanced CT, unenhanced CT should be performed and may show hypodense lesions if conventional CT scan is used (Fig. 16.12; Bressler et al. 1987). With spiral CT, arterial-phase scanning is essential for detecting vascular liver metastases which appear hyperdense (Fig. 16.13; Mignon and Mesurolle 2003; Scatarige et al. 2001a). In a study using multiphase contrast-enhanced spiral CT of 46 patients with liver metastases from RCC, the authors found that 10% of the hepatic lesions were missed in the portal-venous phase; all were smaller than 2 cm and most were seen in the enhanced scans and arterial phase. They concluded that the combination of unenhanced, arterial phase, and portal-venous phase should be used in the initial evaluation of patients with metastatic RCC for improved lesion detection and characterization. For subsequent follow-up monitoring of treatment, the combination of unenhanced and portal-venous phase is preferred. The delayed phase does not contribute significantly to lesion detection (Raptopoulos et al. 2001). Liver metastases vary in size (Figs. 16.14, 16.15). Because most hepatic metastases are large, they may have central necrotic areas which appear hypodense after contrast administration (Figs. 16.16, 16.17; Chae et al. 2005; Federle et al. 1981). Occasionally, these lesions are calcified (Federle et al. 1981), contain fat (Muram and Aisen 2003), or spontaneously rupture (Fig. 16.18) with intraperitoneal hemorrhage (Murakami et al. 2000).

16.4.2 Adrenal Gland

The incidence of adrenal metastases varies from 4.3 to 13.0% (O'Brien and Lynch 1987; Sagalowsky and Molberg 1999; Saitoh et al. 1982; Siemer et al. 2004). Metastases may involve the ipsilateral adrenal gland if it has been spared during surgery (Fig. 16.14; Saitoh et al. 1982) and less frequently the contralateral adrenal gland (Fig. 16.19; Hasegawa et al. 1988; Saitoh et al. 1982). Bilateral involvement of the adrenal gland is possible (Fig. 16.20; Duggan et al. 1987; Selli et al. 1987; Siemer et al. 2004; Yu et al. 1992) as well as tumoral hemorrhage of the remaining adrenal gland (Mignon and Mesurolle 2003). Isolated involvement of the contralateral adrenal gland is possible but rare and is always hematogenous (Mignon et al. 1999). Adrenal metastases may be synchronous (Lau et al. 2003; Selli et al. 1987; Vespasiani et al. 1990) or metachronous (Hasegawa et al. 1988; Lau et al. 2003; Mignon et al. 1999). The latency period after surgical removal of the primary renal tumor can be as long as 19 years for bilateral involvement (Duggan et al. 1987) and 28 years for contralateral involvement (Huisman and Sands 1991). It is known that the risk of ipsilateral adrenal metastasis correlates to the large advanced T-stage tumors of the upper pole. On the other hand, predisposing factors for contralateral involvement are unknown (Mesurolle et al. 1997; Siemer et al. 2004). An aggressive surgical approach is justified with a solitary adrenal metastasis since it carries a better prognosis and prolongs patient survival (Lau et al. 2003; Mignon et al. 1999).

Adrenal involvement is usually detectable preoperatively on CT (Fig. 16.21), MR imaging, or angiography (O'Brien and Lynch 1987; Selli et al. 1987; Siemer et al. 2004). Computed tomography is very sensitive and has an excellent positive predictive value for detecting adrenal involvement (Mignon et al. 1999). It shows a homogeneous or heterogeneous enhancing nodule or mass of varying sizes within the adrenal gland (Mesurolle et al. 1997; Mignon et al. 1999). Differential diagnosis may be difficult with adrenal adenoma. Chemical-shift MR imaging may help. If there is no change of signal from the adrenal lesion between in-phase and out-of-phase sequences, the lesion is a metastasis. It is an adrenal adenoma if the signal intensity decreases between the two sequences (Mignon et al. 1999). Computed tomography may be a less expensive and more widely available diagnostic alternative. A difference of 10 HU in density between unenhanced and contrast-enhanced images has a sensitivity of 75% and specificity around 100% (Mignon et al. 1999). In any case, the hypervascularity of the nodule on CT, MR imaging, or angiography demonstrated by the early and intensive contrast enhancement points to a metastatic nodule from RCC (Mignon et al. 1999). If doubts persist, CT-guided fine-needle-aspiration

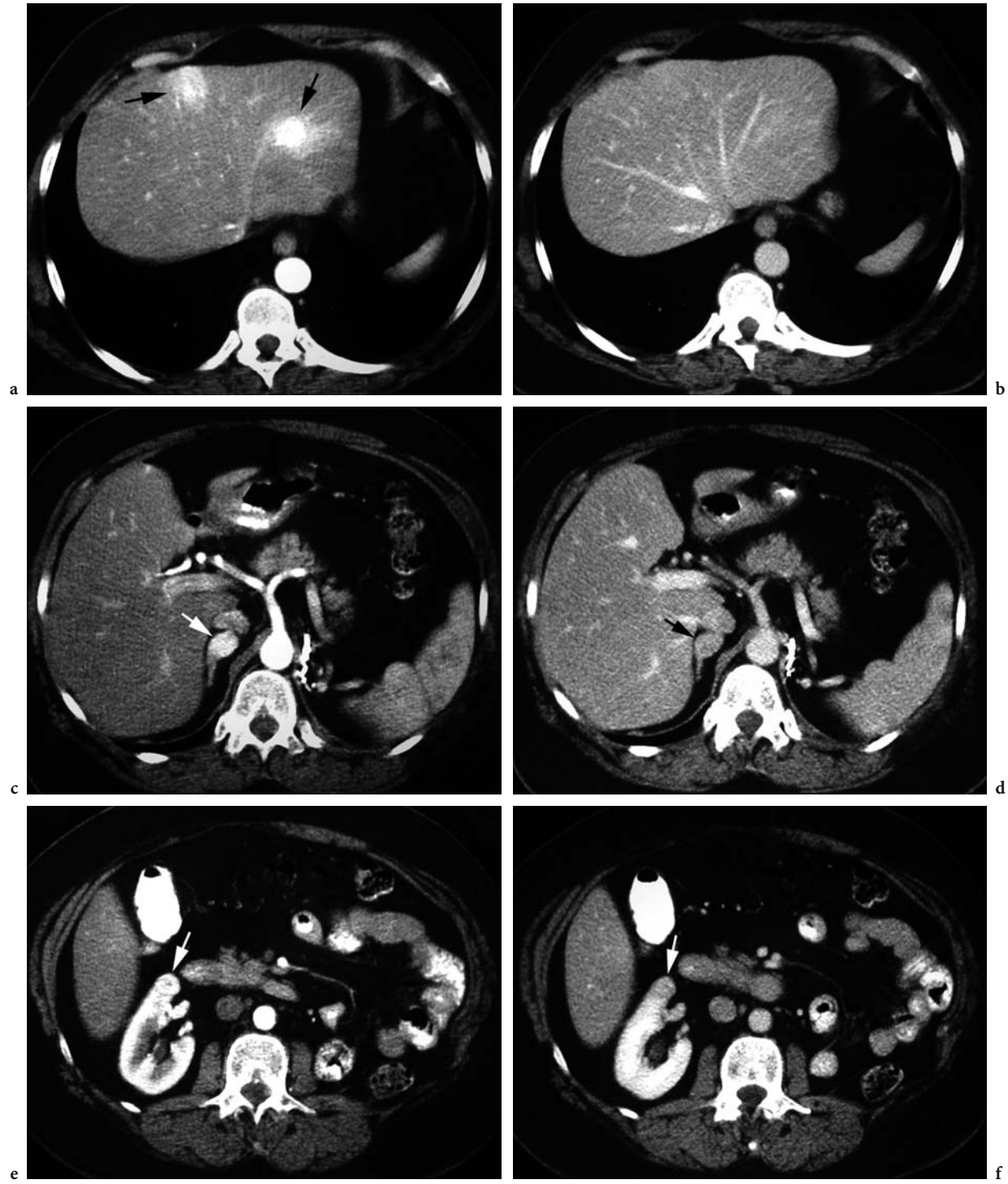

Fig. 16.11a-f. Liver and contralateral adrenal and kidney metastases in a 48-year-old man who underwent left nephrectomy for renal cell carcinoma. Axial contrast-enhanced CT scans show strongly enhancing hepatic metastases (*arrows*, **a**) at the arterial phase, which are **b** invisible at the portal venous phase. Right adrenal metastasis (*arrow*) is also strongly enhancing at **c** the arterial phase but **d** still visible at portal venous phase because of its nodular shape. Conversely, the right kidney metastasis (*arrow*) is difficult to see **e** at arterial phase because it has the same density as the normal renal parenchyma. It is better detected at **f** portal venous phase because it is hypodense (*arrow*) compared with the renal parenchyma.

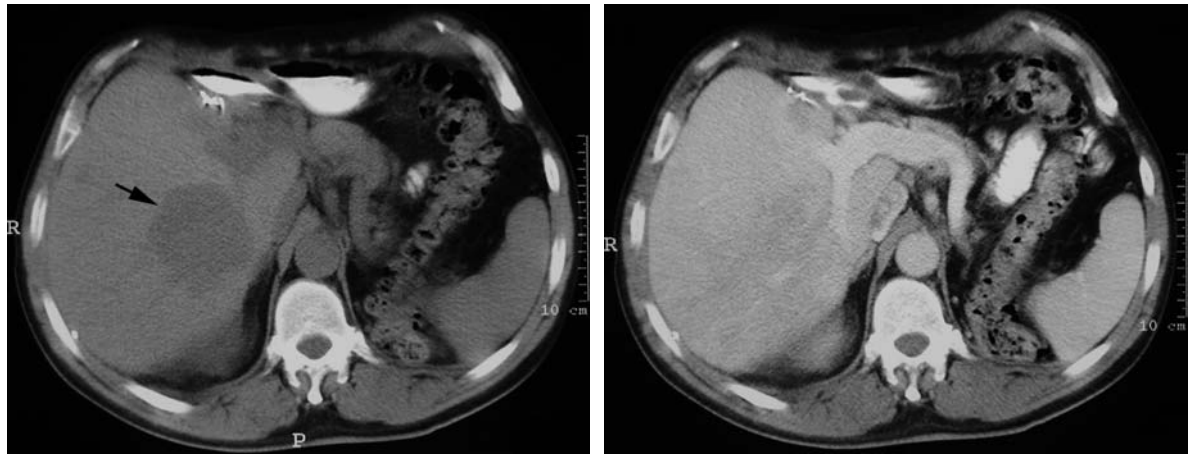

a b

Fig. 16.12a,b. Liver metastasis in a 51-year-old man who underwent left nephrectomy for renal cell carcinoma. **a** Axial unenhanced conventional CT scan shows a large, round hypodense mass lesion in the liver (*arrow*) which is barely detectable (**b**) after contrast injection.

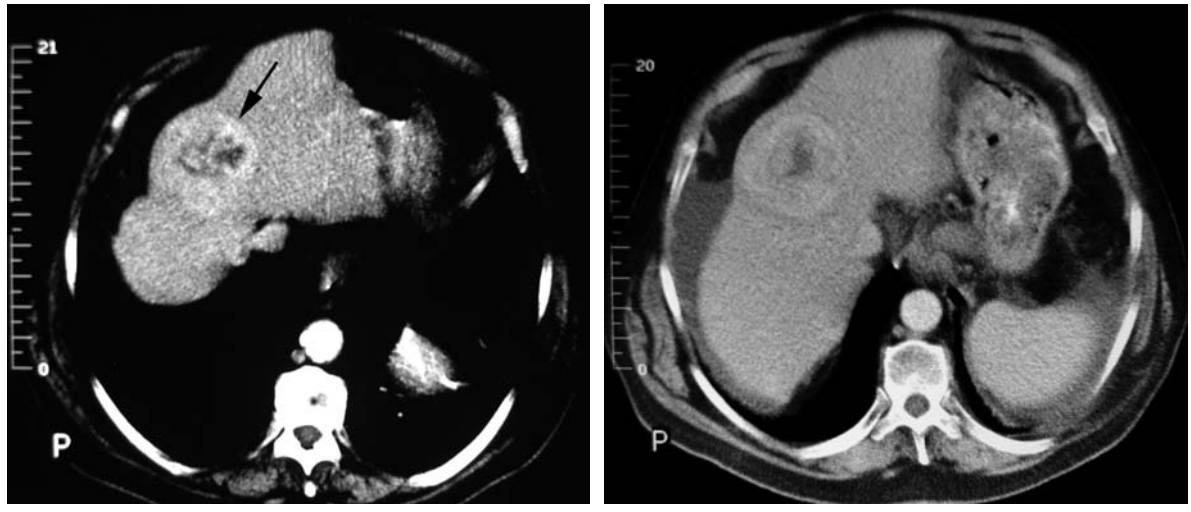

a b

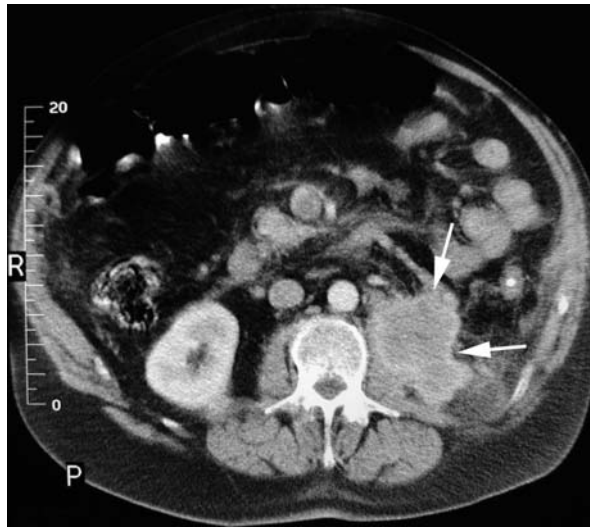

c

Fig. 16.13a-c. Liver metastasis and local recurrence in a 71-year-old man who underwent left nephrectomy for renal cell carcinoma. Axial contrast-enhanced CT scans show a strongly enhancing heterogeneous hepatic mass (*arrow*) with central necrosis **a** at the arterial phase which is less conspicuous **b** at the portal venous phase. There is also an ascites. **c** Axial contrast-enhanced CT scan at portal venous phase at the level of the kidneys shows an enhancing heterogeneous mass (*arrows*) with central necrosis occupying the left kidney fossa and probably invading the psoas muscle.

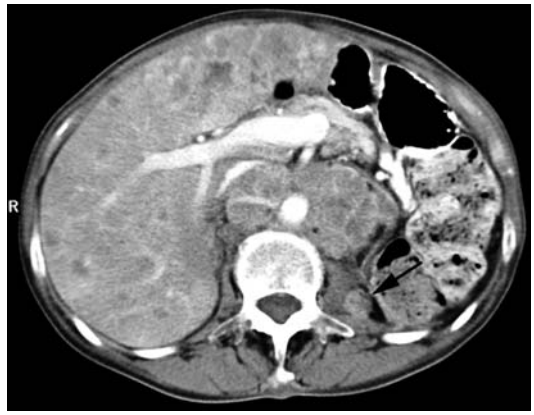

a

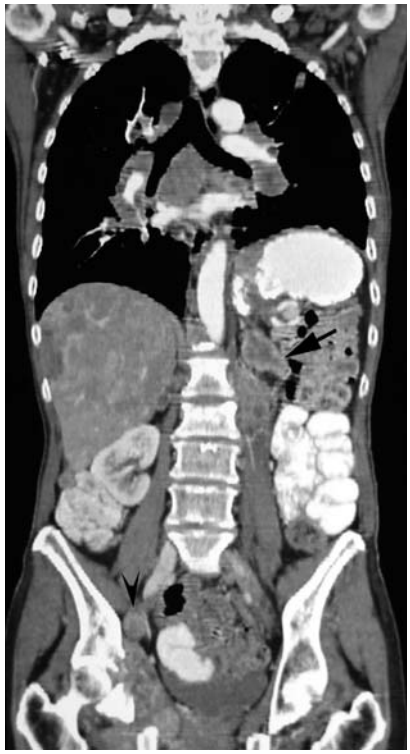

b

Fig. 16.14a,b. Small liver metastases with local recurrence and ipsilateral adrenal gland, bone, lung, and diffuse lymph node metastases in a 60-year-old woman who underwent left nephrectomy for renal cell carcinoma. **a** Axial contrast-enhanced CT scan shows multiple, small heterogeneous hypodense liver lesions with very thin peripheral enhancement. There is also a small heterogeneous enhancing mass in the left renal fossa invading the psoas muscle (*arrow*) and large heterogeneous enhancing retroperitoneal para-aortic adenopathies. **b** Coronal two-dimensional CT reconstruction of whole body confirms the earlier lesions and also shows heterogeneous, enhancing ipsilateral, left adrenal gland (*arrow*) mass, large mediastinal adenopathies, left pulmonary nodule, obturator lymph node enlargement (*arrowhead*), and large heterogeneously enhancing mass destroying the right acetabulum, and superior and inferior pubis rami.

biopsy is a simple, safe, and reliable method for the diagnosis of RCC metastases to the adrenal gland. It should be performed after biological diagnostic exclusion of pheochromocytoma, especially in patients with blood hypertension (Mesurolle et al. 1997; Mignon et al. 1999).

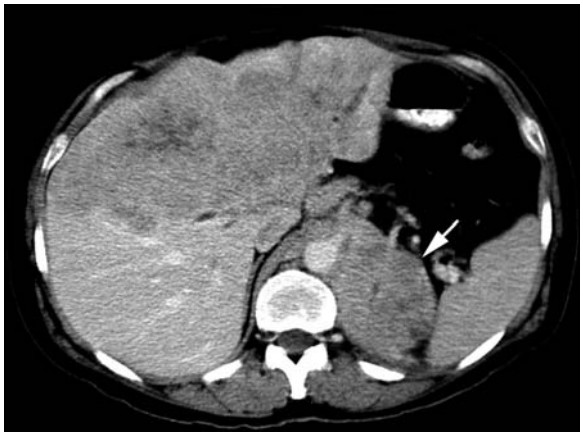

Fig. 16.15. Large liver and adrenal metastases in a 49-year-old man who underwent left radical nephrectomy for renal cell carcinoma. Axial contrast-enhanced CT scan shows a very large heterogeneous hepatic lesion with central necrosis and heterogeneously enhancing tumor in the left adrenal bed (*arrow*) which is invading the left diaphragm.

16.4.3 Spleen

Splenic metastases from RCC are extremely rare. They present a diagnostic dilemma since fine-needle aspiration of splenic tumors is often avoided because of possible hemorrhage (McGregor et al. 2003). Involvement may be synchronous (McGregor et al. 2003) or metachronous (Tatsuta et al. 2001). The latency period can be as long as 22 years (Tatsuta et al. 2001). Renal cell carcinoma may also occasionally secondarily involve the spleen by direct invasion (Suzuki et al. 1982). Splenic metastasis is infrequently diagnosed clinically (McGregor et al. 2003) because it is usually asymptomatic (Tatsuta et al. 2001). Splenectomy is usually the effective treatment because it is associated with complete resection of the tumor. The prognosis associated with splenic metastasis is favorable when there is only a solitary lesion (Tatsuta et al. 2001).

On US and CT, the appearance of spleen metastases varies. They may appear as a large complex heterogeneous mass in the spleen containing both solid and fluid components (Figs. 16.3, 16.22, 16.23; McGregor et al. 2003; Tatsuta et al. 2001). Other appearances include diffuse splenomegaly or small nodules (Tatsuta et al. 2001).

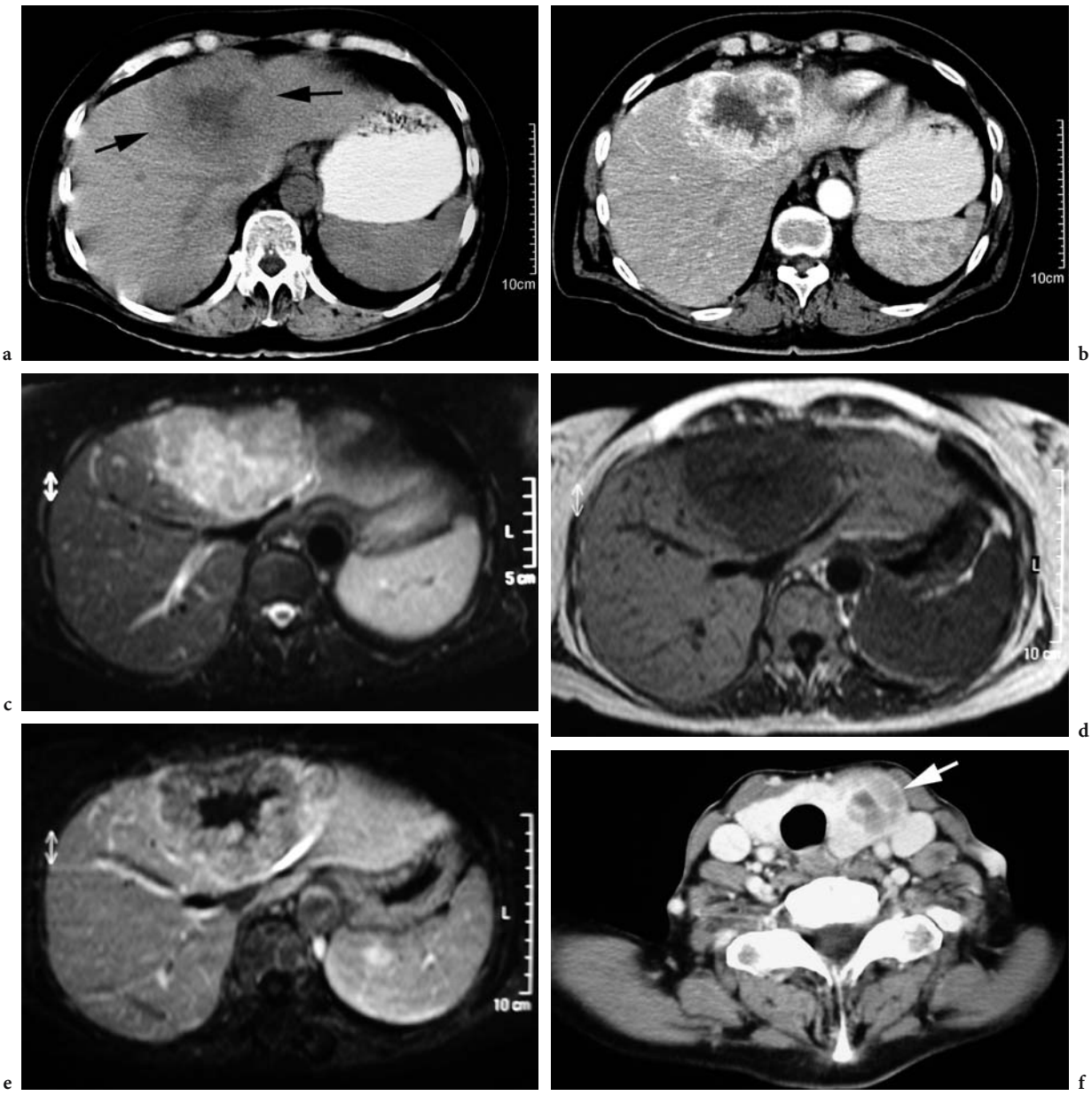

Fig. 16.16a-f. Liver and thyroid metastases in a 69-year-old woman who underwent left nephrectomy for renal cell carcinoma. **a** Axial unenhanced CT scan shows an ill-defined large hypodense hepatic lesion with central necrosis (*arrows*). **b** This lesion strongly heterogeneously enhances after contrast injection and its contours are more conspicuous and its central necrosis is more obvious. This lesion is hyperintense on **c** axial turbo spin T2-weighted MR image and hypointense on **d** fast-field-echo T1-weighted MR image. The tumoral enhancement is less obvious on **e** contrast-enhanced fast-field-echo T1-weighted MR image than on CT. **f** Axial contrast-enhanced CT of the neck shows large heterogeneous nodule of the left thyroid lobe (*arrow*).

16.4.4 Pancreas

Renal cell carcinoma metastases to the pancreas are uncommon and count for only 1–3% of cases (Ghavamian et al. 2000). Nevertheless, RCC is the most commonly reported primary tumor metastasizing to the pancreas (Ghavamian et al. 2000; Klein et al. 1998). They may be synchronous (Zhao et al. 1997) or occur several years after nephrectomy (Dousset et al. 1995; Klein et al. 1998) with a latency period as long as 32 years (Bassi et al. 2003). The pancreas may be the sole site of RCC metastases (Chao et al. 2002). Clinically, patients are often

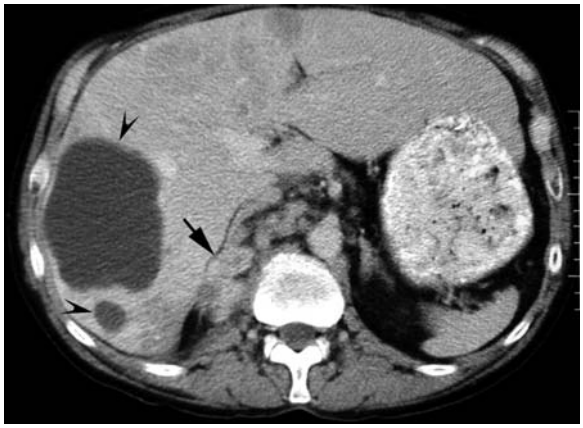

Fig. 16.17. Liver and adrenal metastases in a 59-year-old man who underwent right radical nephrectomy for renal cell carcinoma. Axial contrast-enhanced CT scan shows two well-defined water-density hepatic lesions of different sizes corresponding to cystic metastases (*arrowheads*). There are several other slightly hypodense solid mass liver metastases. There is also a heterogeneously enhancing tumor in the right adrenal bed (*arrow*).

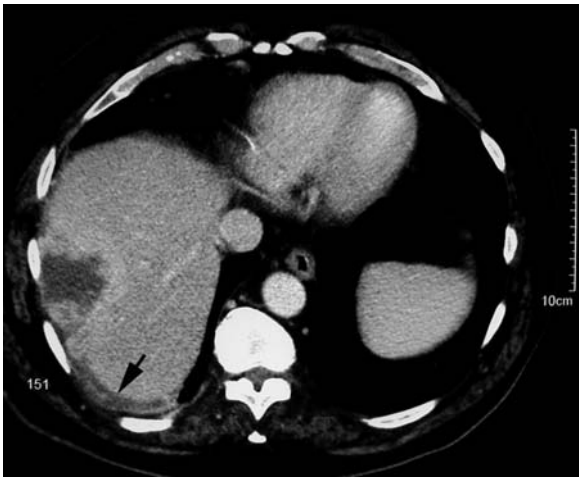

Fig. 16.18. Spontaneous rupture of liver metastasis in a 65-year-old man who underwent nephrectomy for renal cell carcinoma. Axial contrast-enhanced CT scan shows a subcapsular hypodense lesion with slightly peripheral enhancement that spontaneously ruptured with hepatic subcapsular effusion (*arrow*).

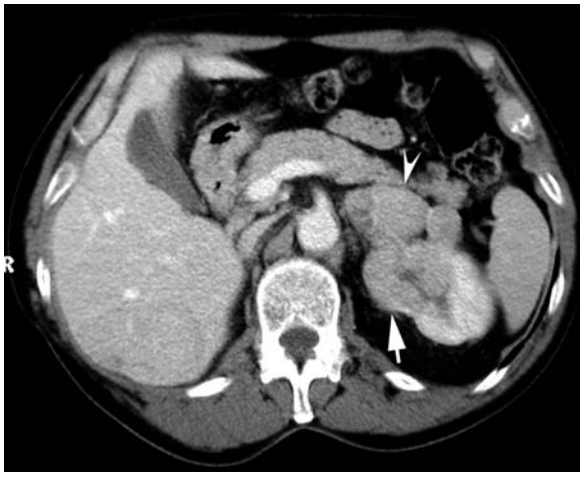

Fig. 16.19. Contralateral adrenal and kidney metastases in a 70-year-old man who underwent right nephrectomy for renal cell carcinoma. Axial contrast-enhanced CT scan at portal venous phase shows heterogeneously enhancing masses of the left adrenal gland (*arrowhead*) and left kidney (*arrow*).

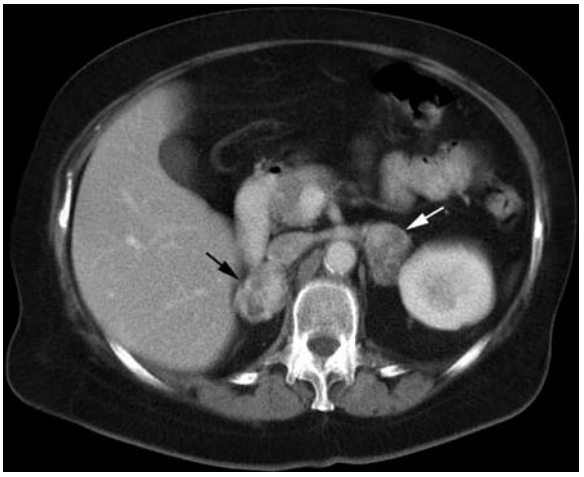

Fig. 16.20. Bilateral adrenal metastases in a 67-year-old man who underwent right nephrectomy for renal cell carcinoma. Axial contrast-enhanced CT scan at portal venous phase shows heterogeneously enhancing masses of both adrenal glands (*arrows*).

asymptomatic (Bassi et al. 2003; Ghavamian et al. 2000). Clinical abnormalities may include palpable abdominal mass, gastrointestinal bleeding, abdominal pain, bile duct obstruction, steatorrhea, and weight loss (Ghavamian et al. 2000; Kassabian et al. 2000). In solitary pancreatic involvement, surgical resection can improve the likelihood of patient survival (Andoh et al. 2004; Ghavamian et al. 2000; Giulini et al. 2003; Kassabian et al. 2000; Marusch et al. 2001). Spontaneous regression of pancreatic metastasis has been reported (Altschuler and Ray 1998). The prognosis of pancreatic metastasis from RCC is much better than that of primary pancreatic adenocarcinoma (Dousset et al. 1995;

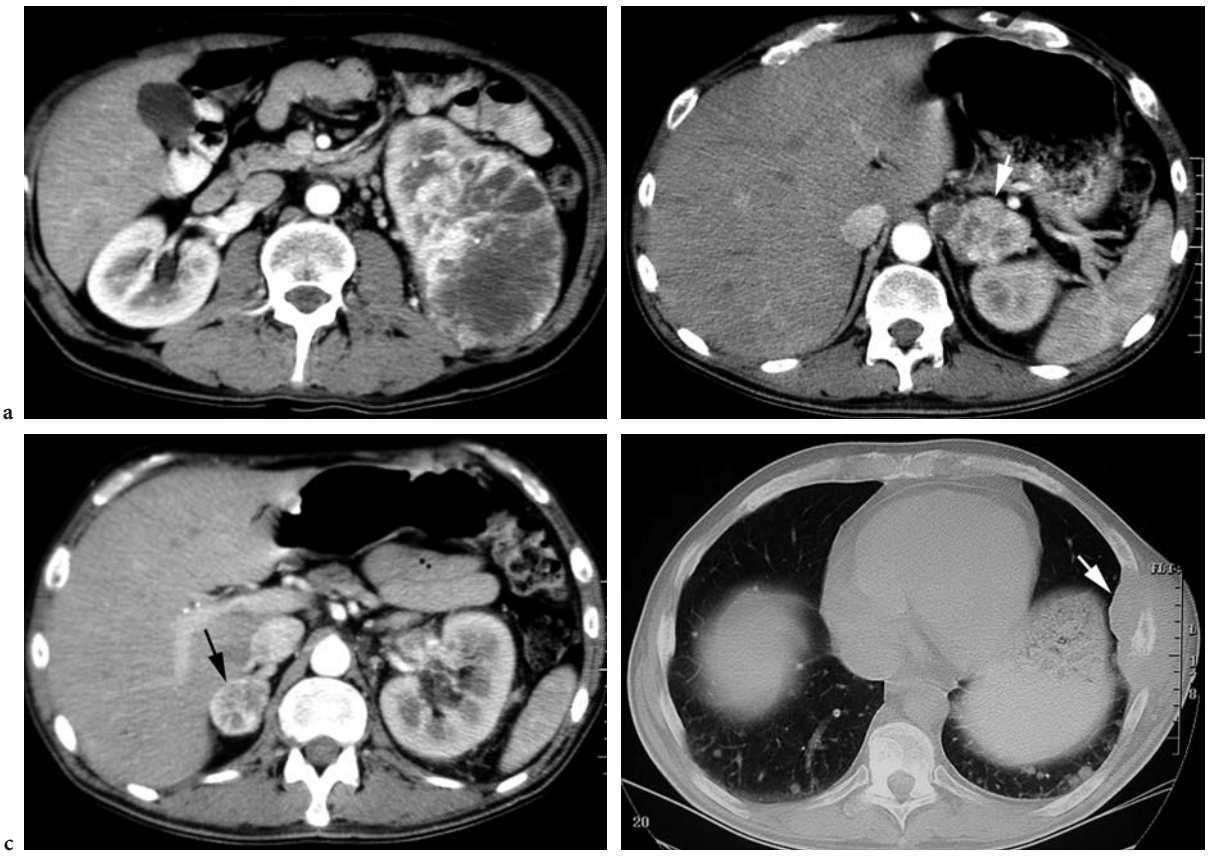

Fig. 16.21a-d. Bilateral adrenal, chest wall, and lung metastases diagnosed preoperatively in a 41-year-old man with renal cell carcinoma. **a** Axial contrast-enhanced CT scan shows heterogeneously enhancing large posterior left renal mass corresponding to the renal cell carcinoma. Axial contrast-enhanced CT scans show heterogeneously enhancing masses of the left (*arrow*, **b**) and right (*arrow*, **c**) adrenal glands. **d** Axial CT scan of the chest shows a large lytic mass involving the left lateral chest wall (*arrow*) and several bilateral small pulmonary nodules.

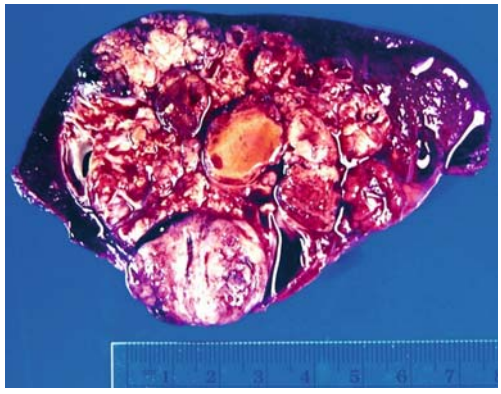

Fig. 16.22. Spleen metastasis in a 65-year-old man with synchronous renal cell carcinoma of the left kidney. Gross specimen shows massive replacement of the splenic parenchyma by metastatic tumor. There are multiple nodules fusing together to form a tumor mass occupying approximately 70% of the splenic parenchyma. Microscopic features of this splenic tumor are of a metastatic papillary carcinoma, identical to the histologic appearance of the primary renal cell carcinoma, chromophil (papillary) type (not shown). (Image courtesy of D.H. McGregor)

Ghavamian et al. 2000; Klein et al. 1998; Rivoire and Voiglio 1996).

On imaging, pancreatic metastases may be solitary or multiple, and usually appear as well-defined soft tissue masses (Ghavamian et al. 2000; Klein et al. 1998). Ultrasound and CT are reliable and highly specific (Bassi et al. 2003). On US or endoscopic US (Dousset et al. 1995), pancreatic metastases may be hypoechoic (Kassabian et al. 2000; Rivoire and Voiglio 1996; Strijk 1989), or hyperechoic (Rypens et al. 1992) due to their hypervascularity. On unenhanced CT, lesions are usually isodense to the pancreatic parenchyma (Altschuler and Ray 1998; Ng et al. 1999), and are rarely reported as mixed isodense and hypodense (Strijk 1989). Calcifications may occur but are very rare (Klein et al. 1998). Spiral CT with its optimization of vascular phases is particularly efficient in demonstrating these hypervascular pancreatic lesions (Klein et al. 1998; Ghavamian et al. 2000; Kassabian et

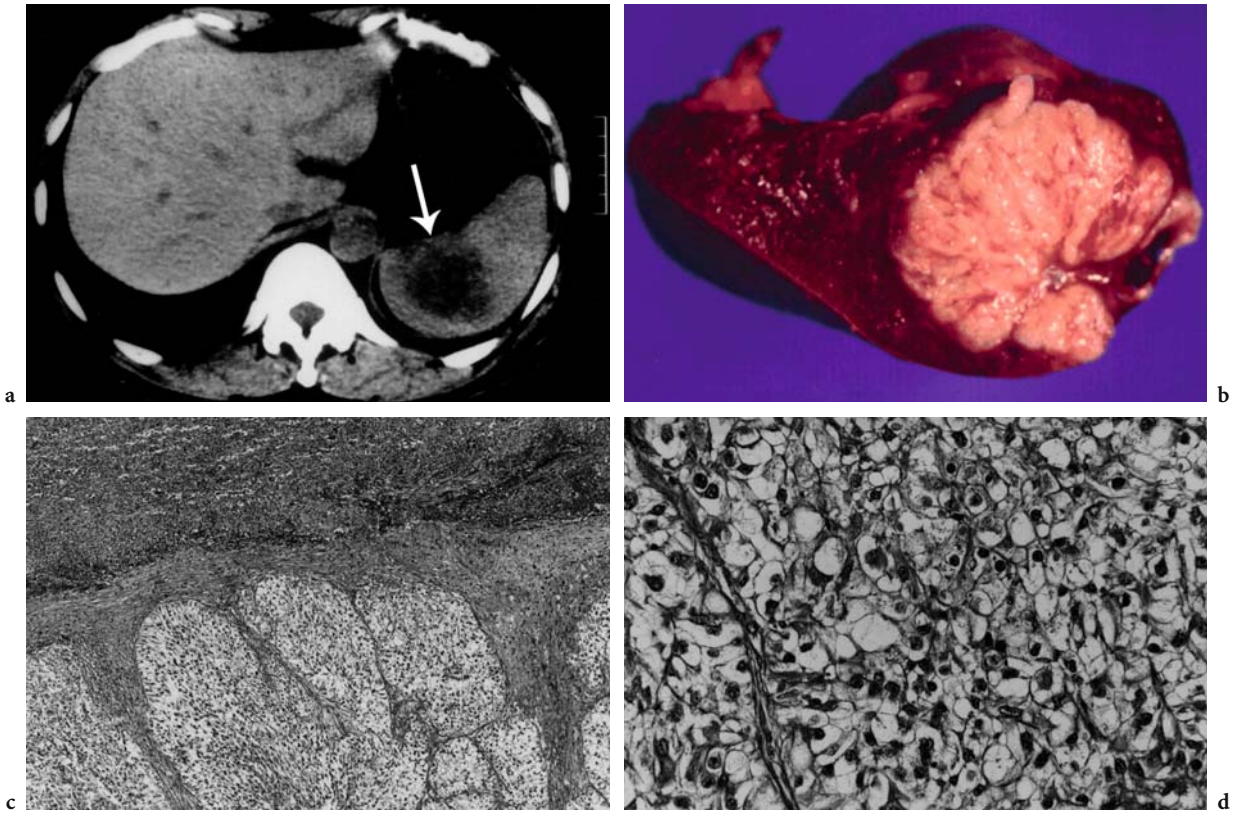

Fig. 16.23a-d. Spleen metastasis in a 69-year-man who underwent left nephrectomy for renal cell carcinoma 17 months previously. **a** Axial unenhanced CT scan shows an ill-defined heterogeneous hypodense mass of 6×6 cm in the spleen (*arrow*). **b** Gross specimen shows a milky-white tumor in the upper half of the spleen, 6 cm in diameter, that did not invade the capsule. Photomicrographs confirm a clear cell carcinoma in the spleen (hematoxylin and eosin stain; original magnification, **c** ×15, **d** ×75). (With permission from Tatsuta et al. 2001)

al. 2000; Scatarige et al. 2001a; Hernandez et al. 2003), which can also be seen on angiography (Andoh et al. 2004; Kassabian et al. 2000; Strijk 1989; Zhao et al. 1997) and on early contrast-enhanced MR imaging (Kelekis et al. 1996). This is unlike primary pancreatic adenocarcinoma which is usually hypovascular and does not enhance after contrast administration (Ghavamian et al. 2000; Scatarige et al. 2001a). This hypervascular effect is pronounced in early phases (i.e., arterial and portal) of enhancement (Fig. 16.24; Ghavamian et al. 2000; Ng et al. 1999). Such metastases may not be appreciated in the delayed phase or on unenhanced CT, especially if they are small (Ng et al. 1999). Smaller lesions tend to be homogeneous and enhance uniformly, whereas larger masses usually contain internal ischemic or necrotic components that appear as central hypodense areas (Figs. 16.25, 16.26; Bassi et al. 2003; Ghavamian et al. 2000; Kassabian et al. 2000; Scatarige et al. 2001b). In this respect the radiological appearance of pancreatic metastases from RCC resembles the appearance of primary RCC (Ghavamian et al. 2000; Klein et al. 1998).

16.4.5 Contralateral Kidney

Contralateral kidney metastases are rare accounting for approximately 1–2% of cases (Janzen et al. 2003). There is still debate on whether tumors that occur in the contralateral kidney after radical or partial nephrectomy represent de novo malignancy or metastasis (Janzen et al. 2003). The synchronous appearance of a single nodule or mass with the primary cancer suggests a possible second contralateral kidney cancer (Mignon and Mesurolle 2003). On the other hand, multiplicity of the lesions in the contralateral kidney or the synchronous appearance of these lesions with other organ metastases indi-

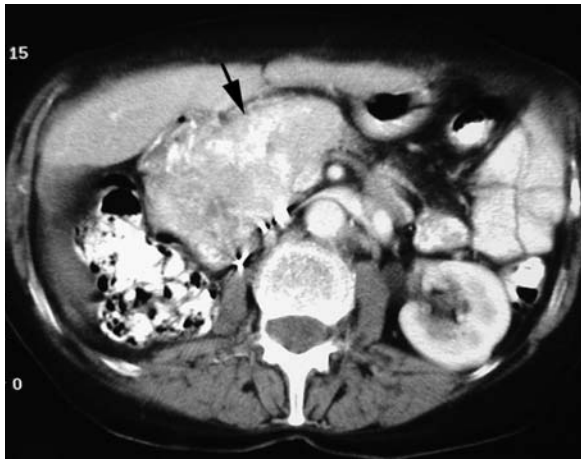

Fig. 16.24. Pancreatic metastasis in a 71-year-old man who underwent right nephrectomy for renal cell carcinoma. Axial contrast-enhanced CT scan at arterial phase shows heterogeneously enhancing very large mass of the head and body of the pancreas (*arrow*).

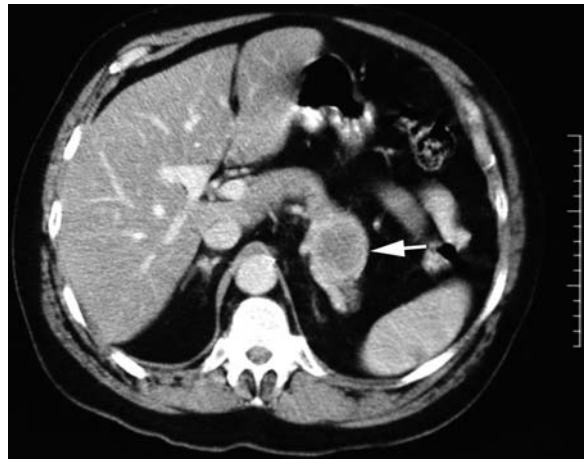

Fig. 16.25. Pancreatic metastasis in a 62-year-old man who underwent right nephrectomy for renal cell carcinoma. Axial contrast-enhanced CT scan at portal venous phase shows heterogeneously enhancing mass in the tail of the pancreas (*arrow*).

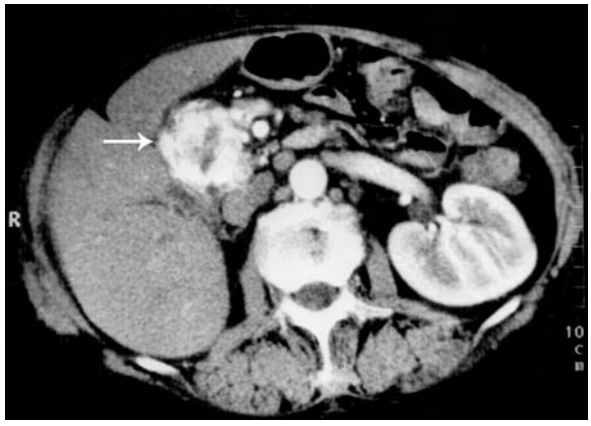

a

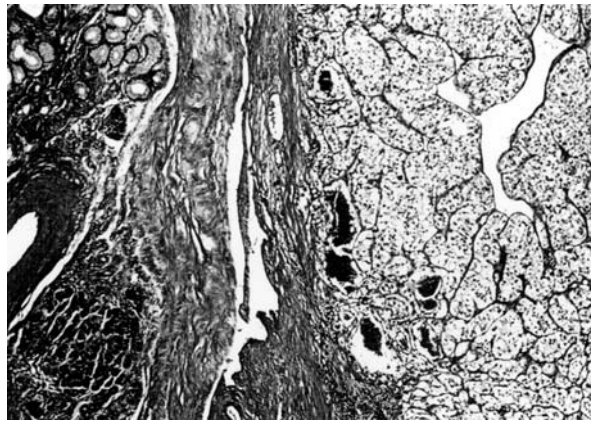

b

Fig. 16.26a,b. Pancreatic metastasis in a 73-year-old woman with renal cell carcinoma. **a** Axial contrast-enhanced CT scan shows large enhancing mass of the head of the pancreas (*arrow*) with central hypodense areas corresponding to necrosis. **b** Photomicrograph shows metastatic cells that are very glycogen rich like the clear cell primary renal tumor (hematoxylin and eosin stain). (Image courtesy of G. Butturini and C. Bassi)

cates metastases (Mignon and Mesurolle, 2003; Scatarige et al. 2001a).

On imaging, contralateral kidney metastases are usually hypoechoic on US and show a strongly enhancing mass on CT. The enhancement may be homogeneous (Chae et al. 2005) or heterogeneous with central necrosis (Fig. 16.27; Scatarige et al. 2001a).

16.4.6 Gallbladder

The gallbladder is only very rarely the site of RCC metastases (Furukawa et al. 1997; Limani et al. 2003; Stattaus et al. 1999). They are usually asymptomatic (Furukawa et al. 1997; Nagler et al. 1994), and usually metachronous (Furukawa et al. 1997) with a latency period as long as 27 years (Aoki et al. 2002). If possible, surgical resection should be performed, as it can provide a better chance of survival (Furukawa et al. 1997; Limani et al. 2003).

Ultrasound may show a polypoid mass in the gallbladder (Furukawa et al. 1997). Color Doppler US may show abundant pulsatile blood flow signal intensity within the mass. Spiral CT at the arterial phase may demonstrate an enhancing polypoid mass in the gallbladder (Fig. 16.28). The density of the lesion is usually higher than that of the

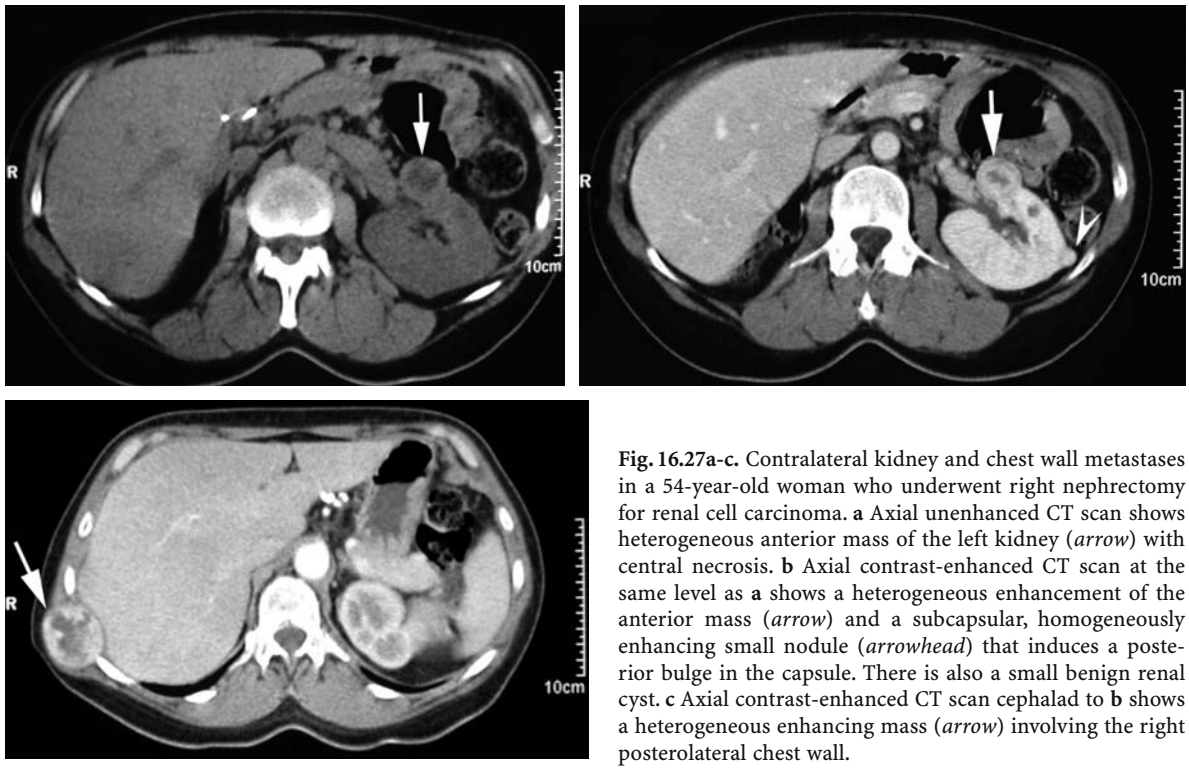

Fig. 16.27a-c. Contralateral kidney and chest wall metastases in a 54-year-old woman who underwent right nephrectomy for renal cell carcinoma. **a** Axial unenhanced CT scan shows heterogeneous anterior mass of the left kidney (*arrow*) with central necrosis. **b** Axial contrast-enhanced CT scan at the same level as **a** shows a heterogeneous enhancement of the anterior mass (*arrow*) and a subcapsular, homogeneously enhancing small nodule (*arrowhead*) that induces a posterior bulge in the capsule. There is also a small benign renal cyst. **c** Axial contrast-enhanced CT scan cephalad to **b** shows a heterogeneous enhancing mass (*arrow*) involving the right posterolateral chest wall.

liver parenchyma (Furukawa et al. 1997). Imaging studies are often futile for differentiating between primary and secondary tumors of the gallbladder (Limani et al. 2003). Primary tumors often coexist with gallstones. A polypoid lesion in an acalculous gallbladder is more consistent with metastasis than primary tumor (Limani et al. 2003) especially in case of hypervascularity on imaging studies (Aoki et al. 2002; Furukawa et al. 1997).

16.4.7 Peritoneum

Intraperitoneal metastatic spread of RCC involving the mesentery and omentum is very uncommon, and is identified in only 1% of patients with metastases at autopsy (Tartar et al. 1991). These widespread diffuse intraperitoneal metastases may be present synchronously to the RCC (Tartar et al. 1991) or may represent advanced recurrence (Scatarige et al. 2001a). Intraperitoneal spread of RCC can occur by one of two mechanisms. Firstly, RCC may break through the renal capsule, the anterior renal fascia, and the apposed posterior parietal peritoneum to spread along the peritoneal surfaces. In the second mechanism, embolic hematogenous metastases reach the omentum, mesentery, or other peritoneal organs with subsequent intraperitoneal spread. Abdominal complaints are the dominant clinical symptoms. Other presentations include abdominal distension due to ascites, early satiety, anorexia, and weight loss (Tartar et al. 1991).

Ultrasound may show cake-like omental thickening and ascites (Tartar et al. 1991). A barium enema may show narrowed bowel segments with an appearance consistent with serosal implants (Tartar et al. 1991). Computed tomography shows patterns of peritoneal carcinomatosis (Fig. 16.29; Scatarige et al. 2001a) which include extensive ascites, widespread omental infiltration (omental cake), and peritoneal soft tissue implants, as well as retroperitoneal metastases (Tartar et al. 1991). It may also show soft tissue masses in the cul-de-sac consisting of "drop" metastases (Tartar et al. 1991).

16.4.8 Esophagus, Stomach, and Duodenum

Esophageal metastases are very uncommon, especially when esophageal involvement is isolated. Clinically, they may be associated with progressive dysphagia. Resection of the esophageal metastasis is an option

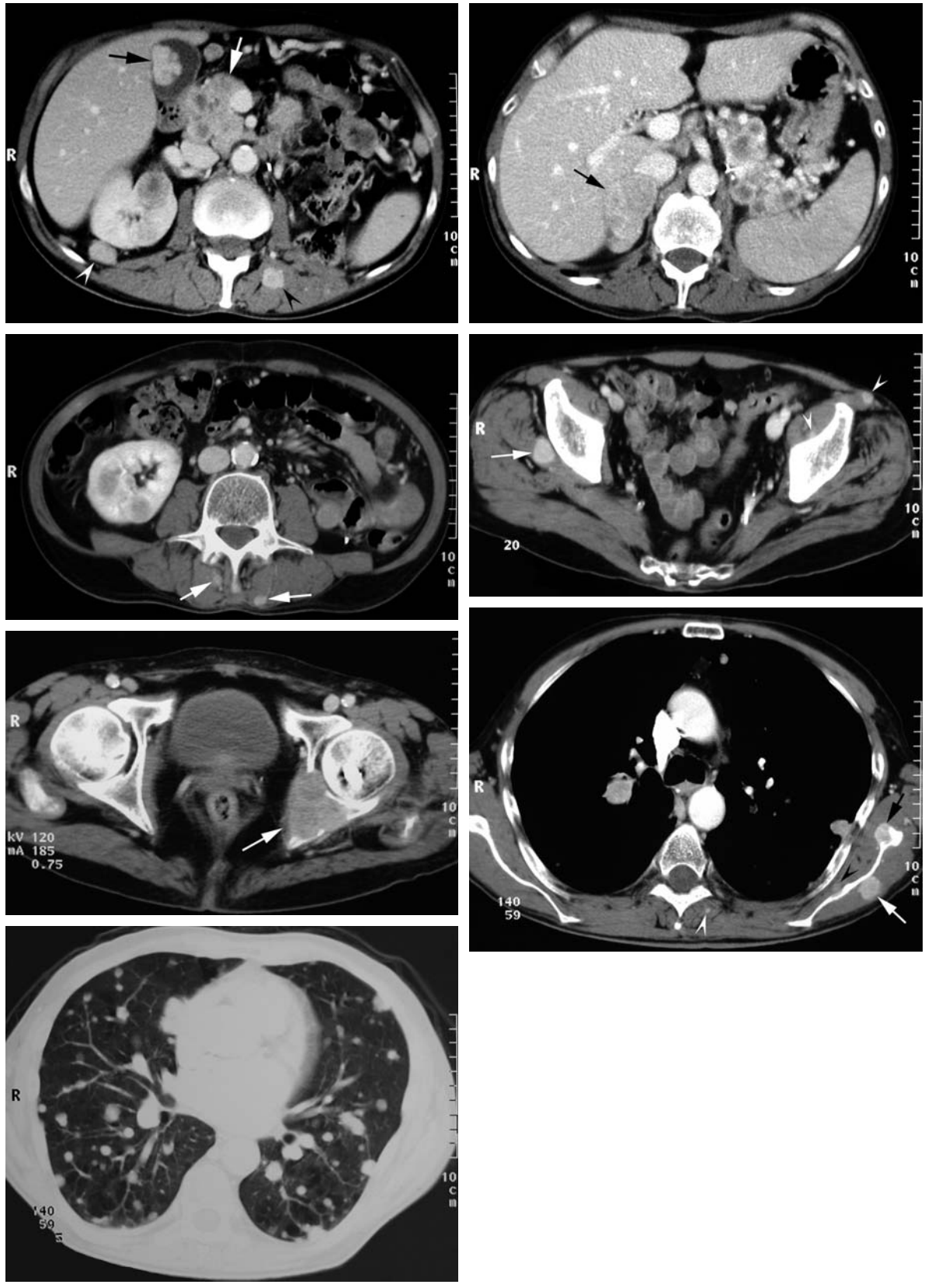

a b c d e f g

Fig. 16.28a-g. Gallbladder, contralateral kidney and adrenal gland, muscle, lung, and bone metastases in a 54-year-old man who underwent left nephrectomy for renal cell carcinoma. **a** Axial contrast-enhanced CT scan shows an enhancing heterogeneous polypoid mass in the gallbladder (*black arrow*). It also shows multiple heterogeneous enhancing masses at the head of the pancreas (*white arrow*) and anterior right kidney, a solid enhancing right posterior perirenal mass (*white arrowhead*), and an enhancing mass in the left erector spinae muscle (*black arrowhead*). **b** Axial contrast-enhanced CT scan cephalad to **a** shows multiple enhancing mixed round and annular masses in the body and tail of the pancreas. There is a large enhancing mass in the contralateral adrenal gland (*arrow*). **c** Axial contrast-enhanced CT scan at portal venous phase and caudad to **a** shows multiple hypodense lesions of varying sizes in the lower pole of the right kidneys. There are bilateral enhancing nodular lesions involving longissimus dorsi muscles (*arrows*). **d** Axial contrast-enhanced CT scan of the pelvis shows multiple nodular enhancing lesions involving right gluteus minimus (*arrow*) and left iliopsoas muscles (*arrowheads*). **e** Axial contrast-enhanced CT scan shows an enhancing destructive mass of the left acetabulum (*arrow*). **f** Axial contrast-enhanced CT scan of the chest shows multiple enhancing nodular lesions of varying sizes involving the left erector spinae (*white arrowhead*), infraspinatus (*white arrow*), and subscapularis (*black arrowhead*) muscles. There is also a enhancing destructive bone lesion of the left scapula (*black arrow*). **g** Axial CT scan of the chest at lung window shows several bilateral pulmonary nodules of varying sizes.

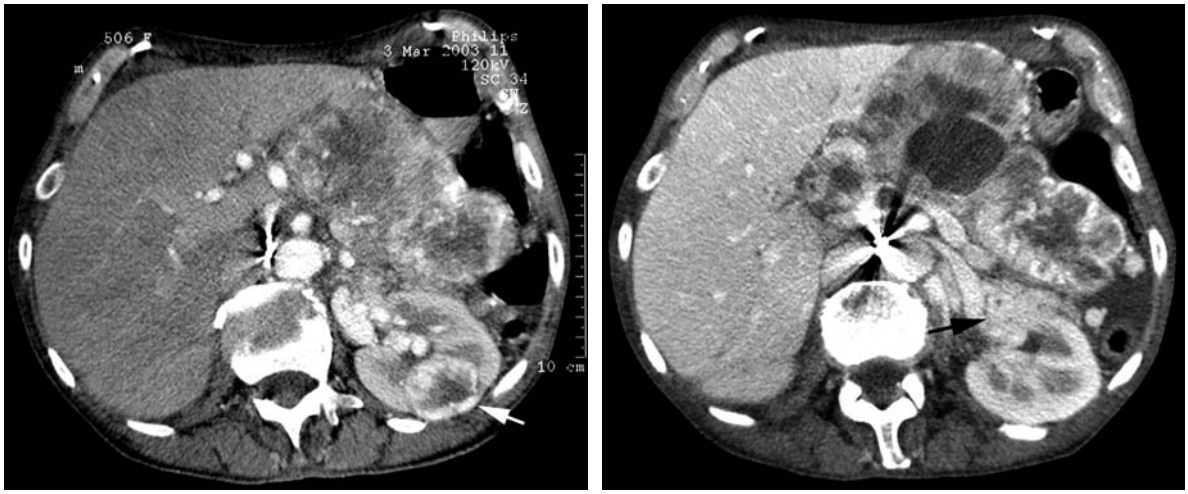

a b

Fig. 16.29a,b. Peritoneal carcinomatosis and contralateral kidney metastases in a 80-year-old woman who underwent right nephrectomy for renal cell carcinoma. **a, b** Axial contrast-enhanced CT scans show extensive widespread heterogeneous peritoneal infiltration with solid and cystic components associated with ascites. There are also heterogeneous enhancing masses of the left kidney of **a** posterior (*arrow*) and **b** anterior (*arrow*) locations.

when isolated, but its presence should be considered an adverse prognostic factor. Esophagography shows an esophageal tumor. Endoscopy may also show the tumor and also allows histological diagnostic biopsies (Monteros-Sanchez et al. 2004).

Stomach metastases from RCC are very rare. They may be synchronous or more frequently metachronous. The latency period can be as long as 9 years (Odori et al. 1998). They are more commonly located in the body and fundus than in the antrum (Adams et al. 2003), and are more likely to be single than multiple (Adams et al. 2003). Clinically, they may be asymptomatic, or associated with hematemesis, anemia, melena, dyspepsia, and/or epigastric pain (Adams et al. 2003; Mascarenhas et al. 2001). Surgical resection is appropriate for isolated gastric metastases because prolonged survival is possible (Mascarenhas et al. 2001). The typical endoscopic appearance is a submucosal nodule with apical depression or ulceration (Adams et al. 2003; Mascarenhas et al. 2001; Odori et al. 1998). Other appearances vary from polypoid lesion (Fig. 16.30) to small or larger ulcers, sometimes with elevated margins (Adams et al. 2003; Mascarenhas et al. 2001). Their appearance may be indistinguishable from that of gastric cancers (Adams et al. 2003). Endoscopy allows biopsies that are positive in more than 90% of the cases (Adams et al. 2003). Endoscopic US is sensitive and may typically show a relatively hypoechoic nodule lying in the submucosal layer (Odori et al. 1998). Computed tomography may show the tumor as a mass in the stomach.

Duodenal metastases are very rare. They may be synchronous (Yavascaoglu et al. 1999) or meta-

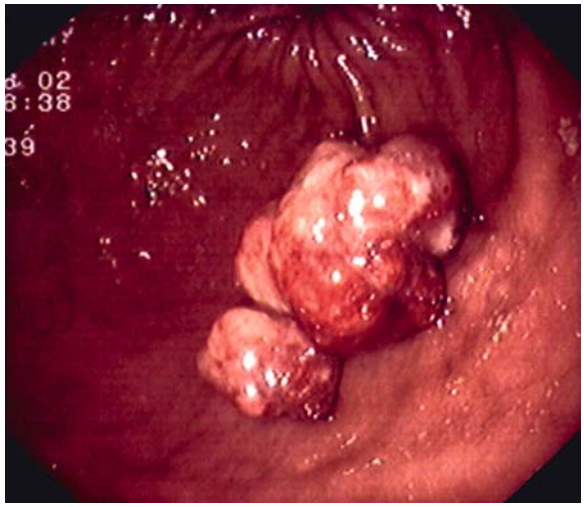

Fig. 16.30. Gastric metastases in a 64-year-old man with advanced renal cell cancer. Endoscopic view shows polypoid metastases in the body of the stomach. (With permission from Adams et al. 2003; image courtesy of I.C. Roberts-Thomson)

chronous with a latency period as long as 11 years (Hashimoto et al. 2001). They usually occur in patients with widespread nodal and visceral involvement, but may also be the only metastatic localization (Hashimoto et al. 2001). Clinically they may present with dyspepsia (Lee et al. 2002) or obstruction (Tharakan et al. 1995), or mainly with gastrointestinal tract bleeding (Hashimoto et al. 2001; Robertson and Gertler 1990; Yavascaoglu et al. 1999). Duodenal metastases are most frequently located in the periampullary region, followed by the duodenal bulb (Hashimoto et al. 2001). Resection en bloc of a single duodenal metastasis may give a favorable prognosis (Gastaca Mateo et al. 1996; Hashimoto et al. 2001). Duodenoscopy shows a large and ulcerative protruding mass that may obstruct the duodenum and a biopsy can be performed during the procedure (Hashimoto et al. 2001; Lee et al. 2002). Angiography typically demonstrates a hypervascular tumor and is particularly useful for demonstrating small hypervascular lesions (Fig. 16.31; Hashimoto et al. 2001). Ultrasound may show a thickened duodenum wall (Hashimoto et al. 2001). Computed tomography may show circumferential wall thickening with high enhancement at the duodenum (Hashimoto et al. 2001; Lee et al. 2002), or a soft tissue enhancing mass at the pancreaticoduodenal region (Yavascaoglu et al. 1999). This tumor enhancement is also well seen at MR imaging (Hashimoto et al. 2001).

16.4.9 Intestine

Renal cell carcinoma metastasis to the intestine is thought to occur by dissemination through Batson's venous plexus (Diaz-Candamio et al. 2000). All segments of the small and large bowels may be involved by renal cancer metastasis.

Metastases in the small intestine are uncommon. Only 4% of RCC metastasize to the small intestine (Yavascaoglu et al. 1999). They are rarely synchronous and usually metachronous with latency period as long as 20 years (Nozawa et al. 2003). These metastases usually show widespread nodal and visceral involvement (Hashimoto et al. 2001). Clinical presentation includes ileus, nausea, abdominal pain, loss of weight, gastrointestinal hemorrhage, intussusception, and/or perforation (Nozawa et al. 2003; Pavlakis et al. 2004; Scatarige et al. 2001a). A hematogenous pathway through pulmonary circulation is considered to play a critical role in the cascade of multiple-step metastases from kidney to small intestine (Nozawa et al. 2003). Histologically, almost all cases show clear cell metastatic RCC. Only one reported case included a sarcomatoid component in part of the primary tumor. These findings are consistent with the concept that sarcomatoid histology suggests high-grade malignancy and poor prognosis (Nozawa et al. 2003). These metastases are classified as polypoid type (Fig. 16.32) in the majority of cases, or Borrmann-2 (Fig. 16.33) or Borrmann-3 type (localized or infiltrating tumor with ulcer, respectively; Nozawa et al. 2003). Management should be aggressive since metastasectomy can extend patent survival (Pavlakis et al. 2004). Barium meal may show single or multiple tumors of varied sizes protruding into the lumen of the small intestine (Nozawa et al. 2003). A CT scan may show single or multiple tumors protruding into the small intestine lumen (Fig. 16.34; Pavlakis et al. 2004).

Metastases to the colon from RCC are extremely rare. They may produce pain in the abdomen (Lee et al. 2002) or melena episodes (Diaz-Candamio et al. 2000) but may also be asymptomatic. They are often metachronous with a latency period as long as 8 years (Diaz-Candamio et al. 2000). Solitary colonic metastasis is possible and it is usually associated with better prognosis and long-term survival. Colonoscopy may reveal a polypoid, exophytic, and nodular mass in the colon, and may also permit biopsy (Diaz-Candamio et al. 2000; Lee et al. 2002). A barium enema study may show a filling defect at the colonic wall that mimics colonic adeno-

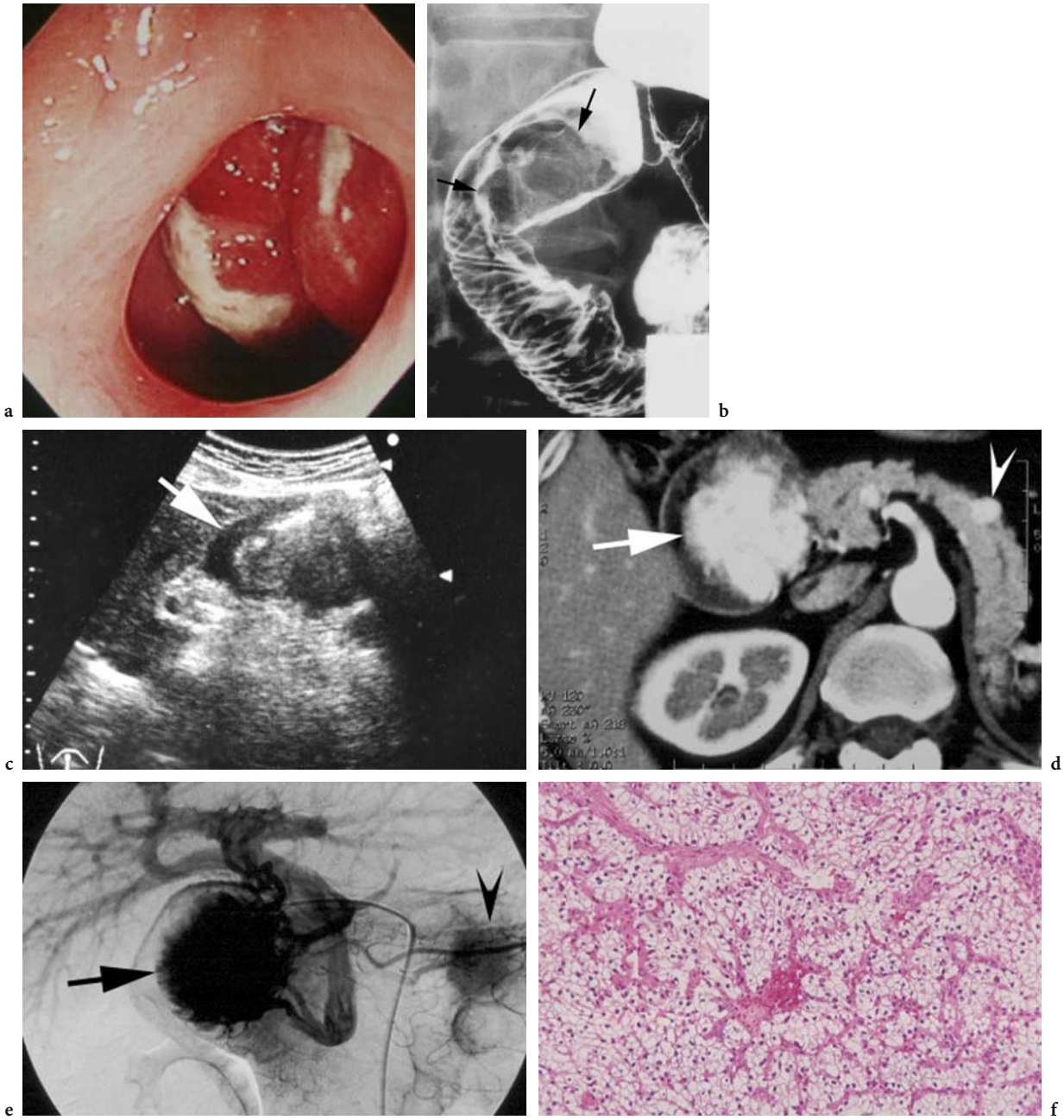

Fig. 16.31a-f. Concomitant duodenal and pancreatic metastases in a 68-year-old man who underwent left nephrectomy 11 years previously for renal cell carcinoma. This patient presented with dyspnea on exertion and severe anemia. **a** Upper gastrointestinal endoscopy reveals an ulcerated bleeding duodenal tumor. **b** Barium meal study of the duodenum discloses the presence of a large tumor of the duodenum bulb (*arrows*). **c** Longitudinal US image of the duodenum shows thickening of the wall of the duodenum (*arrow*) adjacent to the pancreas. **d** Axial contrast-enhanced CT scan shows a large enhanced mass of the duodenum (*arrow*) and a small enhanced nodule in the body of the pancreas (*arrowhead*). **e** Selective common hepatic angiography demonstrates hypervascular tumors in the duodenal wall (*arrow*) and body of the pancreas (*arrowhead*). **f** Photomicrograph of the resected duodenum and pancreas shows clear cell carcinoma compatible with metastasis from renal cell carcinoma (hematoxylin and eosin stain; original magnification, ×100). (With permission from Hashimoto et al. 2001)

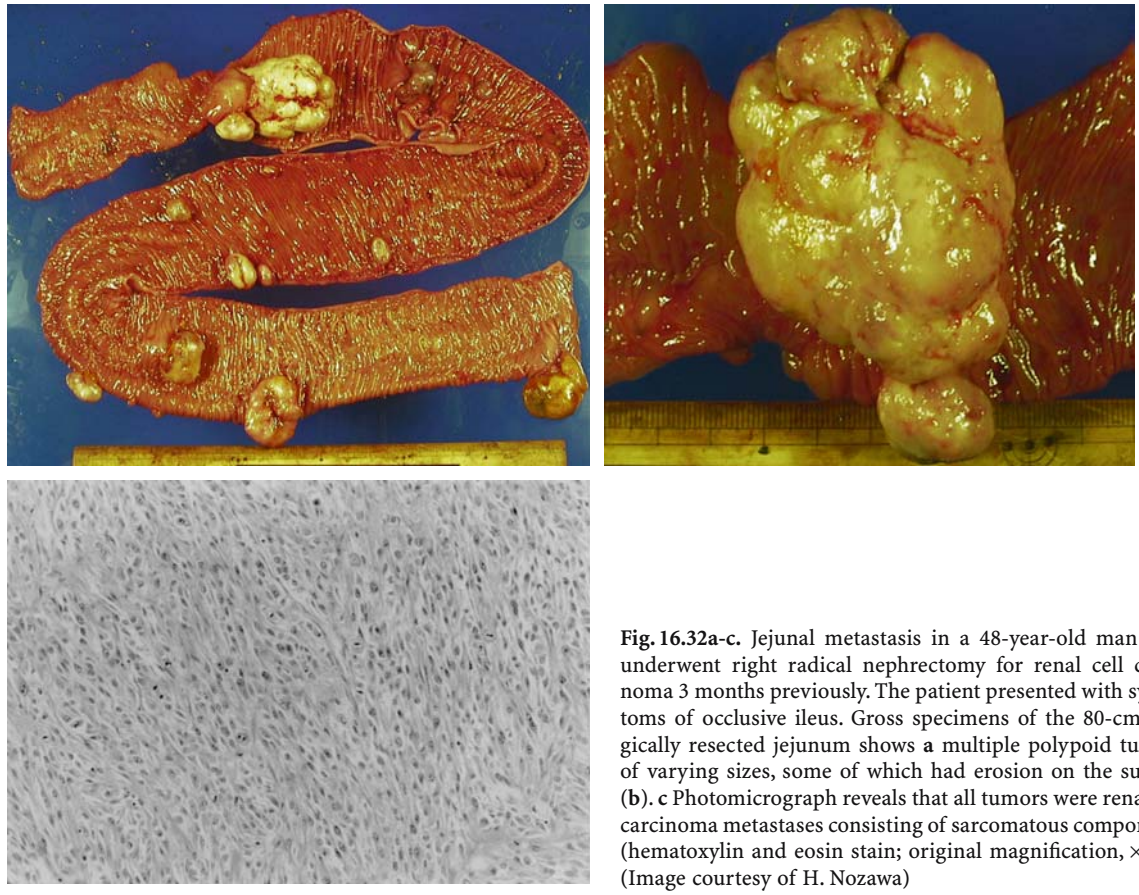

Fig. 16.32a-c. Jejunal metastasis in a 48-year-old man who underwent right radical nephrectomy for renal cell carcinoma 3 months previously. The patient presented with symptoms of occlusive ileus. Gross specimens of the 80-cm surgically resected jejunum shows **a** multiple polypoid tumors of varying sizes, some of which had erosion on the surface (**b**). **c** Photomicrograph reveals that all tumors were renal cell carcinoma metastases consisting of sarcomatous components (hematoxylin and eosin stain; original magnification, ×125). (Image courtesy of H. Nozawa)

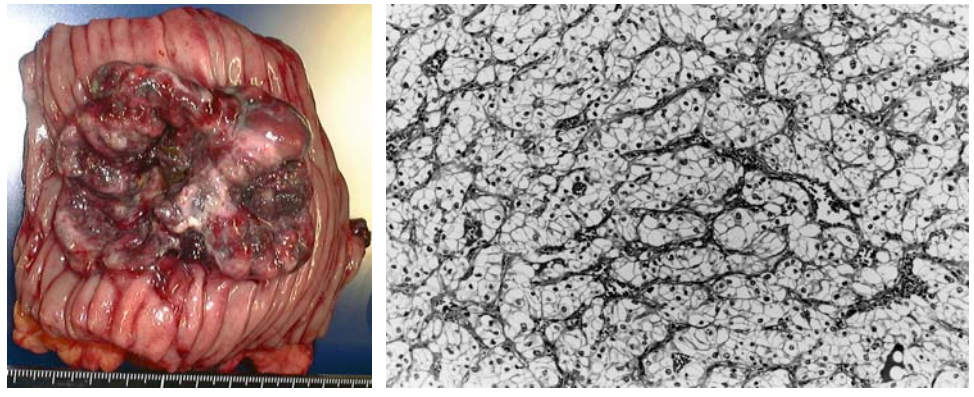

Fig. 16.33a,b. Jejunal metastasis in a 62-year-old man who underwent left nephrectomy for renal cell carcinoma 6 years previously. The patient complained of tarry stools on 10 consecutive days and frequent episodes of shortness of breath. **a** Gross specimen of the surgically resected jejunum shows an ulcerating lesion surrounded by elevated borders typical of a Borrmann-2-like tumor. **b** Photomicrograph reveals clear cell type renal cell carcinoma metastasis (hematoxylin and eosin stain; original magnification, ×125). (Image courtesy of H. Nozawa)

carcinoma (Diaz-Candamio et al. 2000). Spiral CT, especially at arterial phase, may show an early and heavily enhancing irregular mass (Lee et al. 2002) or broad-based polypoid lesion (Diaz-Candamio et al. 2000) protruding into the lumen of the colon.

16.4.10 Genitourinary Tract

All sites in the genitourinary tract may be involved including ureter (Kamota et al. 2003; Lee et al. 1998),

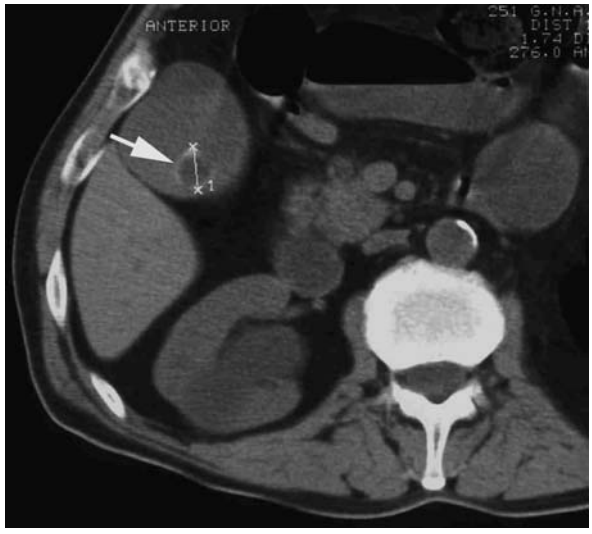

a

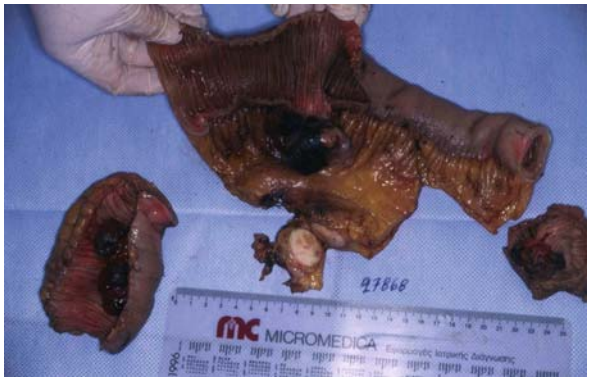

b

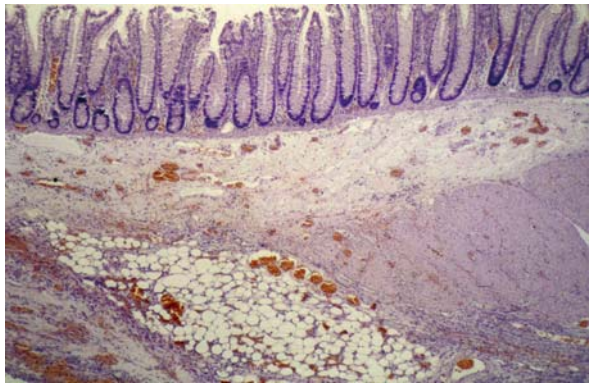

c

Fig. 16.34a-c. Ileal metastasis in a 65-year-old man who underwent left nephrectomy for renal cell carcinoma 2 years previously. The patient experienced vomiting, abdominal dilation secondary to intestinal obstruction, and melena. **a** Axial unenhanced CT scan shows a marked dilation of the small intestine and a lesion protruding into the lumen of the ileum (*arrow*). **b** Gross specimen shows the presence of multiple intra-luminal hemorrhagic lesions. **c** Photomicrograph shows the presence of metastatic renal cell carcinoma in the intestinal wall (hematoxylin eosin stain; original magnification, ×150). (With permission from Pavlakis et al. 2003; image courtesy of G.M. Sakorafas)

bladder (Kamota et al. 2003; Shiraishi et al. 2003), prostate (Mearini et al. 2004), urethra (Mearini et al. 2004), ovary (Insabato et al. 2003), vagina (Yokoyama et al. 1998), Bartholin glands (Leiman et al. 1986), testis (Calleja Escudero et al. 2004; Daniels and Schaeffer 1991; Nabi et al. 2001;), and penis (Daniels and Schaeffer 1991). The mechanism responsible for these metastases is still not entirely clear (Mearini et al. 2004).

Bladder metastasis from RCC is extremely rare with a frequency of 0.3–1.6% (Raviv et al. 2002; Saitoh et al. 1982; Shiraishi et al. 2003). The latency period can be as long as 12 years (Shiraishi et al. 2003). The mechanism is controversial. The localization of the bladder lesion around the ureteral orifice may argue in favor of endoluminal implantation of cancer cells (Shiraishi et al. 2003), a route that has been termed "drop metastasis" (Raviv et al. 2002). The prognosis is poor with most patients dying in the first year (Shiraishi et al. 2003). Nevertheless, a case has been reported with a 6-year survival after resection of bladder metastases. Clinically, patients usually present with painless hematuria (Raviv et al. 2002). A transurethral complete resection is usually possible, but this tumor may necessitate a partial cystectomy (Raviv et al. 2002; Shiraishi et al. 2003). Cystoscopy may show a solitary sessile, spherical tumor protruding into the bladder (Fig. 16.35; Kamota et al. 2003; Shiraishi et al. 2003). Computed tomography shows an enhanced mass within bladder wall (Shiraishi et al. 2003).

Prostate metastases from RCC are extremely rare with the exception of metastasis by direct extension from adjacent structures (Moudouni et al. 2001). Involvement may be synchronous or metachronous to the RCC (Yavascaoglu et al. 1999). In one case report, prostate metastasis appears as a well-defined heterogeneous hyperechoic nodule or mass located in one of the prostate lobes (Fig. 16.36; Mearini et al. 2004), but it can also appear as prostatic hypertrophy mimicking benign prostatic hyperplasia (Moudouni et al. 2001). A unique case of periprostatic metastasis presenting as a periprostatic mass displacing the prostate gland has been reported (Yavascaoglu et al. 1999).

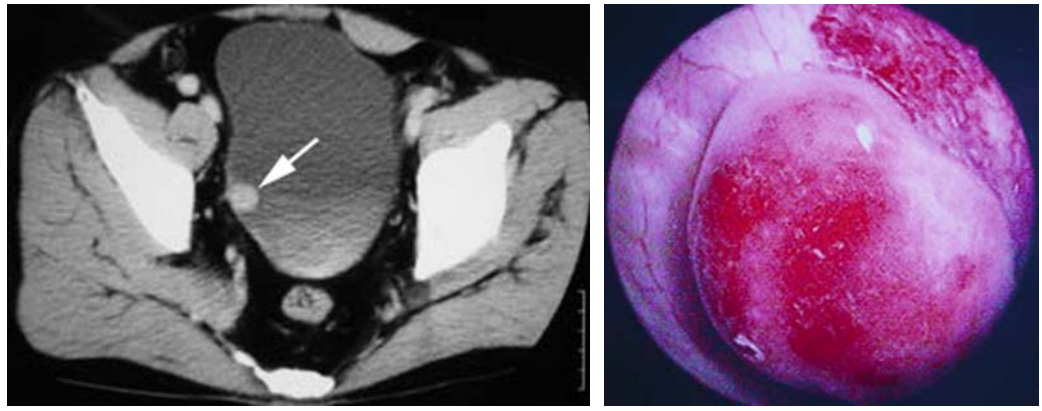

a b

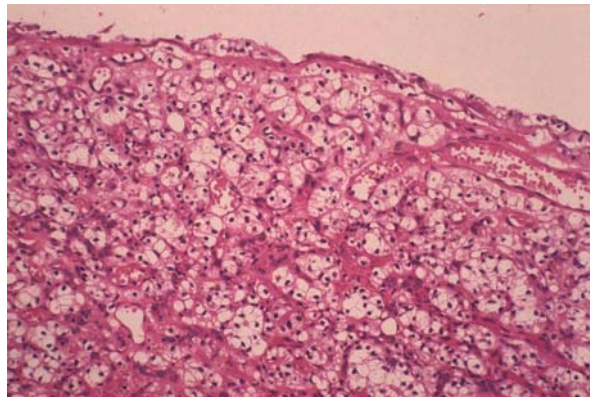

c

Fig. 16.35a-c. Bladder metastasis in a 76-year-old man with renal cell carcinoma who underwent radical nephrectomy 12 years previously. **a** Axial contrast-enhanced CT scan shows a well-defined enhanced mass at the right bladder wall (*arrow*). **b** Cystoscopy shows that the mass appears as a metastasis of right bladder wall. The patient underwent a complete transurethral resection of the bladder tumor. **c** Photomicrograph shows that the tumor has a clear cell pattern that is identical histologically to the primary renal cell carcinoma. There is no transitional epithelium (hematoxylin and eosin stain; original magnification, ×100). (With permission from Shiraishi et al. 2003)

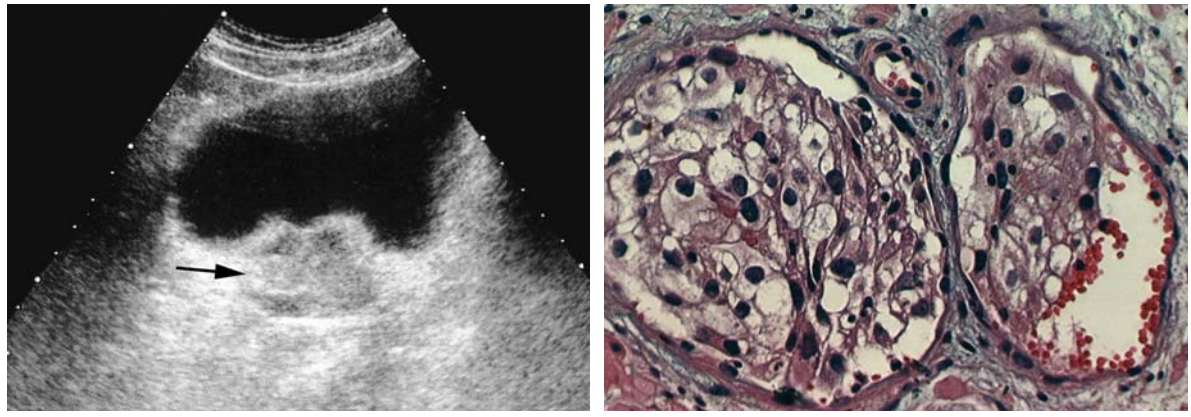

a b

Fig. 16.36a,b. Prostate metastasis in a 48-year-old man with renal papillary adenocarcinoma for which he underwent renal conservative surgery 46 months previously. **a** Transverse US image of the pelvis shows a well-defined mass in the right lobe of the prostate (*arrow*). **b** Fine-needle-aspiration biopsy of this mass shows metastatic renal papillary adenocarcinoma (hematoxylin and eosin stain; original magnification, ×200). (Image courtesy of L. Mearini)

Ovarian metastases from RCC are also very rare. The distinction of ovarian metastasis from an ovarian primary tumor can be difficult, especially when the ovarian metastasis is discovered first and mimics an ovarian clear cell carcinoma. The latency period can be as long as 11 years. On US and CT, they usually appear as a large, solid, or solid and cystic mass (Fig. 16.37), or as one or a few small nodules within a well-defined cystic mass (Fig. 16.38; Insabato et al. 2003).

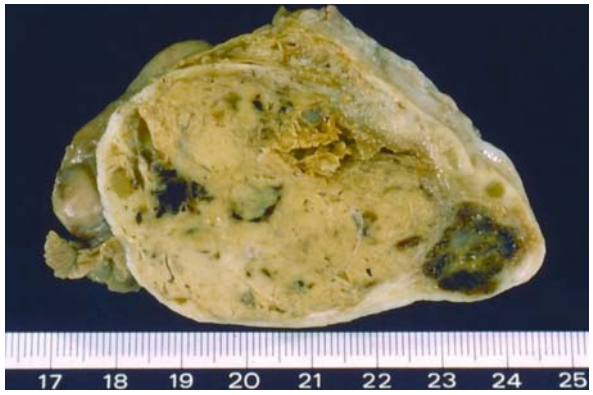

a

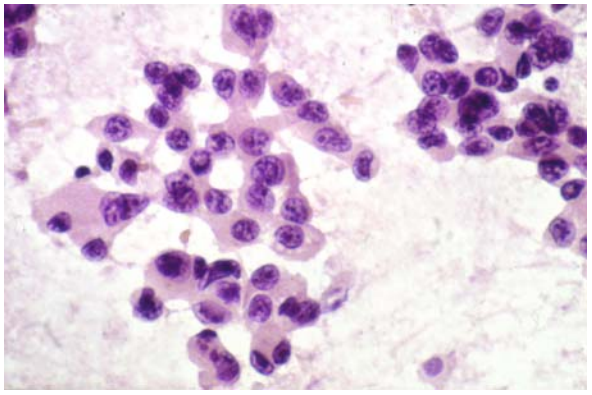

b

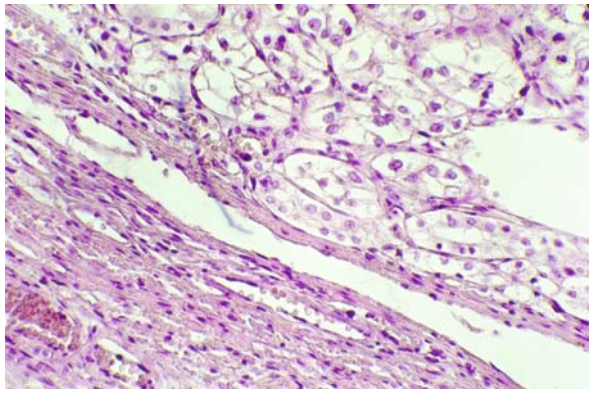

c

Fig. 16.37a-c. Ovarian metastasis in a 49-year-old woman which occurred 14 months after radical nephrectomy for renal cell carcinoma. **a** Macroscopic view of the right ovary shows a large ovarian mass with a yellowish cut surface and areas of necrosis and hemorrhage. **b** Photomicrograph shows the tumor cells with abundant pink cytoplasm and hyperchromatic nuclei with a focal glandular differentiation (hematoxylin and eosin stain; original magnification, ×400). **c** Photomicrograph shows neoplastic clear cell infiltrating the ovarian parenchyma (hematoxylin and eosin stain; original magnification, ×106). (Image courtesy of L. Insabato)

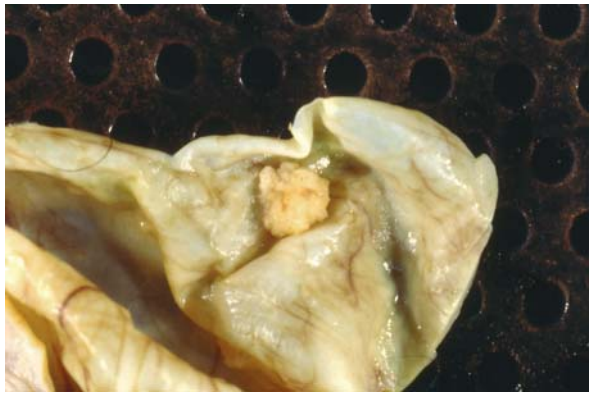

a

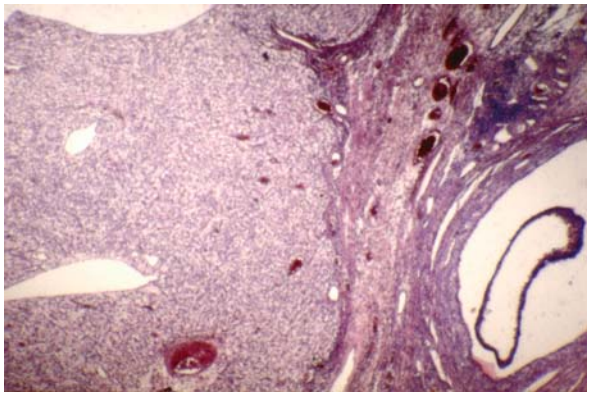

b

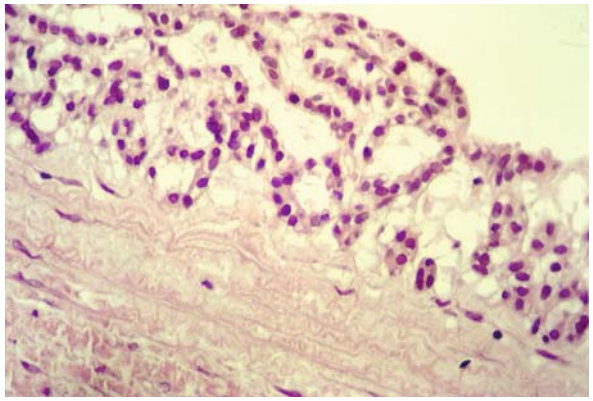

c

Fig. 16.38a-c. Ovarian cystic metastasis in a 17-year-old girl which occurred 2 years after radical nephrectomy for renal cell carcinoma. **a** Macroscopic view of the left ovary shows a metastatic small nodule on the ovarian cyst. **b** Photomicrograph shows papillary proliferation with pleomorphic and hyperchromatic nuclei (Hematoxylin and eosin stain; original magnification, ×106). **c** Photomicrograph of a different nodule shows a clear cell carcinoma with glandular pattern (Hematoxylin and eosin stain; original magnification, ×106). (Image courtesy of L. Insabato)

16.5 Lymph Node Metastases

The incidence of lymph node metastases in RCC varies from 14 to 30% (Johnsen and Hellsten 1997). The presence of regional lymph node metastases is an important predictor of multifocal distant metastases (Johnsen and Hellsten 1997) and hence carries a poor prognosis, with reported 5-year survival rates of 5–30% (Pantuck et al. 2003; Thrasher and Paulson 1993). The presence of regional lymph node metastases is associated with distant metastatic dissemination via the thoracic duct, mediastinal lymph nodes, and the left subclavian lymph node (Mignon and Mesurolle 2003). The traditional view that RCC involving "locoregional" lymph nodes is potentially curable by classic radical nephrectomy has very little evidence to support it (Pantuck et al. 2003; Russo 2003). Moreover, it is now known that regional lymph node metastasis confers immunotherapy resistance and a graver prognosis than pulmonary metastasis (Russo 2003).

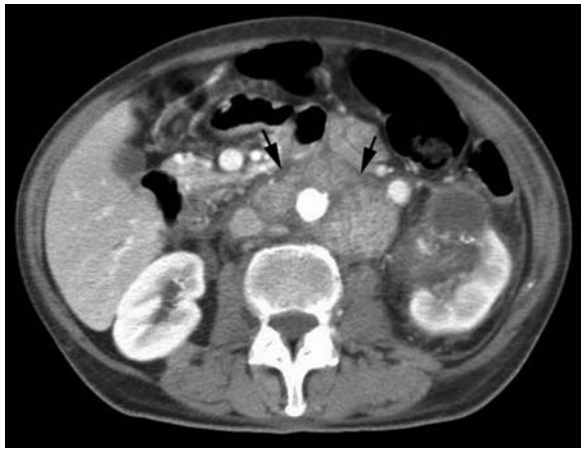

Fig. 16.39. Lymph node metastasis in 67-year-old woman synchronous with renal cell carcinoma. Axial contrast-enhanced CT scan shows large heterogeneous enhancing retroperitoneal and para-aortic lymph node mass (*arrows*) associated with a large heterogeneous hypodense anterior mass of the left kidney corresponding to cystic renal cell carcinoma.

Lymph nodes close to the renal vascular pedicle are the most frequently involved (Scatarige et al. 2001a). Para-aortic and retroperitoneal lymph nodes are also frequently involved (Figs. 16.3, 16.39, 16.40). In a large series by Saitoh et al. (1982), para-aortic and retroperitoneal lymph nodes were involved in 24–35% of patients. More advanced patterns of recurrence include mesenteric lymphadenopathy (Scatarige et al. 2001a). In fact, lymph nodes at any site may be involved (Fig. 16.41): neck and clavicle; hilus of lungs (Fig. 16.42); pancreas; hilus of liver; stomach (Fig. 16.43); axilla; and inguinal region (Saitoh et al. 1982; Savas et al. 1998; Yamashita et al. 2000). Involvement of mediastinal lymph nodes (Fig. 16.44) may result from retrograde extension through thoracic duct tributaries (Tartar et al. 1991), may be isolated (Merine and Fishman 1988; Yamashita et al. 2000), and may present as an anterior mass leading to confusion with more common tumors such as thymus, thyroid, or germ cell neoplasms, and lymphomas (Koc et al. 1999; Mattana et al. 1996).

Computed tomography is the examination of choice and shows that metastatic nodes may enhance (Fig. 16.45), particularly if the primary tumor is very

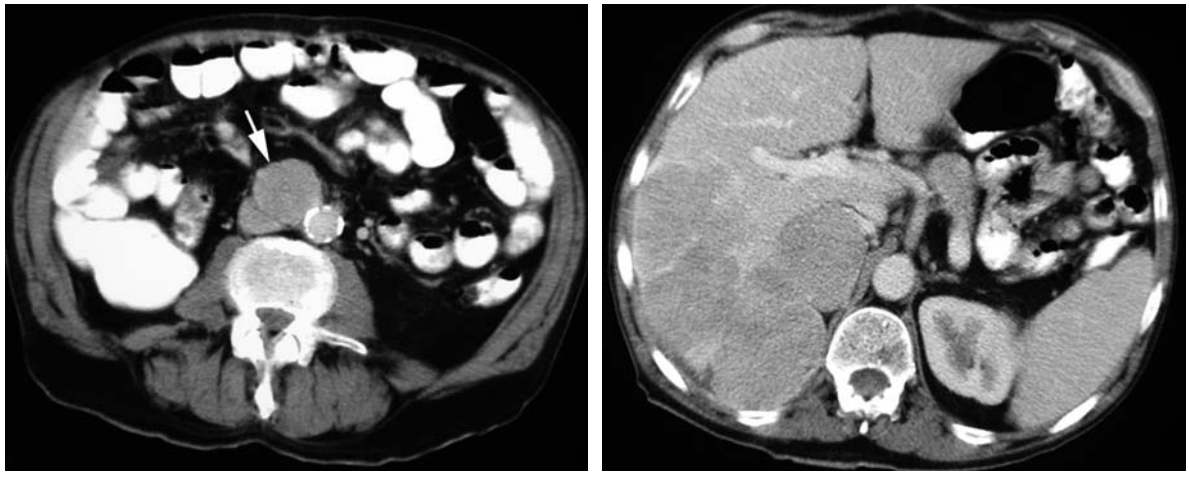

Fig. 16.40a,b. Lymph node and liver metastases in 73-year-old man who underwent right nephrectomy for renal cell carcinoma. **a** Axial contrast-enhanced CT scan shows interaortocaval lymph node enlargement (*arrow*). **b** Axial contrast-enhanced CT scan cephalad to **a** shows large confluent, slightly hypodense hepatic masses.

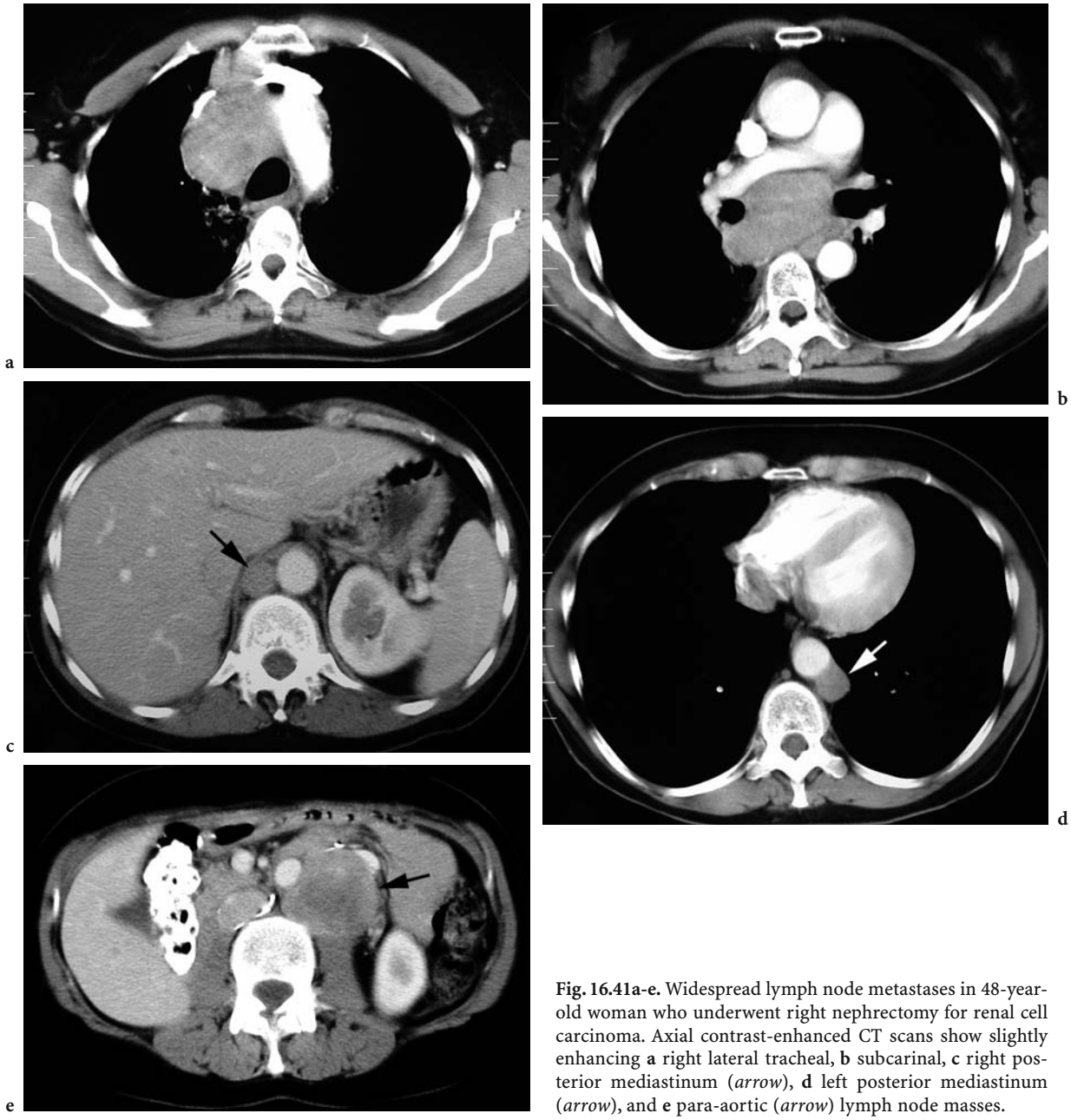

Fig. 16.41a-e. Widespread lymph node metastases in 48-year-old woman who underwent right nephrectomy for renal cell carcinoma. Axial contrast-enhanced CT scans show slightly enhancing **a** right lateral tracheal, **b** subcarinal, **c** right posterior mediastinum (*arrow*), **d** left posterior mediastinum (*arrow*), and **e** para-aortic (*arrow*) lymph node masses.

vascular (Yamashita et al. 2000). Nevertheless, in a study aiming to assess the predictive value of CT for the diagnosis of regional lymph node metastases, Studer et al. (1990) showed the enlargement of regional lymph nodes frequently may be caused by inflammatory changes, especially in the presence of tumor necrosis. They concluded that the radiological finding should not be interpreted as metastatic disease, unless it has been proved cytologically by fine-needle aspiration.

16.6 Central Nervous System Metastases

16.6.1 Brain

The reported incidence of brain metastasis is 2%. Only 2–10% of patients with a recurrence of RCC developed brain metastases (Janzen et al. 2003; Nussbaum et al. 1996; Seaman et al. 1995). Brain metastases are gen-

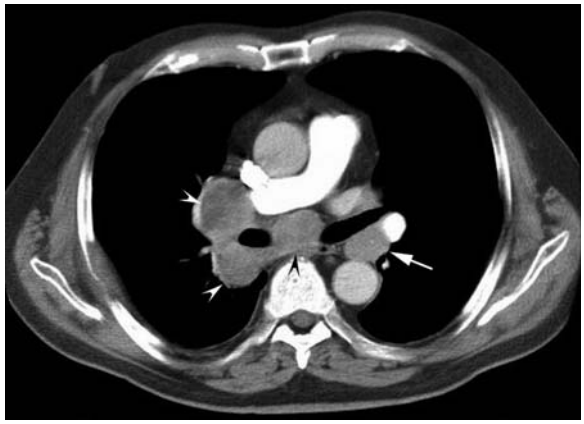

Fig. 16.42. Lymph node metastases in a 72-year-old man who underwent nephrectomy for renal cell carcinoma. Axial contrast-enhanced CT scan shows enlargement of right hilar bronchopulmonary (*white arrowheads*), subcarinal (*black arrowhead*), and para-aortic (*arrow*) lymph nodes.

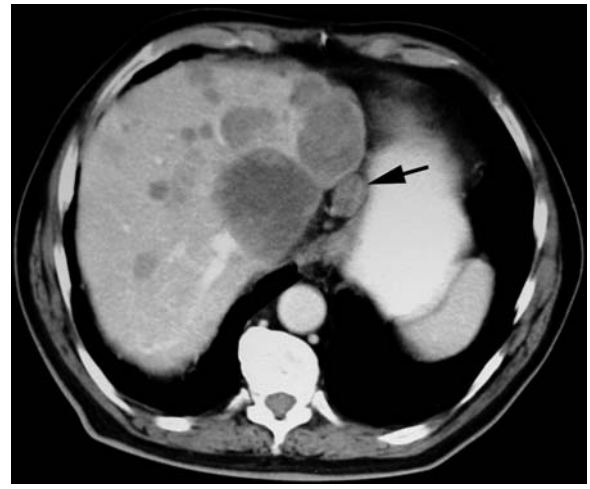

Fig. 16.43. Lymph node and liver metastases in 77-year-old man who underwent right nephrectomy for renal cell carcinoma. Axial contrast-enhanced CT scan shows enlargement of left gastric lymph node (*arrow*) and several hypodense liver masses of varying sizes.

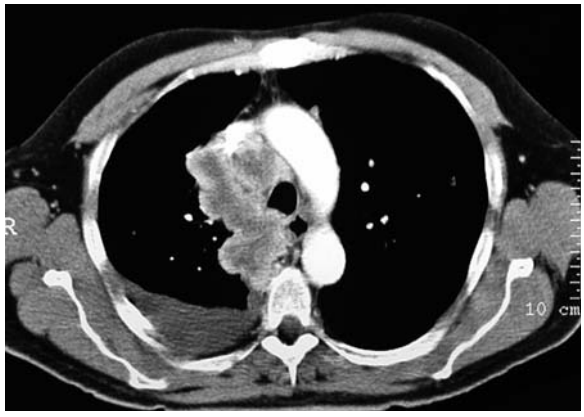

Fig. 16.44. Lymph node metastasis in a 63-year-old man who underwent nephrectomy for renal cell carcinoma. Axial contrast-enhanced CT scan shows large heterogeneous enhancing right mediastinal lymph node mass with mass effect on the trachea. There is also a right pleural effusion.

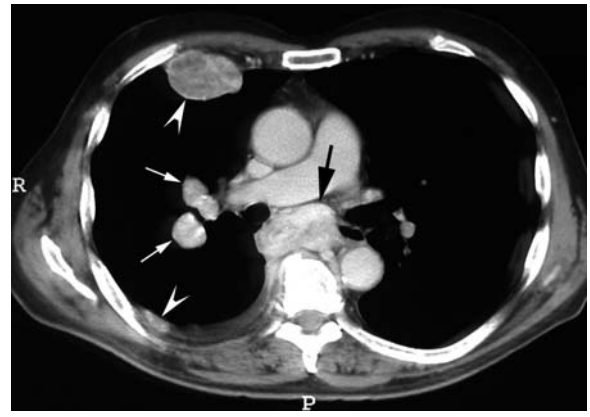

Fig. 16.45. Lymph node, lung, and pleural metastases in 76-year-old man who underwent nephrectomy for renal cell carcinoma. Axial contrast-enhanced CT scan shows strongly enhancing heterogeneous subcarinal lymphadenopathy (*black arrow*) and right pulmonary parahilar masses (*white arrows*). There are also two heterogeneously enhancing right pleural based masses (*arrowheads*) with pleural effusion.

erally believed to result from hematogenous spread of circulating tumor cells or frank tumor emboli. The sequence of events that initiates metastatic spread to the brain remains largely unknown (Klos and O'Neill 2004). The latency period is variable and can be as long as 18 years (Radley et al. 1993). The brain is rarely the sole site of metastasis (Ishikawa et al. 1990; Janzen et al. 2003). Resection of a solitary metastasis is associated with a significantly improved survival, although the survival time is short (Janzen et al. 2003). Spontaneous regression of cerebral metastases is a very rare event that may involve the brain alone (Guthbjartsson and Gislason 1995) or in association with other metastatic locations (Omland and Fossa 1989).

Clinically, brain metastases may present with focal or generalized symptoms. Headache is the most common symptom. Other symptoms include focal weakness, mental change, seizure, gait ataxia, sensory disturbance, and/or speech problems (Klos and O'Neill, 2004; Marshall et al. 1990). Unusual but characteristic clinical syndromes have

been described in patients with brain metastases, including sagittal sinus occlusion, subdural effusion, miliary metastases that produce a progressive confusional state, and diabetes insipidus (Klos and O'Neill 2004; Yokoyama et al. 1998;). Asymptomatic brain lesions are often seen in patients with metastatic RCC (Saidi et al. 1998; Seaman et al. 1995). This is especially true in the modern imaging era when more asymptomatic lesions are found with the aid of CT and MR imaging (Klos and O'Neill 2004; Seaman et al. 1995).

Surgical excision remains an important therapy for selected patients with large brain tumors. The best outcome after surgical resection is achieved in patients with a solitary, surgically accessible tumor and in patients without systemic disease (Hoshi et al. 2002; Vleeming et al. 1994). Whole-brain radiotherapy (WBRT) is another therapeutic alternative and is usually recommended for patients with multiple brain metastases (Klos and O'Neill 2004). Gamma-knife radiosurgery is an effective noninvasive modality of treatment. It is a stereotactically guided high-precision irradiation method focusing ionizing radiation within the target volume in a single-dose application. The metastases from kidney cancers are ideal targets because of their spherical shape and sharp margins. Gamma-knife radiosurgery offers high local control rate and improved quality of life and survival (Hoshi et al. 2002).

Magnetic resonance imaging is the imaging modality of choice for brain metastases because of its superior resolution over CT, especially in evaluating the posterior fossa (Klos and O'Neill 2004) and pituitary gland (Uchino et al. 1996; Yokoyama et al. 1998). Magnetic resonance imaging can detect a lesion as small as 1.9 mm (Klos and O'Neill 2004). For emergency evaluation of patients and because it is widely accessible, CT is especially helpful when clinical deterioration is rapid (Klos and O'Neill 2004).

Typically, the lesions are multiple, at the gray–white junction, have relatively smooth margins, are nodular enhancing lesions, and are tightly focused while surrounded by abundant vasogenic edema (Fig. 16.46; Destian et al. 1989; Klos and O'Neill 2004). Lesions are usually supratentorial but sometimes may be located in the posterior fossa (Fig. 16.47; Uchino et al. 1996). Nussbaum et al. (1996) reported 56% of patients with single brain metastases and 44% with multiple locations. When a solitary lesion is found on CT, MR imaging should be performed before surgical treatment is planned. Not only is management different than with multiple metastases, but so is the prognosis (Klos and O'Neill 2004). Lesions measuring less than 5 mm often have less surrounding edema (Chae et al. 2005; Klos and O'Neill 2004). All lesions show enhancement, including homogeneous, nearly homogeneous, or ring enhancement (Uchino et al. 1996). A cystic appearance is very rare (Ishikawa et al. 1990). Because of their hypervascularity, these lesions are sometimes hemorrhagic (Destian et al. 1989; Hodgson et al. 1994; Klos and O'Neill 2004). Intracranial brain metastases are typically intraaxial. Uncommon locations include extraaxial locations (Fig. 16.48), as reported in a 4-year-old boy with two large extraaxial brain metastases from clear cell sarcoma of the kidney (Park et al. 1997), and the choroid plexus with unilateral (Fig. 16.49) or exceedingly rarely bilateral involvement (Hillard et al. 2003). The pituitary gland may also be involved (Djimi et al. 2003; Koshiyama et al. 1992; Uchino et al. 1996; Yokoyama et al. 1998).

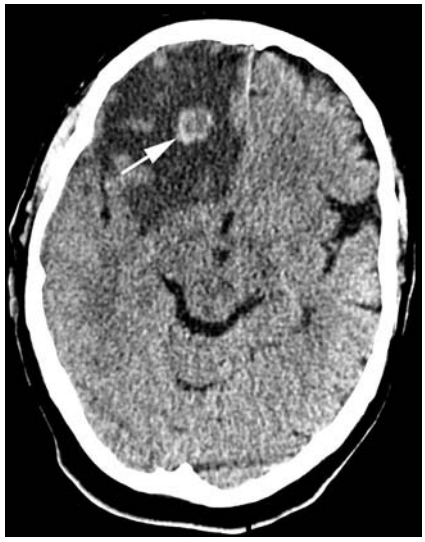

Fig. 16.46. Brain metastasis in a 74-year-old man who underwent nephrectomy for renal cell carcinoma. Axial contrast-enhanced CT scan shows a small right frontal annular lesion (*arrow*) at the gray–white junction surrounded by abundant vasogenic edema.

Recently developed imaging techniques, such as MR spectroscopy, SPECT technology, and increased contrast dose with delayed imaging, and the latest imaging techniques utilizing transfer of magnetization, dynamic contrast-enhanced MR imaging (Fig. 16.50), and PET, may offer improved diagnostic utility, but further studies are needed to identify whether these modalities will provide an appropriate and cost-effective advantage over current imaging techniques (Klos and O'Neill 2004; Kremer et al. 2003).

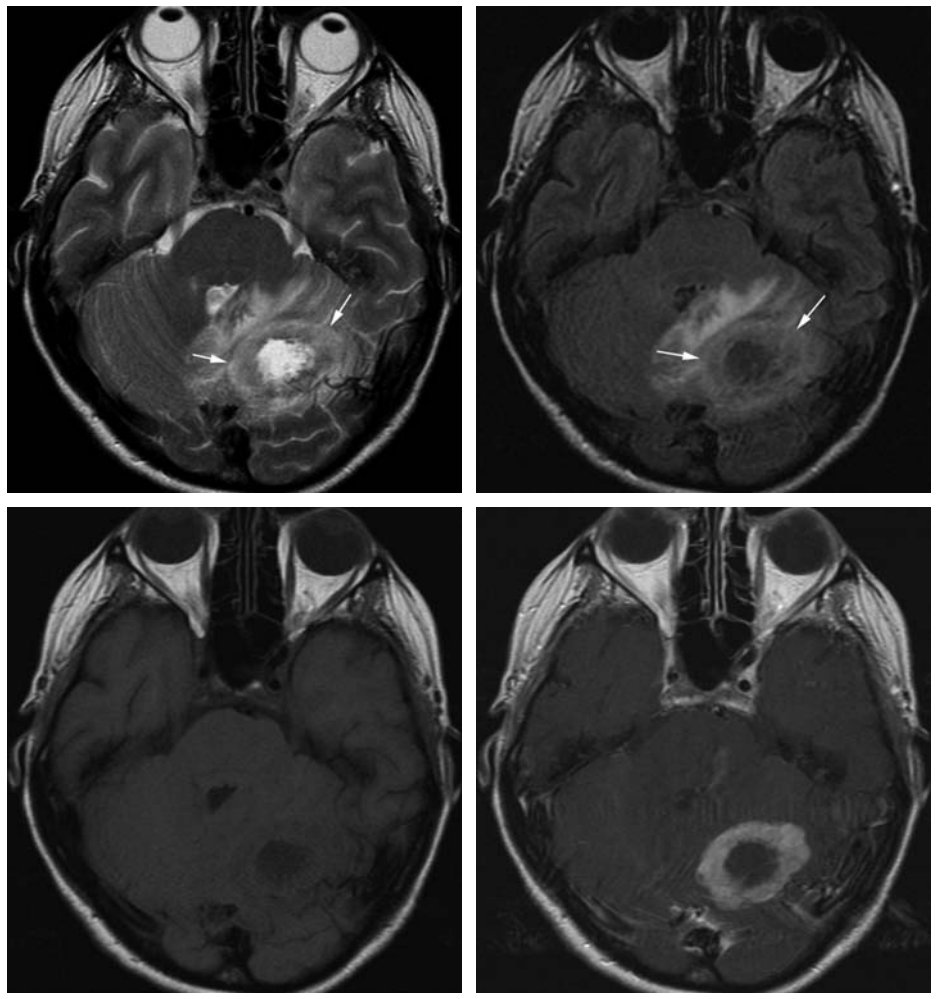

Fig. 16.47a-d. Unique cerebellar metastasis in a 46-year-old woman treated for renal cell carcinoma. Axial **a** T2-weighted and **b** fluid-attenuated inversion recovery (FLAIR) MR images show a large left cerebellar lobe lesion which has a slightly hyperintense thick peripheral ring (*arrow*) and is surrounded by hyperintense vasogenic edema with mass effect on the fourth ventricle. The frank central hyperintensity on T2-weighted and hypointensity on FLAIR images corresponds to necrosis. **c** Axial unenhanced T1-weighted MR image shows that the ring and edema are difficult to discern. Only the hypointense necrosis and mass effect on the fourth ventricle are obvious. **d** Axial contrast-enhanced T1-weighted MR image demonstrates a characteristic strong ring enhancement of the lesion. (Image courtesy of F. Lafitte)

16.6.2 Spinal Cord, Cauda Equina, and Epidural Space

Intramedullary spinal cord metastases are very rare and make up only 4–8.5% of central nervous system metastases. Clinical symptoms include progressive pain, autonomic dysfunction, and/or neurological deficits, e.g., Brown-Sequard syndrome (Fakih et al. 2001; Schijns et al. 2000). There is a rapid progression of neurological deficits and treatment is urgent (Schijns et al. 2000). Occasionally, patients present first with symptoms from spinal cord metastases that precede the detection of the primary RCC (Fakih et al. 2001; Schijns et al. 2000). On the other hand, most reported cases are associated with brain metastases. Treatment options include surgery as well as radiotherapy with or without chemotherapy (Fakih et al. 2001). Magnetic resonance imaging is very sensitive for the detection of intramedullary metastases. The MR imaging characteristics of intramedullary metastases are the presence of peritumoral edema and contrast enhancement of the lesion. T2-weighted sequences principally show hyperintensity due to edema, and when normal may exclude intramedullary metastasis. Administration of contrast improves sensitivity and makes the MR

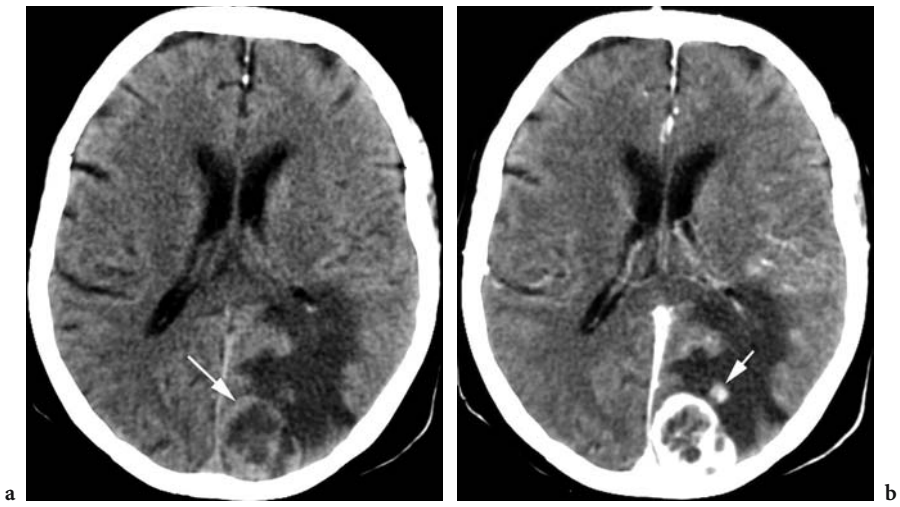

Fig. 16.48a,b. Brain metastases in 72-year-old man who underwent left nephrectomy for renal cell carcinoma. **a** Axial unenhanced CT scan shows a superficially located parasagittal left occipital heterogeneous large mass with broad base (*arrow*) near the vertex and surrounded by abundant vasogenic edema. **b** Axial contrast-enhanced CT scan at the same level shows the mass heterogeneously enhancing and also discloses an additional small rounded enhancing lesion (*arrow*) within the same vasogenic edema.

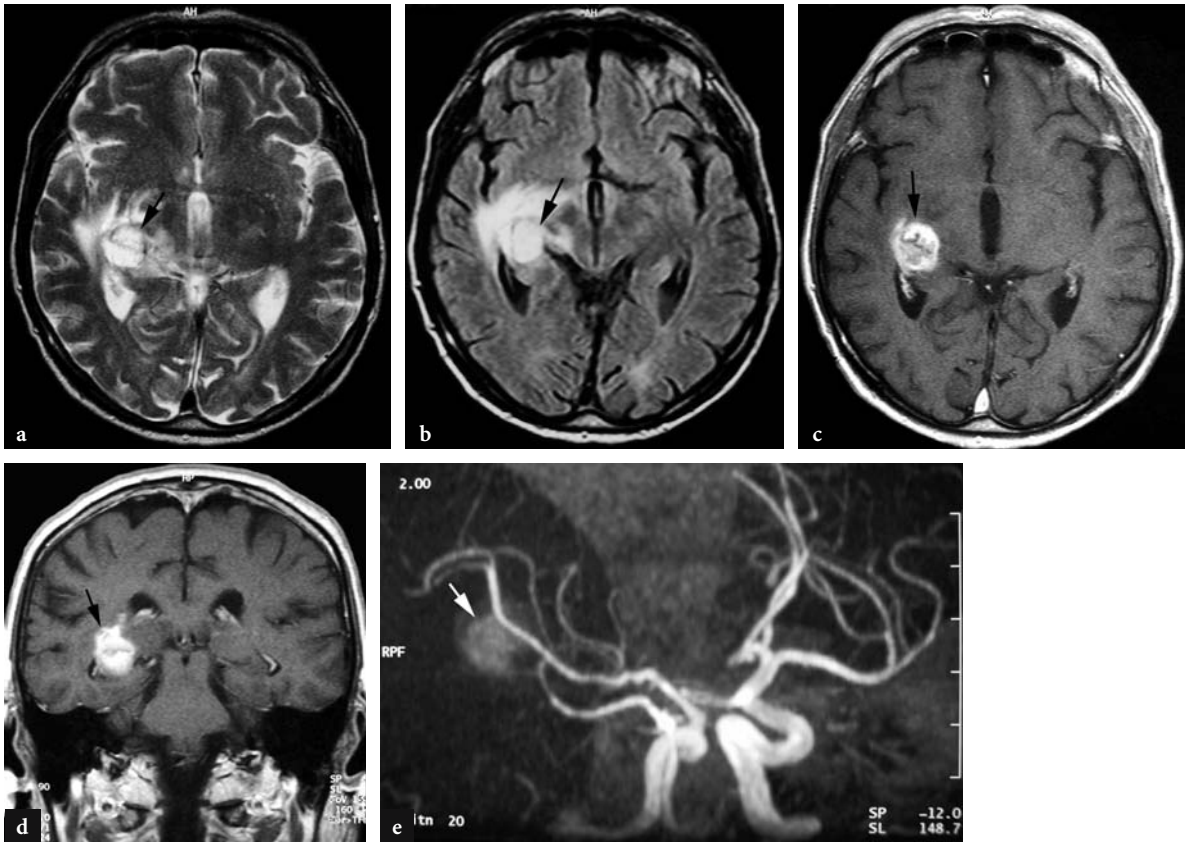

Fig. 16.49a-e. Brain metastases in a 72-year-old man who underwent nephrectomy for renal cell carcinoma. Axial **a** T2-weighted and **b** FLAIR MR images show a hyperintense round lesion within the right trigone (*arrow*) and surrounded by a vasogenic edema. **c** Axial and **d** coronal contrast-enhanced T1-weighted MR images demonstrate a heterogeneously enhancing mass of the choroid plexus of the trigone (*arrow*). **e** Cerebral MR angiogram reveals tumor blush in region of the right trigone (*arrow*).

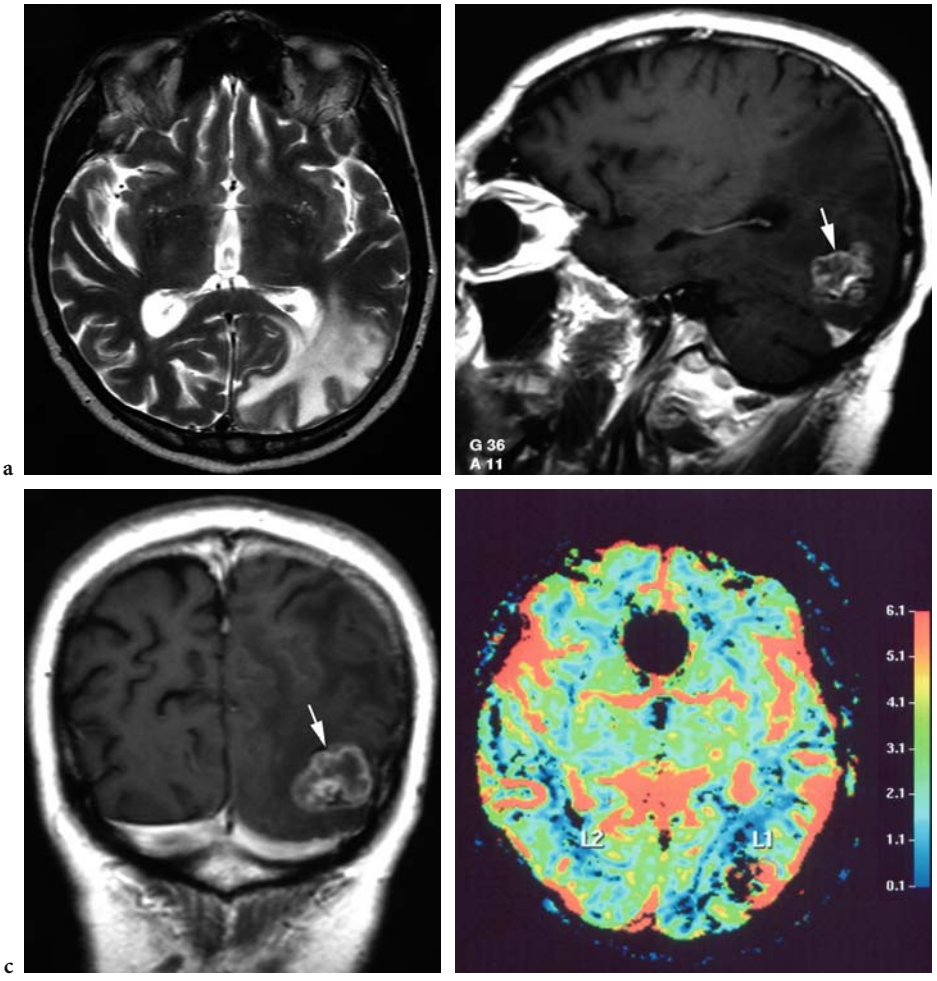

Fig. 16.50a-e. Brain metastasis in a 68-year-old man with renal cell carcinoma. **a** Axial T2-weighted MR image shows an extensive vasogenic edema around the trigone of the left lateral ventricle. **b** Sagittal and **c** coronal contrast-enhanced T1-weighted images show a heterogeneous ring enhancement (*arrow*) with central necrosis. There is an extensive hypointense surrounding edema. **d** Axial cerebral blood volume (CBV) map image of the metastasis shows a peripheral hypervascular ring with central necrosis. **e** Time–concentration curves show a much higher CBV (8.6) in the tumor than in the contralateral white matter [1.3, maximum relative CBV (rCBVmax) of 6.61]. (Image courtesy of S. Grand)

imaging more specific in distinguishing between edema and the tumor which is generally well circumscribed (Fig. 16.51; Fakih et al. 2001; Schijns et al. 2000).

Cauda equina metastases from renal cancer are exceedingly rare and only a few cases have been published (Takada et al. 2003; Maxwell et al. 1999). Clinical symptoms include characteristic cramping pain provoked by light percussion on the lumbar spine, becoming severe when sleeping in the flexion or sitting position (Takada et al. 2003), or lower back pain radiating to both legs without sensorial or motor deficit (Maxwell et al. 1999). Magnetic resonance imaging is a useful and sensi-

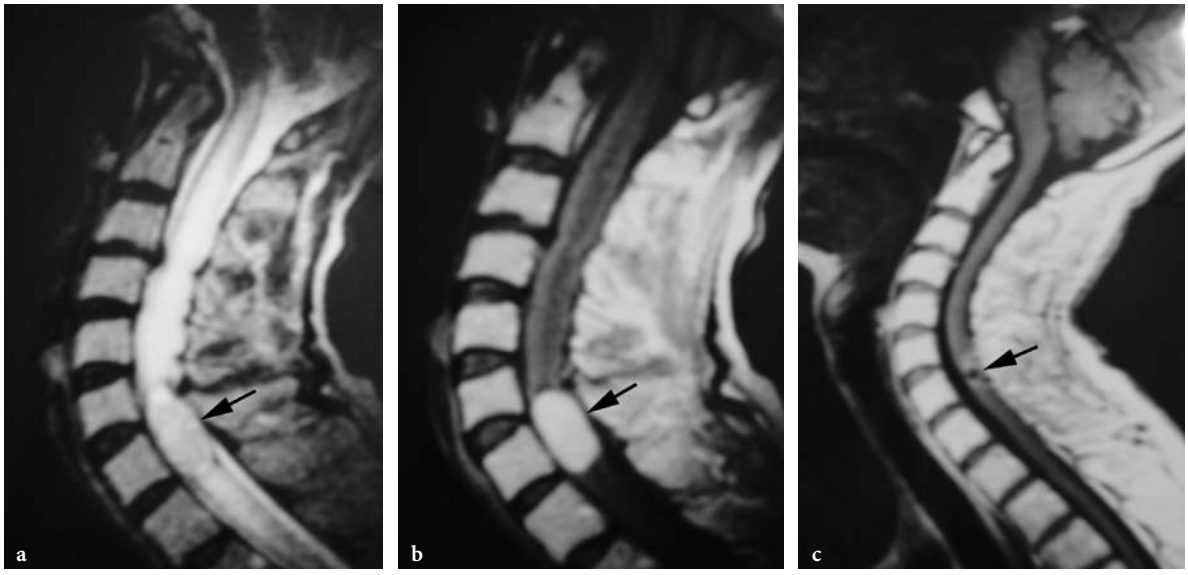

Fig. 16.51a-c. Spinal cord metastasis as a first manifestation of renal cell carcinoma in a 70-year-old woman who developed Brown-Sequard syndrome within 6 weeks. **a** Sagittal T2-weighted MR image of the cervical spine demonstrates a solitary lesion (*arrow*) at the level of C7 isointense to the spinal cord, but slightly bulging its contours. The hyperintense areas above and below the lesion correspond to edema. **b** Sagittal contrast-enhanced T1-weighted MR image displays a clear enhancement of the well-demarcated intramedullary lesion (*arrow*). The edema is now hypointense but less so than the cerebrospinal fluid. **c** Sagittal contrast-enhanced T1-weighted MR image obtained 6 weeks after surgery shows surgical sequela at the site of the tumor (*arrow*), which has been completely removed, and the complete disappearance of edema. (Image courtesy of O.E.M. Schijns)

tive but less specific tool for detecting cauda equine intradural metastases. It shows various appearance patterns and intensities, because the lesion may contain necrotic tissues and/or old hemorrhage. Administration of contrast media is mandatory to improve tumor conspicuity (Fig. 16.52; Takada et al. 2003).

Metastasis to the epidural space is relatively uncommon but has been described in several cancers including kidney cancer (Trufflandier et al. 2002). Although suspicion of epidural involvement is based on progressive pain with axial or radicular distribution, early symptoms are often nonspecific. Imaging diagnosis of epidural compression is clinically important because early treatment of spinal epidural metastasis improves patient survival and function (Fig. 16.53). A complete study of the spine with MR imaging has been shown to be highly sensitive and specific for detection of epidural metastases and incomparable for the diagnosis of cord compression (Kim et al. 2000). A case report using PET/CT in an asymptomatic patient showed promising results in the diagnosis of epidural involvement; however, the place of PET/CT in the management of epidural involvement has yet to be defined (Fig. 16.54; Jadvar et al. 2004).

16.7 Head and Neck Metastases

Metastases of RCC to the head and neck region are rare; however, RCC is one of the most common infraclavicular primary tumors to metastasize to the nose and paranasal sinuses (Janzen et al. 2003; Navarro et al. 2000; Simo et al. 2000). These metastases are usually vascular and may either precede the diagnosis of the primary renal neoplasm or occur many years after treatment of the primary tumor (Som et al. 1987). Individual case reports suggest that surgical resection of solitary distant metastases can improve survival (Janzen et al. 2003; Navarro et al. 2000).

16.7.1 Parotid Gland

Renal cell carcinoma metastasizing to the parotid gland is extremely rare (Adil et al. 1999). Parotid metastasis may be the first clinical sign of the RCC (Coppa and Oszczakiewicz 1990; Park and Hlivko 2002). The most common presenting complaint is parotid mass; pain and tenderness occur

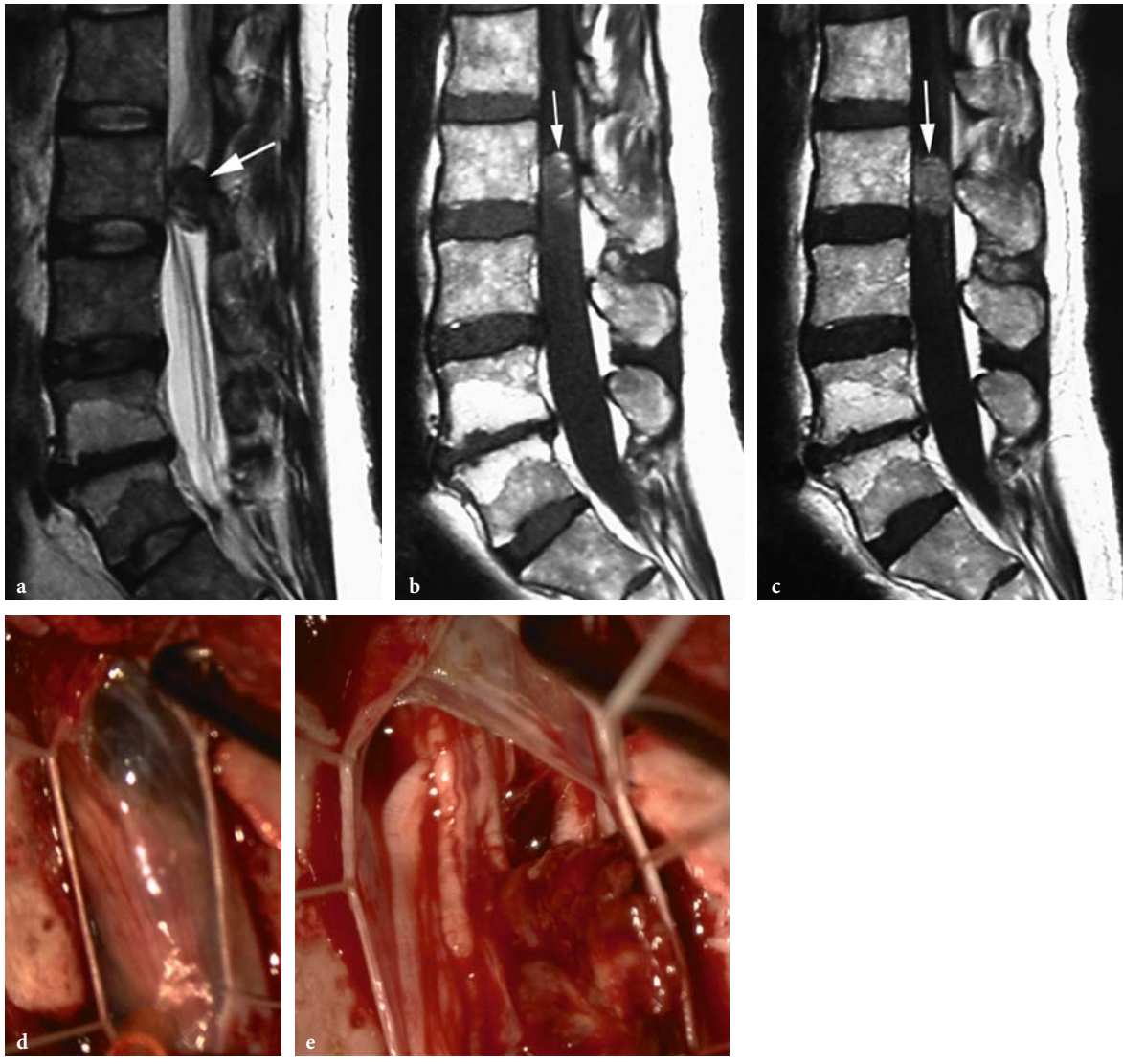

Fig. 16.52a-e. Cauda equina intradural metastasis from renal cell carcinoma in a 61-year-old man with a 10-month history of worsening lower back pain that radiated to both legs. **a** Sagittal spin-echo T2-weighted MR image shows intradural hypointense lesion (*arrow*) involving the cauda equina at the level of L2. **b** Sagittal unenhanced T1-weighted MR image shows small heterogeneous hyperintense areas within the ill-defined tumoral lesion (*arrow*). **c** Sagittal contrast-enhanced T1-weighted MR image shows a slight but homogeneous enhancement of the lesion (*arrow*) which appears more conspicuous. Intraoperative photographs **d** before and **e** after dural opening clearly show brown necrotic encapsulated tumor, which displays several nerves that run directly to the tumor. Macroscopically, the tumor contains old hemorrhagic and necrotic tissue corresponding to the imaging findings. (Image courtesy of M. Doita)

rarely (Park and Hlivko 2002). Usually, parotid metastasis presents as a solitary mass measuring 1.0–15.0 cm (Park and Hlivko 2002). Bilateral involvement of the parotids has been rarely reported and can be synchronous (Ravi et al. 1992) or metachronous (Li et al. 2001). Fine-needle-aspiration biopsy with immunohistochemical studies can provide crucial information, since the diagnosis of clear cell carcinoma of the parotid represents a challenge at the microscopic level as well (Som et al. 1987; Park and Hlivko 2002). Parotidectomy with facial nerve preservation should be considered the therapy of choice for a solitary parotid metastasis (Park and Hlivko 2002).

Ultrasound shows a well-circumscribed hypoechoic mass at the parotid gland (Li et al. 2001). Computed tomography demonstrates homogeneous enhancement (Park and Hlivko 2002), or it may be heterogeneous due to central necrosis of the parotid mass (Li et al. 2001).

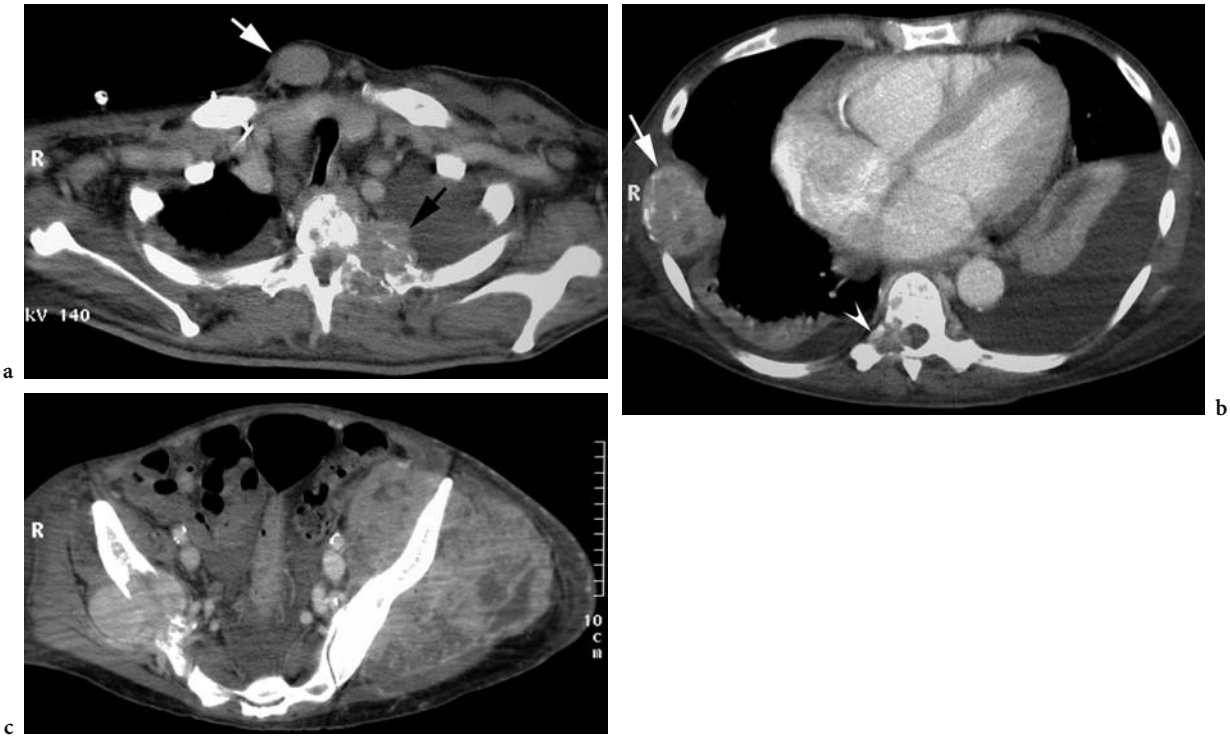

Fig. 16.53a-c. Epidural, chest wall, bone, and subcutaneous metastases in a 55-year-old man who underwent right nephrectomy for renal cell carcinoma. **a** Axial contrast-enhanced CT scan shows a large left paravertebral enhancing lytic lesion of upper thoracic vertebra (*black arrow*) which extends into the spinal canal with anterior and left epidural involvement and spinal cord compression. There is also an oval subcutaneous mass (*white arrow*) in front of the thyroid gland and bilateral pleural effusion. **b** Axial contrast-enhanced CT scan caudad to **a** shows a second lower thoracic right paravertebral lytic lesion (*arrowhead*) with extension to the spinal canal and right epidural involvement. There is a lateral chest wall heterogeneous mass (*arrow*) with rib lysis. **c** Axial contrast-enhanced CT scan of the pelvis shows large heterogeneous enhancing lytic masses involving both ilia.

16.7.2 Eye and Adnexa

Ocular metastases from RCC involve the iris, ciliary body, choroid, eyelid, orbit (Haimovici et al. 1997; Kindermann et al. 1981; Ware et al. 1999), and extraocular muscles (Slamovits and Burde 1988). Ocular metastases may rarely be the initial presenting sign of RCC (Haimovici et al. 1997).

Orbital metastasis from RCC is rare (Kindermann et al. 1981). Clinically, it is not specific and can appear like any other space-occupying lesion in the orbit with signs of exophthalmia, hyperemia of the conjunctiva, diplopia, or as a palpable mass (Kindermann et al. 1981; Schmidt et al. 1994). Among metastatic orbital carcinomas, RCC may be unique in producing pulsating exophthalmia due to its vascularity (Kindermann et al. 1981). In this respect, orbital metastasis from RCC can be confused with orbital hemangiomas (Kindermann et al. 1981). Because an orbital metastasis from renal carcinoma may present as a well-circumscribed, pseudoencapsulated retrobulbar lesion, it can be confused with an orbital benign lesion (Bersani et al. 1994). Ultrasound and CT usually show a well-delineated mass that is often hypervascular and separate from the globe (Fig. 16.55; Kindermann et al. 1981; Schmidt et al. 1994).

Choroidal metastases from RCC are uncommon. The choroidal involvement may be the sole or the initial manifestation of metastatic disease. Clinically, signs are variable (Haimovici et al. 1997) and defective vision may be encountered (Hammad et al. 2003; Srinivasan and Gray 2003). Choroidal metastases may cause diagnostic confusion with primary choroidal melanoma (Kindermann et al. 1981). The diagnostic efficacy of fine-needle-aspiration biopsy appears to be somewhat dependent on technical factors and the availability of an experienced cytopathologist (Haimovici et al. 1997). Choroidal metastases respond well to external beam or proton irradiation (Haimovici et al. 1997). They may also spontaneously regress after removal of the

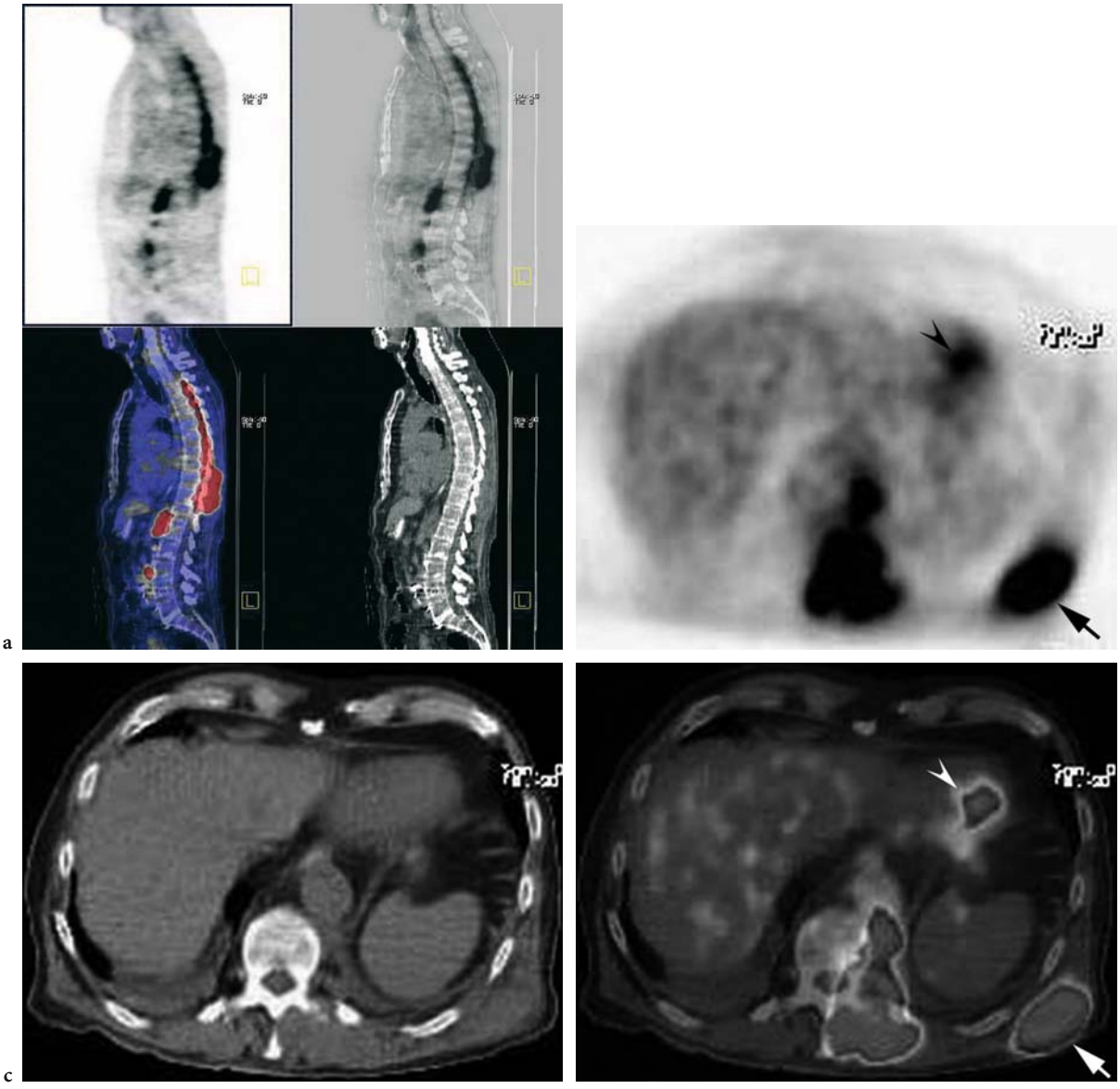

Fig. 16.54a-d. Epidural and muscle metastases in an 82-year-old man with a history of transitional cell carcinoma treated with left nephrectomy. **a** Sagittal PET/CT images demonstrate intense hypermetabolism along the distribution of the epidural space from T1 to T10 (*upper left panel:* FDG-PET alone; *upper right panel:* combined more PET and less CT; *lower left panel:* combined less PET and more CT; *lower right panel:* CT alone). Axial **b** PET, **c** CT, and **d** fused PET/CT images show the disease at the lower thoracic level, and also disclose disease in the left latissimus dorsi muscle (*arrow*). Note the normal anterior uptake of the heart (*arrowhead*). A subsequent MR imaging of the thoracic spine (not shown) confirmed the epidural disease without evidence for metastatic cord compression. (Image courtesy of H. Jadvar)

primary tumor (Hammad et al. 2003). The ophthalmoscopic, fluorescein angiographic, and US characteristics are diverse and nonspecific (Haimovici et al. 1997). Examination of the fundus shows nonpigmented (Haimovici et al. 1997) or lightly pigmented (i.e., discrete yellowish or reddish-orange) subretinal masses (Srinivasan and Gray 2003). Fluorescein angiography shows variable fluorescein-staining tumors (Haimovici et al. 1997). Ultrasound may show variable reflectivity, and a regular, or less frequently slightly irregular, internal structure (Haimovici et al. 1997), and often a marked vascularity (Fig. 16.56; Hammad et al. 2003).

Metastases to the extraocular muscles are exceedingly rare. They may be bilateral. When they appear as the initial manifestation of metastatic RCC, the metastases can be difficult to distinguish from other pathologies common to the site. Imaging modalities,

Fig. 16.55a-c. Orbital metastasis in a 58-year-old man with renal cell carcinoma. **a** Axial contrast-enhanced CT scan shows a large mass occupying the right orbit that enhances dramatically. There is central necrosis. This mass extends into the right nasal cavity and lateral mass of the ethmoid through bony destruction of the lateral wall of the right nasal cavity. **b** The same slice as **a** at bone window shows an involvement of the greater wing of sphenoidal bone and destruction of the frontal process of the zygomatic bone (*arrow*). **c** Axial contrast-enhanced CT scan cephalad to **a** shows marked right eye proptosis by the large mass.

such as US, CT, and MR imaging, may show bilateral diffuse enlargement of the extraocular muscles (Slamovits and Burde 1988).

Iris and conjunctival involvement are very rare. The involved iris appears fleshy and vascular and the conjunctival lesion appears as a highly vascular nodule. Iridocyclectomy and excision of the conjunctival nodule are considered the treatment of choice (Ware et al. 1999).

16.7.3 Nose and Sinuses

Metastases to the nose and paranasal sinuses are rare; however, RCC is the most frequent infraclavicular primary tumor to metastasize to the nose and paranasal sinuses. Clinically, it is seen as an intranasal mass causing nasal obstruction, recurrent epistaxis, facial pain, and induration (Simo et al. 2000; Szymanski et al. 2004). Orbital symptoms, such as diplopia and proptosis, are not rare. An orbital mass may be seen and has been described once as the presenting symptom of a metastasis to the paranasal sinuses (Homer and Jones 1995). The final diagnosis usually depends on the clinical history and the histology of the lesion. This metastasis is assumed to have a very poor prognosis. Nevertheless, recent publications show that these tumors seem to respond to high-dose radiation and when solitary can be successfully treated surgically (Simo et al. 2000).

On imaging, appearances, although suggestive of malignancy, are usually nonspecific. Renal metastases to the sinusal cavities have an appearance similar to that of melanoma, extramedullary plasmacytoma, esthesioneuroblastoma, meningioma, other vascular metastases (i.e., thyroid, adrenal), lymphoma, and the primary malignant lesions (i.e., nasopharyngeal carcinoma, chordoma) at this site. The strong enhancement, soft tissue, and bone destruction, and lack of tumoral calcification, should suggest kidney cancer metastasis as the diagnosis (Som et al. 1987). Angiography usually shows a highly

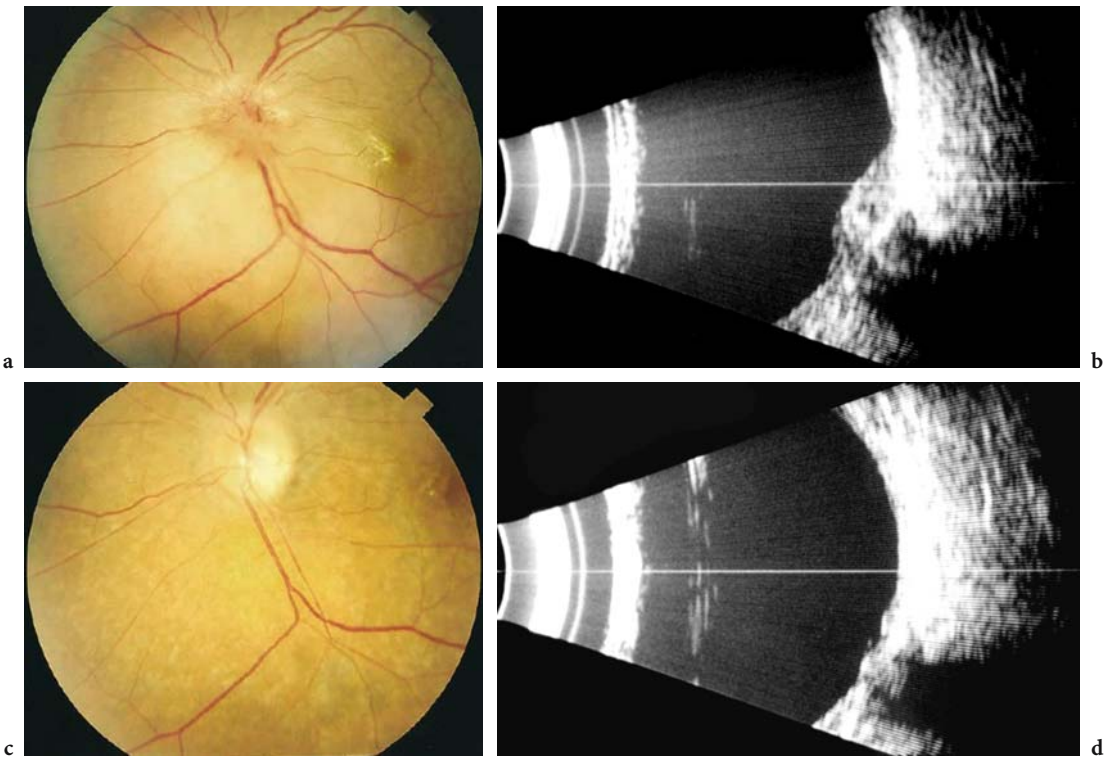

Fig. 16.56a-d. Spontaneous regression of choroidal metastasis in a 48-year-old woman 6 weeks after nephrectomy for renal cell carcinoma. **a** Fundus photograph of the left eye shows elevated choroidal lesion corresponding to the metastasis with swollen optic disc and adjacent exudative retinal detachment. **b** Longitudinal US image demonstrates choroidal lesion and retinal detachment. **c** Fundus photograph of the left eye performed 6 weeks after nephrectomy shows resolution of both optic disk swelling and retinal detachment. **d** Longitudinal US image performed at the same time shows no evidence of residual metastasis from renal cell carcinoma. (Image courtesy of W.A.J. VAN HEUVEN)

vascular mass. Computed tomography is thought to be the radiological investigation of choice in assessing the extent of metastatic lesions, especially to the bone. Magnetic resonance imaging is very helpful in precisely assessing tumoral extension, especially into the brain (Fig. 16.57), and in assessing residual disease after radiotherapy (SIMO et al. 2000).

16.7.4 Tongue

Lingual metastasis is extremely rare, and no more than 20 cases have been reported in the literature (TOMITA et al. 1998). Possible routes of metastasis to the tongue include the systemic circulation, the venous circulation, and the lymphatic circulation (OKABE et al. 1992). Metastasis to the tongue may be interpreted as a manifestation of widespread metastatic disease. Most of the tongue metastases are located in the basal region. This may be due to richer vascular supply, or to the relative immobility of this area (OKABE et al. 1992). Prognosis is poor, and treatment is mainly palliative.

Magnetic resonance imaging is the best imaging modality for the diagnosis and may demonstrate a mass within the tongue with enhancement after contrast intravenous administration (TOMITA et al. 1998).

16.7.5 Thyroid Gland

The thyroid gland is the most common site in the head and neck of metastases from kidney cancers (SOM et al. 1987), and RCC is the most common neoplasm to metastasize to the thyroid gland (HEFFESS et al. 2002). Nonetheless, RCC metastasis to the thyroid gland is a rare event, although it must be considered in the differential diagnosis of any thyroid gland clear cell neoplasm (DAL FABBRO et al. 1987; GIUFFRIDA et al. 2003; HEFFESS et al. 2002). The tumor generally affects a single lobe as a solitary mass measuring 1.0–15.0 cm (BENOIT et

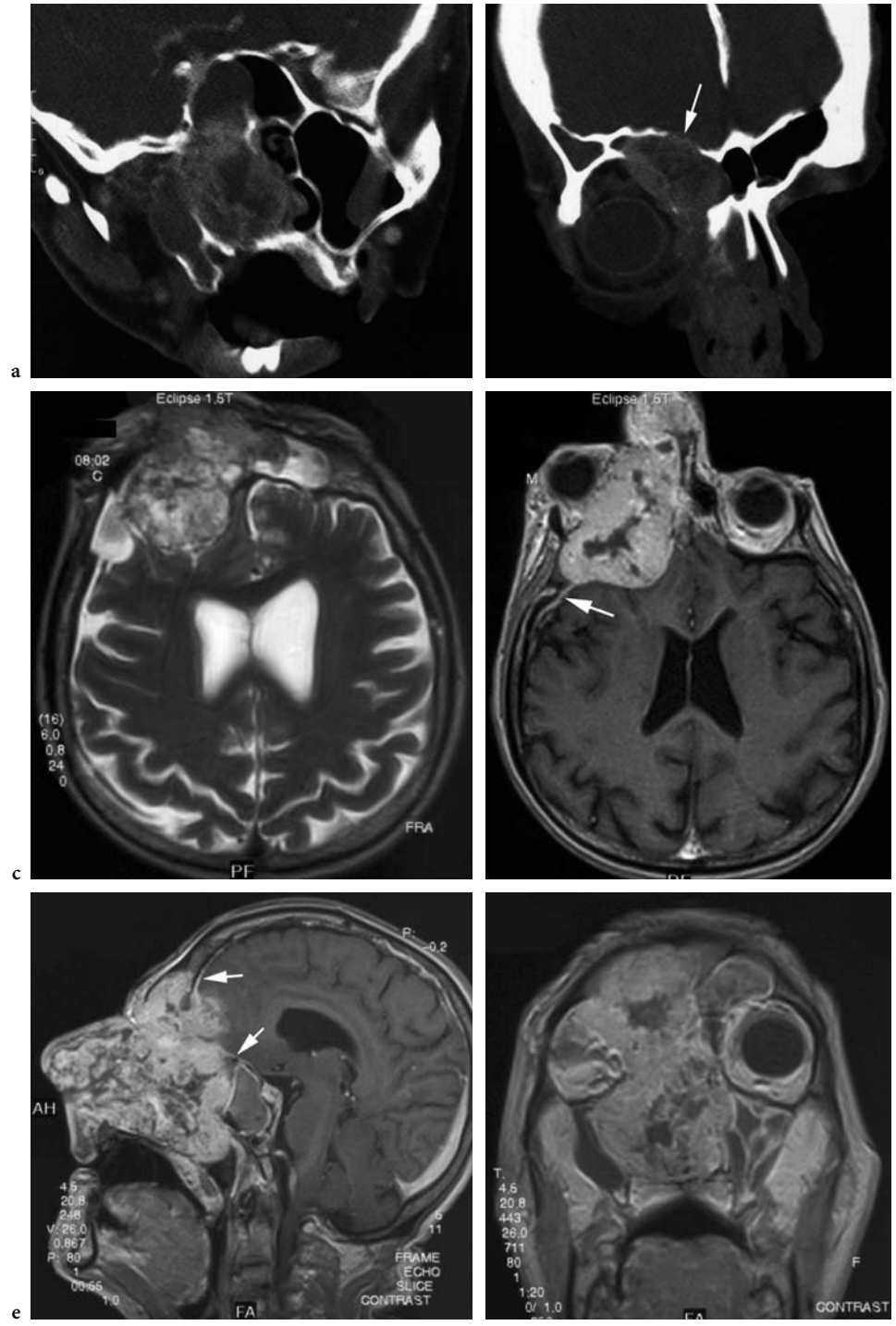

Fig. 16.57a-f. Nasal and paranasal sinus metastases in a 69-year-man concomitant to renal cell carcinoma of the left kidney. **a** Coronal oblique CT scan shows a large soft tissue mass occupying the right maxillary sinus, the right ethmoid cells, the sphenoidal sinus, and the lateral wall of the right nasal cavity, with extensive destruction of nasosinusal (bone) septum. **b** Coronal oblique CT scan anterior to **a** shows an extension of the tumoral mass into the right orbit and the frontal sinus with intracranial extension (*arrow*) through bony destruction of the upper wall of the frontal sinus. **c** Axial T2-weighted MR image shows the heterogeneous hyperintense mass, strongly enhancing after **d** contrast administration on axial T1-weighted image. There is central tumoral necrosis and marked right-eye proptosis. A dural tail enhancement (*arrow*) is also observed, probably due to meningeal involvement. **e** Sagittal and **f** coronal contrast-enhanced T1-weighted MR images demonstrate the extensive involvement of the nose and paranasal sinuses and confirms the meningeal involvement (*arrows*) as well. (Image courtesy of M. Szymanski)

al. 2004; Heffess et al. 2002; Hudson et al. 1991). Occasionally, the disease may be multifocal or bilateral (Heffess et al. 2002). A metastatic tumor in the thyroid could be the initial presentation of renal carcinoma (Benoit et al. 2004; Dal Fabbro et al. 1987; Heffess et al. 2002). Macroscopically, masses in the thyroid gland are well circumscribed, encapsulated, lobulated, and soft to partially necrotic (Heffess et al. 2002). The true metastatic nature of the tumor is recognized only after tumor sampling with pathological assessment; therefore, all patients with a solitary thyroid mass require a fine-needle-aspiration biopsy or a core-needle biopsy of the mass. Architectural, cytological, histological, histochemical, and immunohistochemical features are sufficiently distinctive to allow differentiation between primary neoplasm and metastatic RCC (Giuffrida et al. 2003; Heffess et al. 2002; May et al. 2003). Importantly, the differentiation between follicular carcinoma of the thyroid and metastasis is rendered possible by a combination of TTF-1, thyroglobulin, and CD 10 (Fig. 16.58; May et al. 2003), whereas clear cell carcinoma of the thyroid and metastasis can be distinguished by PAS staining (Dal Fabbro et al. 1987). Surgical treatment of a metastatic thyroid gland may prolong survival (Benoit et al. 2004; Heffess et al. 2002; May et al. 2003). This is particularly true with solitary metastases because of an unusually good prognosis (Heffess et al. 2002; May et al. 2003).

Imaging is not specific since both primary and secondary thyroid neoplasms have the same radiological appearance (Fig. 16.59). Ultrasound shows a heterogeneous hypoechoic mass. Radioiodine scintigraphy very often shows a "cold" nodule (Heffess et al. 2002).

16.8 Skeletal Muscle and Diaphragmatic Metastases

Skeletal muscle metastases from RCC are extremely rare (Schatteman et al. 2002); most are asymptomatic and occur in patients with advanced disease (Munk et al. 1992; Pretorius and Fishman 2000) but may occasionally be associated with pain (Pretorius and Fishman, 2000) or paraneoplastic syndrome such as erythrocytosis (Alimonti et al. 2003). They may be isolated (Scatarige et al. 2001a) or they may be the initial manifestation of the renal tumor, making the differentiation between primary soft tissue tumor and renal metastasis difficult (Schatteman et al. 2002). The latency period can be as long as 16 years (Nabeyama et al. 2001). The erector spinae muscle is a favored site for skeletal muscle metastases (Fig. 16.28; Scatarige et al. 2001a), but other sites of involvement include deltoid (Fig. 16.60; Alimonti et al. 2003; Schatteman et al. 2002), gluteals (Fig. 16.28; Pretorius and Fishman 2000), trapezius (Munk et al. 1992), triceps brachii, biceps brachii, rectus abdominis (Fig. 16.61), and vastus lateralis (Nabeyama et al. 2001).

On imaging, renal metastases to the skeletal muscle tend to enhance uniformly (Scatarige et al. 2001a; Schatteman et al. 2002) and usually have regular contours (Pretorius and Fishman, 2000) or sometimes lobulated contours (Munk et al. 1992). Magnetic resonance imaging is the gold standard because of its superior intrinsic soft tissue contrast (Pretorius and Fishman 2000). Magnetic resonance imaging also accurately shows the boundaries of the metastasis with the surrounding normal tissues (Fig. 16.62; Schatteman et al. 2002). In general, the metastasis is hyperintense on T2-weighted images, hypointense on T1-weighted images, and enhances homogeneously after contrast administration (Munk et al. 1992). If hemorrhagic, the metastasis would appear slightly hyperintense on unenhanced T1-weighted images (Nabeyama et al. 2001). Magnetic resonance imaging has another advantage over CT with its ability to reveal changes suggestive of edema in the surrounding tissues, visible as a hyperintensity on T2-weighted images (Munk et al. 1992; Pretorius and Fishman 2000).

Diaphragmatic metastases are exceedingly rare. Ultrasound may occasionally show a diaphragmatic mass (Pilecki et al. 2002), but CT, and more efficiently MR imaging, accurately localizes the involvement to the diaphragm.

16.9 Cutaneous Metastases

Cutaneous metastases are rare and occasionally involve the initial surgical nephrectomy incision. Their incidence is reported to be 2.8% of which 20% were diagnosed at presentation. The majority of these lesions were multiple. None of the patients experienced a recurrence 10 or more years after initial surgery (Newmark et al. 1994). Cutaneous metastases to the nephrectomy scar respond favorably to surgical excision (Newmark et al. 1994).

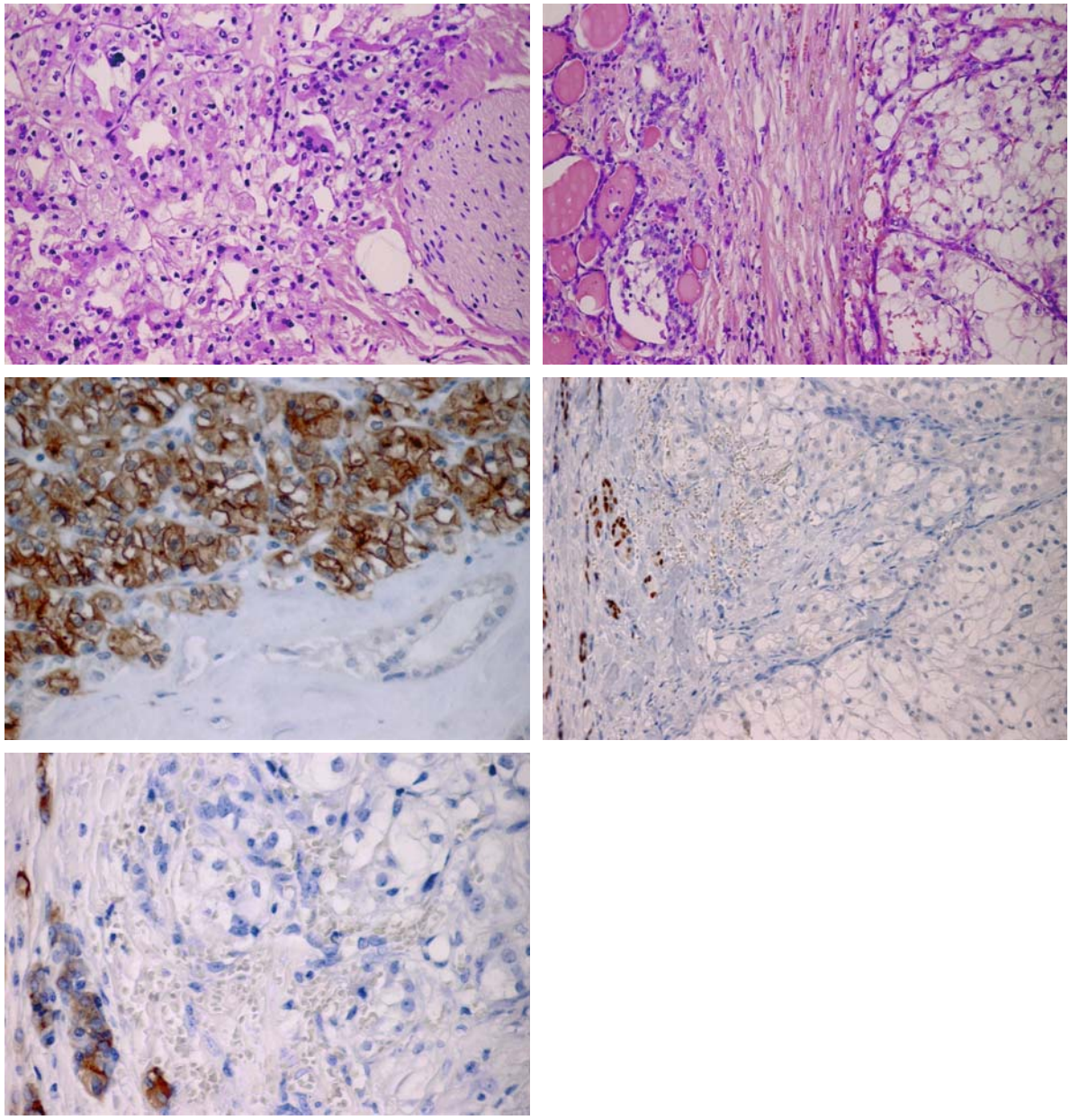

Fig. 16.58a-e. Thyroid metastasis in a 56-year-old man who underwent right nephrectomy for renal cell carcinoma 10 years previously. **a** Photomicrograph shows clear cell carcinoma of the right kidney (hematoxylin and eosin stain; original magnification, ×200). **b** Photomicrograph shows the thyroid metastasis with the same clear cell carcinoma histology (hematoxylin and eosin stain; original magnification, ×200). **c** Photomicrograph shows expression of CD10 by the thyroid metastasis (immunoperoxidase stain; original magnification, ×420). **d** Photomicrograph shows nuclear evidence of TTF-1 in the normal thyroid (*left side* of the slide) but not in the thyroid metastasis (immunoperoxidase stain; original magnification, ×200). **e** Photomicrograph shows expression of thyroglobulin in the residual normal thyroid tissue (*left side* of the slide) but not in the thyroid metastasis (immunoperoxidase stain; original magnification, ×420). (With permission from May et al. 2003)

The use of CT and MR imaging can greatly assist in delineating the extent of the lesion and planning surgical treatment (Fig. 16.63; Newmark et al. 1994). In a case report, contrast-enhanced CT showed a slightly heterogeneous nonenhancing extracavitary lesion. This lesion was heterogeneously hypointense on T1- and hyperintense on T2-weighted images (Newmark et al. 1994).

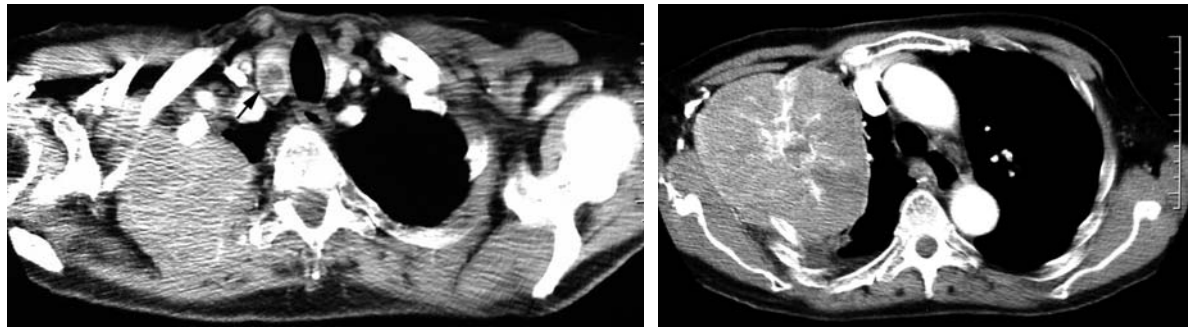

Fig. 16.59a,b. Thyroid and chest wall metastases in a 66-year-old woman who underwent left nephrectomy for renal cell carcinoma. **a** Axial contrast-enhanced CT scan shows a heterogeneously enhancing lesion of the right thyroid lobe (*arrow*) with central necrosis associated with a large right chest wall enhancing mass. This mass involves the right superior rib and is best seen on **b**.

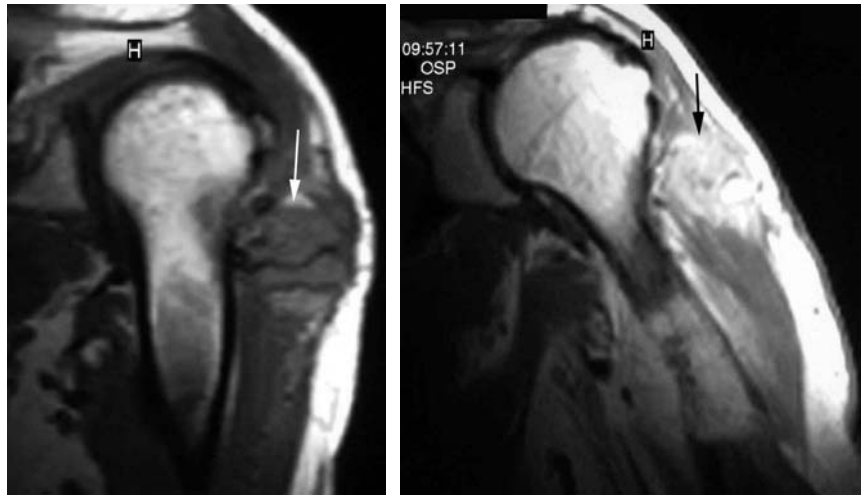

Fig. 16.60a,b. Muscle metastasis in a 63-year-old man with clear cell renal carcinoma 3 months after radical nephrectomy and who presented with deltoid swelling and paraneoplastic erythrocytosis. **a** Coronal unenhanced T1-weighted MR image shows an ill-defined and slightly hyperintense oval mass involving the left deltoid muscle (*arrow*). **b** Sagittal contrast-enhanced T1-weighted MR image shows strong enhancement of the mass (*arrow*). There is no adjacent involvement of the skin. (Image courtesy of A. Alimonti and S. Tormenta)

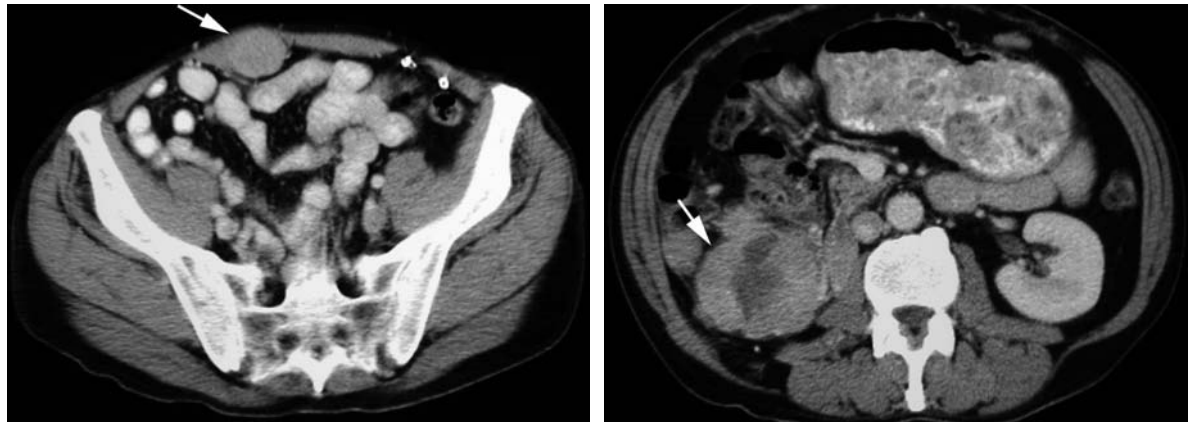

Fig. 16.61a,b. Muscle metastasis and local recurrence in a 59-year-old man who underwent right nephrectomy for renal cell carcinoma. **a** Axial contrast-enhanced CT demonstrates a homogeneously slightly enhancing mass to the right rectus abdominis muscle (*arrow*). **b** Axial contrast-enhanced CT scan cephalad to **a** shows a heterogeneously enhancing mass (*arrow*) in the right renal fossa.

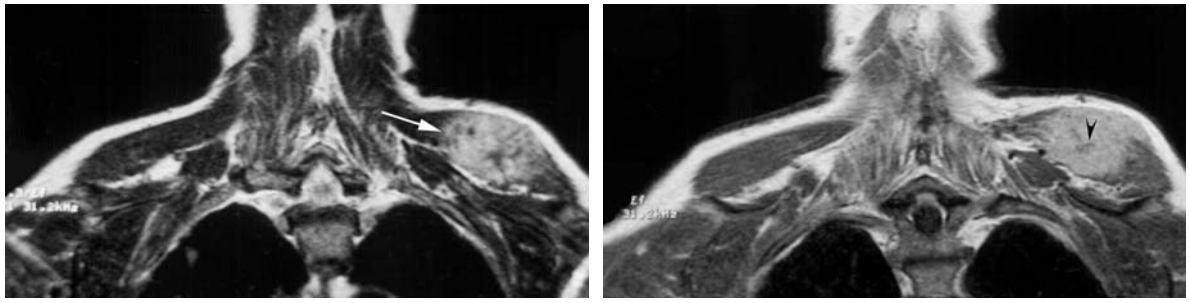

Fig. 16.62a,b. Muscle metastasis in a 63-year-old man with clear cell renal carcinoma 2 years after nephrectomy. **a** Coronal T2-weighted MR image shows well-defined and slightly heterogeneous hyperintense rounded mass involving the left deltoid muscle (*arrow*). **b** Coronal contrast-enhanced T1-weighted MR image shows a strong enhancement of the mass with central hypointensity corresponding to tumoral necrosis (*arrowhead*). There is no adjacent involvement of the skin. (Image courtesy of P. Schatteman)

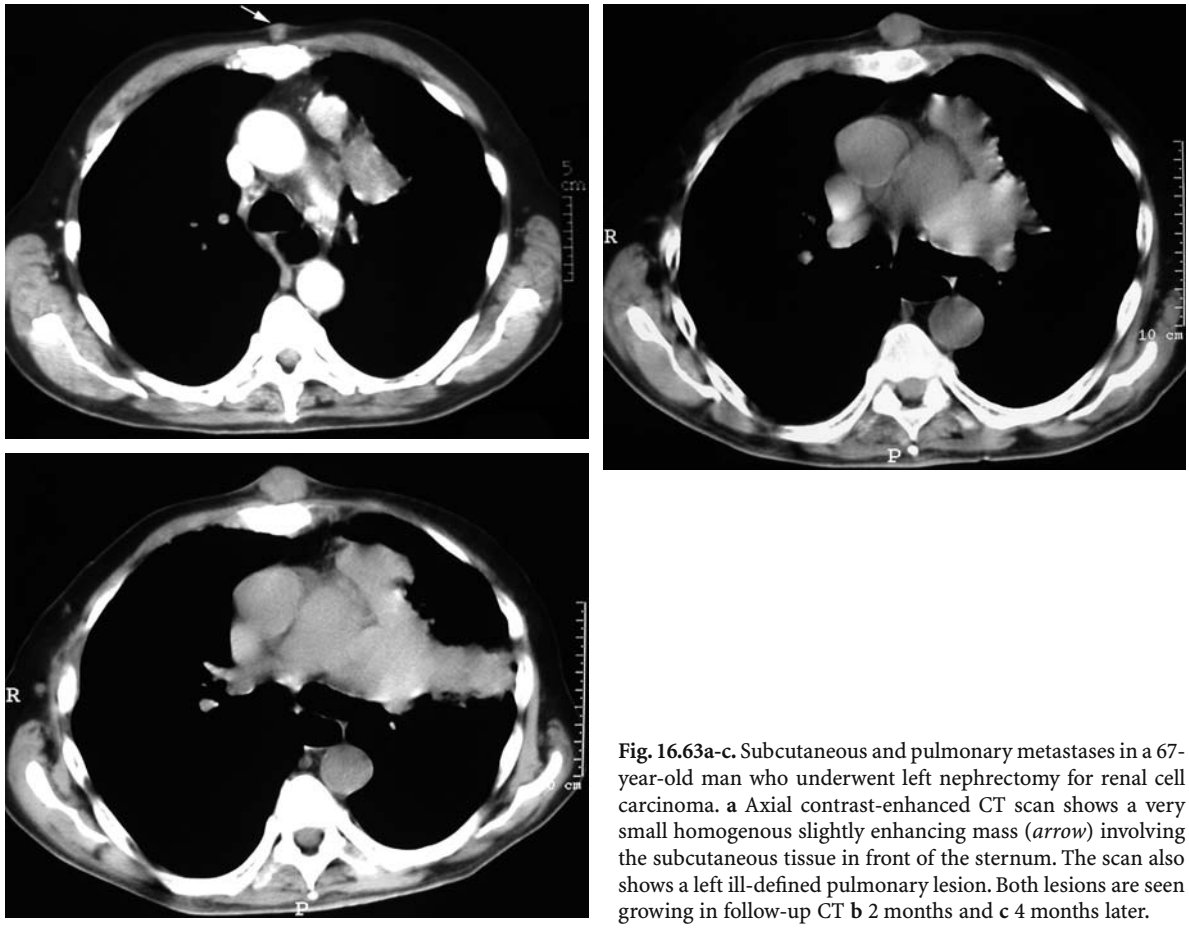

Fig. 16.63a-c. Subcutaneous and pulmonary metastases in a 67-year-old man who underwent left nephrectomy for renal cell carcinoma. **a** Axial contrast-enhanced CT scan shows a very small homogenous slightly enhancing mass (*arrow*) involving the subcutaneous tissue in front of the sternum. The scan also shows a left ill-defined pulmonary lesion. Both lesions are seen growing in follow-up CT **b** 2 months and **c** 4 months later.

16.10 Local Recurrence

Local recurrence of RCC in the renal fossa is an uncommon event following radical nephrectomy (Itano et al. 2000; Janzen et al. 2003), although the risk may be higher after partial nephrectomy (Janzen et al. 2003). Isolated late recurrence is rare with less than a 2% incidence at 5-year follow-up. It is controversial whether this entity is a remnant of microscopic disease or a form of metastatic disease (Itano et al. 2000). The clinical disease-free interval is reported to be as long as 45 years after nephrectomy (Tapper et al. 1997). An isolated recurrence of

RCC in the renal bed may behave as a solitary metastasis and select patients may benefit from surgical resection (Itano et al. 2000).

Recurrent renal carcinoma usually appears as an enhancing mass or nodule in the surgical site after nephrectomy (Figs. 16.13, 16.14; Nakada et al. 2002; Scatarige et al. 2001a). The mass may be heterogeneous (Tapper et al. 1997) with central necrosis (Fig. 16.61; Chae et al. 2005). The recurrence often involves the quadratus lumborum and psoas muscles (Fig. 16.64). It can displace or invade nearby structures such as the spine. The adrenal bed may be involved in case of cephalic extent which can involve the ipsilateral adrenal gland if the latter was spared at the time of nephrectomy (Scatarige et al. 2001a; Tapper et al. 1997). Locally recurrent renal carcinoma may directly invade the ascending or descending colon (Scatarige et al. 2001a). The recurrence may also extend posteriorly towards the surgical scar (Fig. 16.65; Tapper et al. 1997). Following nephron-sparing surgery, local recurrence is suggested when an enhancing nodule develops in the wedge-shaped partial nephrectomy defect (Scatarige et al. 2001a).

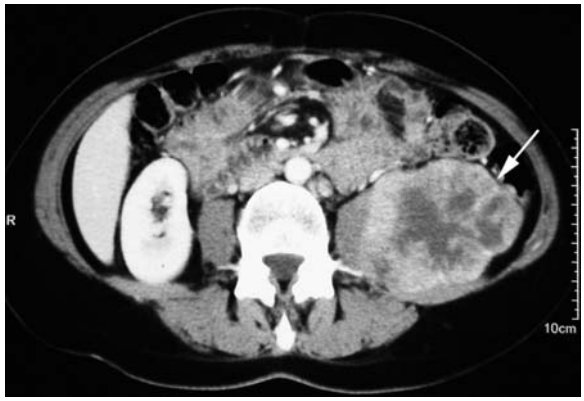

Fig. 16.64. Local recurrence in a 48-year-old woman who underwent left nephrectomy for renal cell carcinoma. Axial contrast-enhanced CT scan shows a large heterogeneously enhancing mass (*arrow*) with central necrosis of the left renal fossa and invading the left quadratus lumborum and psoas muscles.

16.11 Conclusion

Metastatic lesions from kidney cancer are seen in virtually every organ: the lung; pleura; pancreas; adrenal gland; liver; contralateral kidney; bone; lymph nodes; muscles; etc. These lesions can mas-

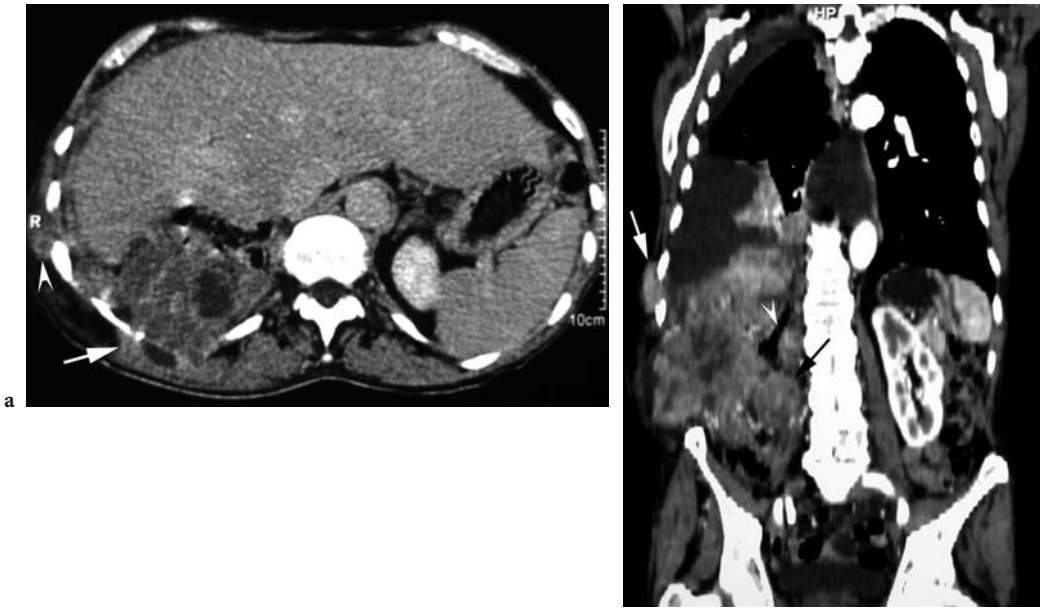

Fig. 16.65a,b. Local recurrence, chest wall, and pleural metastases in a 72-year-old man who underwent right nephrectomy for renal cell carcinoma. **a** Axial contrast-enhanced CT scan shows a large heterogeneously enhancing mass with central necrosis of the right renal fossa, extending posteriorly towards the surgical scar and invading the right latissimus dorsi muscle (*arrow*). It also shows a small heterogeneous mass of the lateral right chest wall (*arrowhead*). **b** Coronal contrast-enhanced two-dimensional CT reconstruction shows the large recurrent renal cell carcinoma mass that is locally and directly invading the ascending colon (*arrowhead*) and the right psoas muscle (*black arrow*). It also shows the right chest wall mass (*white arrow*) and important right pleural and pericardial effusions.

querade as another primary tumor. It is important to distinguish metastatic spread of RCC from primary tumors, as this knowledge is essential for the correct diagnosis and for determining the most effective treatment. Imaging studies are essential, as are histopathological examinations. Whole-body spiral CT is currently the method of choice for evaluating the postsurgical nephrectomy site for the presence of recurrent lesions and for detecting the usual anatomical sites of metastases. Like the primary tumor, metastatic lesions tend to be hypervascular and intravenous contrast administration is very useful. Other radiological modalities may be of interest when exploring particular organs, such as US for the liver and MR imaging for the brain and spine. Knowledge of the mechanisms, risk factors, and clinical timing of recurrent disease in surgically treated renal cancer aids the radiologist in understanding and detecting the patterns of recurrence observed on imaging.

Acknowledgements

We extend sincere thanks to Drs. A. Alimonti, C. Bassi, G. Butturini, M. Doita, S. Grand, M. Hashimoto, L. Insabato, H. Jadvar, F. Lafitte, M. May, D.H. McGregor, L. Mearini, H. Nozawa, I.C. Roberts-Thomson, G.M. Sakorafas, P. Schatteman, O.E.M. Schijns, K. Shiraishi, M. Szymanski, M. Tatsuta, S. Tormenta, and W.A.J. van Heuven for providing us with their excellent images.

References

Adams LA, Kaushik SP, Teo M, Roberts-Thomson IC (2003) Gastrointestinal: gastric metastases. J Gastroenterol Hepatol 18:343

Adil G, Murat D, Ayhan O, Ozgur TM, Ibrahim Y, Fuat PA, Rifki F (1999) Renal cell carcinoma metastasis to the parotid gland. BJU Int 83:861–862

Alimonti A, Cosimo S di, Maccallini V, Ferretti G, Pavese I, Satta F, Palma M di, Vecchione A (2003) A man with a deltoid swelling and paraneoplastic erythrocytosis: case report. Anticancer Res 23:5181–5184

Allen G, Klingman R, Ferraris VA, Fisher H, Harte F, Singh A (1991) Transesophageal echocardiography in the surgical management of renal cell carcinoma with intracardiac extension. J Cardiovasc Surg (Torino) 32:833–836

Altschuler EL, Ray A (1998) Spontaneous regression of a pancreatic metastasis of a renal cell carcinoma. Arch Fam Med 7:516–517

Andoh H, Kurokawa T, Yasui O, Shibata S, Sato T (2004) Resection of a solitary pancreatic metastasis from renal cell carcinoma with a gallbladder carcinoma: report of a case. Surg Today 34:272–275

Aoki T, Inoue K, Tsuchida A, Kasuya K, Kitamura K, Koyanagi Y, Shimizu T (2002) Gallbladder metastasis of renal cell carcinoma: report of two cases. Surg Today 32:89–92

Arkless R (1965) Renal carcinoma: how it metastasizes. Radiology 84:496–501

Badoual C, Tissier F, Lagorce-Pages C, Delcourt A, Vieillefond A (2002) Pulmonary metastases from a chromophobe renal cell carcinoma: 10 years' evolution. Histopathology 40:300–302

Barthwal MS, Chatterji RS, Jawed KZ (2003) Endobronchial metastases from renal cell carcinoma. J Assoc Physicians India 51:1027–1028

Bassi C, Butturini G, Falconi M, Sargenti M, Mantovani W, Pederzoli P (2003) High recurrence rate after atypical resection for pancreatic metastases from renal cell carcinoma. Br J Surg 90:555–559

Benoit L, Favoulet P, Arnould L, Margarot A, Franceschini C, Collin F, Fraisse J, Cuisenier J, Cougard P (2004) Metastatic renal cell carcinoma of the thyroid gland: about seven cases and review of the literature. Ann Chir 129:218–223

Bersani TA, Costello JJ Jr, Mango CA, Streeten BW (1994) Benign approach to a malignant orbital tumor: metastatic renal cell carcinoma. Ophthal Plast Reconstr Surg 10:42–44

Bressler EL, Alpern MB, Glazer GM, Francis IR, Ensminger WD (1987) Hypervascular hepatic metastases: CT evaluation. Radiology 162:49–51

Calleja Escudero J, Pascual Samaniego M, Martin Blanco S, Castro Olmedo C de, Gonzalo V, Fernandez del Busto E (2004) Intrascrotal metastasis in a renal cell carcinoma. Acta Urol Esp 28:311–313

Carroll JC, Quinn CC, Weitzel J, Sant GR (1994) Metastatic renal cell carcinoma to the right cardiac ventricle without contiguous vena caval involvement. J Urol 151:133–134

Chae EJ, Kim JK, Kim SH, Bae SJ, Cho KS (2005) Renal cell carcinoma: analysis of postoperative recurrence patterns. Radiology 234:189–196

Chang CH, Shiau YC, Shen YY, Kao A, Lin CC, Lee CC (2003) Differentiating solitary pulmonary metastases in patients with renal cell carcinomas by 18F-fluoro-2-deoxyglucose positron emission tomography: a preliminary report. Urol Int 71:306–309

Chao K, Hurley J, Neerhut G, Kiroff G (2002) Multiple pancreatic metastases from renal cell carcinoma. Aust NZ J Surg 72:310–312

Cheng AS (2003) Cardiac metastasis from a renal cell carcinoma. Int J Clin Pract 57:437–438

Coppa GF, Oszczakiewicz M (1990) Parotid gland metastasis from renal carcinoma. Int Surg 75:198–202

Dal Fabbro S, Monari G, Barbazza R (1987) A thyroid metastasis revealing an occult renal clear-cell carcinoma. Tumori 73:187–190

Daniels GF Jr, Schaeffer AJ (1991) Renal cell carcinoma involving penis and testis: unusual initial presentations of metastatic disease. Urology 37:369–373

Destian S, Sze G, Krol G, Zimmerman RD, Deck MD (1989) MR imaging of hemorrhagic intracranial neoplasms. Am J Roentgenol 152:137–144

Diaz-Candamio MJ, Pombo S, Pombo F (2000) Colonic metastasis from renal cell carcinoma: helical-CT demonstration. Eur Radiol 10:139–140

Djimi H, Donnio A, Ayeboua L, Vally P, Olindo S, Cabre P, Ventura E, Landau M, Richer R, Merle H (2003) Hypophysis metastasis of a hypernephroma tumor revealed by a chiasma syndrome. J Fr Ophtalmol 26:976–979

Dousset B, Andant C, Guimbaud R, Roseau G, Tulliez M, Gaudric M, Palazzo L, Chaussade S, Chapuis Y (1995) Late pancreatic metastasis from renal cell carcinoma diagnosed by endoscopic ultrasonography. Surgery 117:591–594

Duggan MA, Forestell CF, Hanley DA (1987) Adrenal metastases of renal-cell carcinoma 19 years after nephrectomy. Fine needle aspiration cytology of a case. Acta Cytol 31:512–516

Essadki O, Chartrand-Lefebvre C, Finet JF, Grenier P (1998) Cystic pulmonary metastasis simulating a diagnosis of histiocytosis X. J Radiol 79:886–888

Fakih M, Schiff D, Erlich R, Logan TF (2001) Intramedullary spinal cord metastasis (ISCM) in renal cell carcinoma: a series of six cases. Ann Oncol 12:1173–1177

Federle MP, Jeffrey RB Jr, Minagi H (1981) Case report. Calcified liver metastasis from renal cell carcinoma. J Comput Assist Tomogr 5:771–772

Flanigan RC, Yonover PM (2001) The role of radical nephrectomy in metastatic renal cell carcinoma. Semin Urol Oncol 19:98–102

Flanigan RC, Salmon SE, Blumenstein BA, Bearman SI, Roy V, McGrath PC, Caton JR Jr, Munshi N, Crawford ED (2001) Nephrectomy followed by interferon alfa-2b compared with interferon alfa-2b alone for metastatic renal-cell cancer. N Engl J Med 345:1655–1659

Flanigan RC, Campbell SC, Clark JI, Picken MM (2003) Metastatic renal cell carcinoma. Curr Treat Options Oncol 4:385–390

Furukawa H, Mizuguchi Y, Kanai Y, Mukai K (1997) Metastatic renal cell carcinoma to the gallbladder: color Doppler sonography and CT findings. Am J Roentgenol 169:1466–1467

Gastaca Mateo MA, Ortiz de Urbina Lopez J, Diaz Aguirregoitia J, Martinez Fernandez G, Campo Hiriart M, Echevarria Garcia-San Frechoso A (1996) Duodenal metastasis of renal cell adenocarcinoma. Rev Esp Enferm Dig 88:361–363

Ghavamian R, Klein KA, Stephens DH, Welch TJ, LeRoy AJ, Richardson RL, Burch PA, Zincke H (2000) Renal cell carcinoma metastatic to the pancreas: clinical and radiological features. Mayo Clin Proc 75:581–585

Giuffrida D, Ferrau F, Pappalardo A, Aiello RA, Bordonaro R, Cordio S, Giorgio CG, Squatrito S (2003) Metastasis to the thyroid gland: a case report and review of the literature. J Endocrinol Invest 26:560–563

Giulini SM, Portolani N, Bonardelli S, Baiocchi GL, Zampatti M, Coniglio A, Baronchelli C (2003) Distal pancreatic resection with splenic preservation for metastasis of renal carcinoma diagnosed 24 years later from the nephrectomy. Ann Ital Chir 74:93–96

Griniatsos J, Michail PO, Menenakos C, Hatzianastasiou D, Koufos C, Bastounis E (2003) Metastatic renal clear cell carcinoma mimicking stage IV lung cancer. Int Urol Nephrol 35:15–17

Gupta D, Merino MI, Farhood A, Middleton LP (2001) Metastases to breast simulating ductal carcinoma in situ: report of two cases and review of the literature. Ann Diagn Pathol 5:15–20

Guthbjartsson T, Gislason T (1995) Spontaneous regression of brain metastasis secondary to renal cell carcinoma. Scand J Urol Nephrol 29:215–217

Haimovici R, Gragoudas ES, Gregor Z, Pesavento RD, Mieler WF, Duker JS (1997) Choroidal metastases from renal cell carcinoma. Ophthalmology 104:1152–1158

Hammad AM, Paris GR, van Heuven WA, Thompson IM, Fitzsimmons TD (2003) Spontaneous regression of choroidal metastasis from renal cell carcinoma. Am J Ophthalmol 135:911–913

Hasegawa J, Okumura S, Abe H, Kanamori S, Yoshida K, Akimoto M (1988) Renal cell carcinoma with solitary contralateral adrenal metastasis. Urology 32:52–53

Hashimoto M, Miura Y, Matsuda M, Watanabe G (2001) Concomitant duodenal and pancreatic metastases from renal cell carcinoma: report of a case. Surg Today 31:180–183

Heffess CS, Wenig BM, Thompson LD (2002) Metastatic renal cell carcinoma to the thyroid gland: a clinicopathologic study of 36 cases. Cancer 95:1869–1878

Hernandez DJ, Kavoussi LR, Ellison LM (2003) Laparoscopic distal pancreatectomy for metastatic renal cell carcinoma. Urology 62:551

Hillard VH, Musunuru K, Hasan I, Zia S, Hirschfeld A (2003) Long-term management of bilateral metastases of renal cell carcinoma to the choroid plexus. Acta Neurochir (Wien) 145:793–797

Hodgson TJ, Howell SJ, Kean DM (1994) Case report: metastatic renal cell carcinoma presenting as intracerebral haemorrhage. Clin Radiol 49:213–214

Homer JJ, Jones NS (1995) Renal cell carcinoma presenting as a solitary paranasal sinus metastasis. J Laryngol Otol 109:986–989

Hoshi S, Jokura H, Nakamura H, Shintaku I, Ohyama C, Satoh M, Saito S, Fukuzaki A, Orikasa S, Yoshimoto T (2002) Gamma-knife radiosurgery for brain metastasis of renal cell carcinoma: results in 42 patients. Int J Urol 9:618-625; discussion 626; author reply 627

Hudson MA, Kavoussi LR, Catalona WJ (1991) Bilateral renal cell carcinoma with metastasis to thyroid. Urology 37:145–148

Huisman TK, Sands JP Jr (1991) Renal cell carcinoma with solitary metachronous contralateral adrenal metastasis. Experience with 2 cases and review of the literature. Urology 38:364–368

Insabato L, Rosa G de, Franco R, D'Onofrio V, Vizio D di (2003) Ovarian metastasis from renal cell carcinoma: a report of three cases. Int J Surg Pathol 11:309–312

Ishikawa J, Umezu K, Yamashita H, Maeda S (1990) Solitary brain metastasis from renal cell carcinoma 14 years after nephrectomy: a case report. Hinyokika Kiyo 36:1439–1441

Itano NB, Blute ML, Spotts B, Zincke H (2000) Outcome of isolated renal cell carcinoma fossa recurrence after nephrectomy. J Urol 164:322–325

Jadvar H, Cham D, Gamie S, Henderson RW (2004) Fusion positron emission tomography-computed tomography demonstration of epidural metastases. Clin Nucl Med 29:39–40

Janzen NK, Kim HL, Figlin RA, Belldegrun AS (2003) Surveillance after radical or partial nephrectomy for localized renal cell carcinoma and management of recurrent disease. Urol Clin North Am 30:843–852

Johnsen JA, Hellsten S (1997) Lymphatogenous spread of renal cell carcinoma: an autopsy study. J Urol 157:450–453

Kamota S, Harabayashi T, Suzuki S, Takeyama Y, Mitsui T, Mouri G, Hashimoto A, Nakamura M, Shinohara N, Nonomura K, Koyanagi T (2003) Ureteral and bladder metastases of renal cell carcinoma following synchronous renal cell carcinoma and bladder cancer; a case report. Nippon Hinyokika Gakkai Zasshi 94:705–708

Kassabian A, Stein J, Jabbour N, Parsa K, Skinner D, Parekh D, Cosenza C, Selby R (2000) Renal cell carcinoma metastatic to the pancreas: a single-institution series and review of the literature. Urology 56:211–215

Kelekis NL, Semelka RC, Siegelman ES (1996) MRI of pancreatic metastases from renal cancer. J Comput Assist Tomogr 20:249–253

Kim JK, Learch TJ, Colletti PM, Lee JW, Tran SD, Terk MR (2000) Diagnosis of vertebral metastasis, epidural metastasis, and malignant spinal cord compression: Are T1-weighted sagittal images sufficient? Magn Reson Imaging 18:819–824

Kindermann WR, Shields JA, Eiferman RA, Stephens RF, Hirsch SE (1981) Metastatic renal cell carcinoma to the eye and adnexae: a report of three cases and review of the literature. Ophthalmology 88:1347–1350

Klein KA, Stephens DH, Welch TJ (1998) CT characteristics of metastatic disease of the pancreas. Radiographics 18:369–378

Klos KJ, O'Neill BP (2004) Brain metastases. Neurologist 10:31–46

Koc M, Polat P, Erem T, Buyukavci M, Ozbey I, Gundogdu C, Suma S (1999) Quiz case of the month. Diagnosis: clear-cell renal cell carcinoma (RCC) with metastasis to lung, mediastinal and abdominal lymph nodes and bones. Eur Radiol 9:1935–1936

Kolosseus RC, Temes RT, Feddersen RM, Williamson M, Smith AY (1995) Intrapulmonary lymph nodes masquerading as renal cell carcinoma metastases. Urology 46:249–250

Koshiyama H, Ohgaki K, Hida S, Takasu K, Yumitori K, Shimatsu A, Koh T (1992) Metastatic renal cell carcinoma to the pituitary gland presenting with hypopituitarism. J Endocrinol Invest 15:677-681

Kremer S, Grand S, Berger F, Hoffmann D, Pasquier B, Remy C, Benabid AL, Bas JF (2003) Dynamic contrast-enhanced MRI: differentiating melanoma and renal carcinoma metastases from high-grade astrocytomas and other metastases. Neuroradiology 45:44–49

Lau WK, Zincke H, Lohse CM, Cheville JC, Weaver AL, Blute ML (2003) Contralateral adrenal metastasis of renal cell carcinoma: treatment, outcome and a review. BJU Int 91:775–779

Lee G, Sharma SD, Bullock KN (1998) An unusual case of renal cell carcinoma with two rare metastases. Scand J Urol Nephrol 32:239–240

Lee JG, Kim JS, Kim HJ, Kim ST, Yeon JE, Byun KS, Bak YT, Lee CH (2002) Simultaneous duodenal and colon masses as late presentation of metastatic renal cell carcinoma. Korean J Intern Med 17:143–146

Leiman G, Markowitz S, Veiga-Ferreira MM, Margolius KA (1986) Renal adenocarcinoma presenting with bilateral metastases to Bartholin's glands: primary diagnosis by aspiration cytology. Diagn Cytopathol 2:252–255

Li L, Friedrich RE, Schmelzle R, Donath K (2001) Metachronous bilateral metastases of renal cell carcinoma to the parotid region. J Oral Maxillofac Surg 59:434–438

Lim DJ, Carter MF (1993) Computerized tomography in the preoperative staging for pulmonary metastases in patients with renal cell carcinoma. J Urol 150:1112–1114

Limani K, Matos C, Hut F, Gelin M, Closset J (2003) Metastatic carcinoma of the gallbladder after a renal cell carcinoma. Acta Chir Belg 103:233–234

Lokich J (1997) Spontaneous regression of metastatic renal cancer. Case report and literature review. Am J Clin Oncol 20:416–418

Mahnken AH, Tacke J (2000) Myocardial heart metastasis in rapidly progressing renal cell carcinoma. Rofo 172:488–490

Marshall ME, Pearson T, Simpson W, Butler K, McRoberts W (1990) Low incidence of asymptomatic brain metastases in patients with renal cell carcinoma. Urology 36:300–302

Marusch F, Koch A, Dietrich F, Hoschke B, Gastinger I (2001) Singular late metastasis of renal cell carcinoma in the pancreas. An unusual pancreatic tumor. Zentralbl Chir 126:391–395

Mascarenhas B, Konety B, Rubin JT (2001) Recurrent metastatic renal cell carcinoma presenting as a bleeding gastric ulcer after a complete response to high-dose interleukin-2 treatment. Urology 57:168

Mattana J, Kurtz B, Miah A, Singhal PC (1996) Renal cell carcinoma presenting as a solitary anterior superior mediastinal mass. J Med 27:205–210

Maxwell M, Borges LF, Zervas NT (1999) Renal cell carcinoma: a rare source of cauda equina metastasis. Case report. J Neurosurg Spine 90:129–132

May M, Marusch F, Kaufmann O, Seehafer M, Helke C, Hoschke B, Gastinger I (2003) Solitary renal cell carcinoma metastasis to the thyroid gland: a paradigm of metastasectomy? Chirurg 74:768–774

McGregor DH, Wu Y, Weston AP, McAnaw MP, Bromfield C, Bhattatiry MM (2003) Metastatic renal cell carcinoma of spleen diagnosed by fine-needle aspiration. Am J Med Sci 326:51–54

Mearini L, Zucchi A, Pizzirusso G, Costantini E, Mearini E (2004) Renal papillary adenocarcinoma with unusual metastases: case report and review of the literature. Arch Ital Urol Androl 76:88–90

Merine D, Fishman EK (1988) Mediastinal adenopathy and endobronchial involvement in metastatic renal cell carcinoma. J Comput Tomogr 12:216–219

Mesurolle B, Mignon F, Travagli JP, Meingan P, Vanel D (1997) Late presentation of solitary contralateral adrenal metastasis of renal cell carcinoma. Eur Radiol 7:557–558

Mignon F, Mesurolle B (2003) Local recurrence and metastatic dissemination of renal cell carcinoma: clinical and imaging characteristics. J Radiol 84:275–284

Mignon F, Mesurolle B, Sissakian JF, Bruckert F, Guichoux F, Barre O, Chagnon S, Lacombe P (1999) Late solitary metastasis of a renal cancer to the contralateral adrenal gland. J Radiol 80:939–942

Mizuo T, Ohashi H, Tanizawa A, Okuno T (1990) Complete resolution of multiple pulmonary metastases of renal cell carcinoma following intravenous drip infusion of r-interleukin 2: a case report. Hinyokika Kiyo 36:931–935

Monteros-Sanchez AE de los, Medina-Franco H, Arista-Nasr J, Cortes-Gonzalez R (2004) Resection of an esophageal metastasis from a renal cell carcinoma. Hepatogastroenterology 51:163–164

Motzer RJ, Bander NH, Nanus DM (1996) Renal-cell carcinoma. N Engl J Med 335:865–875

Moudouni SM, En-Nia I, Rioux-Leclerq N, Manunta A, Guille F, Lobel B (2001) Prostatic metastases of renal cell carcinoma. J Urol 165:190–191

Munk PL, Gock S, Gee R, Connell DG, Quenville NF (1992) Case report 708: Metastasis of renal cell carcinoma to skeletal muscle (right trapezius). Skeletal Radiol 21:56–59

Murakami R, Taniai N, Kumazaki T, Kobayashi Y, Ogura J, Ichikawa T (2000) Rupture of a hepatic metastasis from renal cell carcinoma. Clin Imaging 24:72–74

Muram TM, Aisen A (2003) Fatty metastatic lesions in 2 patients with renal clear-cell carcinoma. J Comput Assist Tomogr 27:869–870

Nabeyama R, Tanaka K, Matsuda S, Iwamoto Y (2001) Multiple intramuscular metastases 15 years after radical nephrectomy in a patient with stage IV renal cell carcinoma. J Orthop Sci 6:189–192

Nabi G, Gania MA, Sharma MC (2001) Solitary delayed contralateral testicular metastasis from renal cell carcinoma. Indian J Pathol Microbiol 44:487–488

Nagler J, McSherry CK, Miskovitz P (1994) Asymptomatic metachronous metastatic renal cell adenocarcinoma to the gallbladder. Report of a case and guidelines for evaluation of intraluminal polypoid gallbladder masses. Dig Dis Sci 39:2476–2479

Nakada SY, Johnson DB, Hahnfield L, Jarrard DF (2002) Resection of isolated fossa recurrence of renal-cell carcinoma after nephrectomy using hand-assisted laparoscopy. J Endourol 16:687–688

Navarro F, Vicente J, Villanueva MJ, Sanchez A, Provencio M, Espana P (2000) Metastatic renal cell carcinoma to the head and neck area. Tumori 86:88–90

Newmark JR, Newmark GM, Epstein JI, Marshall FF (1994) Solitary late recurrence of renal cell carcinoma. Urology 43:725–728

Ng CS, Loyer EM, Iyer RB, David CL, DuBrow RA, Charnsangavej C (1999) Metastases to the pancreas from renal cell carcinoma: findings on three-phase contrast-enhanced helical CT. Am J Roentgenol 172:1555–1559

Nozawa H, Tsuchiya M, Kobayashi T, Morita H, Kobayashi I, Sakaguchi M, Mizutani T, Tajima A, Kishida Y, Yakumaru K, Kagami H, Sekikawa T (2003) Small intestinal metastasis from renal cell carcinoma exhibiting rare findings. Int J Clin Pract 57:329–331

Nussbaum ES, Djalilian HR, Cho KH, Hall WA (1996) Brain metastases. Histology, multiplicity, surgery, and survival. Cancer 78:1781–1788

O'Brien WM, Lynch JH (1987) Adrenal metastases by renal cell carcinoma. Incidence at nephrectomy. Urology 29:605–607

Odori T, Tsuboi Y, Katoh K, Yamada K, Morita K, Ohara A, Kuroiwa M, Sakamoto H, Sakata T (1998) A solitary hematogenous metastasis to the gastric wall from renal cell carcinoma four years after radical nephrectomy. J Clin Gastroenterol 26:153–154

Ohgou T, Okahara M, Kishimoto T (1998) Renal cell carcinoma with many transvenous pleural metastases. Nihon Kokyuki Gakkai Zasshi 36:369–373

Okabe Y, Ohoka H, Miwa T, Nagayama I, Furukawa M (1992) View from beneath: pathology in focus. Renal cell carcinoma metastasis to the tongue. J Laryngol Otol 106:282–284

Omland H, Fossa SD (1989) Spontaneous regression of cerebral and pulmonary metastases in renal cell carcinoma. Scand J Urol Nephrol 23:159–160

Pantuck AJ, Zisman A, Dorey F, Chao DH, Han KR, Said J, Gitlitz BJ, Figlin RA, Belldegrun AS (2003) Renal cell carcinoma with retroperitoneal lymph nodes: role of lymph node dissection. J Urol 169:2076–2083

Park DY, Kim YM, Chi JG (1997) Intracranial metastasis from clear cell sarcoma of the kidney: a case report. J Korean Med Sci 12:473–476

Park YW, Hlivko TJ (2002) Parotid gland metastasis from renal cell carcinoma. Laryngoscope 112:453–456

Pavlakis GM, Sakorafas GH, Anagnostopoulos GK (2004) Intestinal metastases from renal cell carcinoma: a rare cause of intestinal obstruction and bleeding. Mt Sinai J Med 71:127–130

Pilecki SE, Cieslinski K, Lasek WL, Purzycka-Jazdon AM, Lambrecht W (2002) Metastasis of renal carcinoma to the diaphragm. Wiad Lek 55:120–124

Pretorius ES, Fishman EK (2000) Helical CT of skeletal muscle metastases from primary carcinomas. Am J Roentgenol 174:401–404

Pursner M, Petchprapa C, Haller JO, Orentlicher RJ (1997) Renal carcinoma: bilateral breast metastases in a child. Pediatr Radiol 27:242–243

Rabinovitch RA, Zelefsky MJ, Gaynor JJ, Fuks Z (1994) Patterns of failure following surgical resection of renal cell carcinoma: implications for adjuvant local and systemic therapy. J Clin Oncol 12:206–212

Radley MG, McDonald JV, Pilcher WH, Wilbur DC (1993) Late solitary cerebral metastases from renal cell carcinoma: report of two cases. Surg Neurol 39:230–234

Raptopoulos VD, Blake SP, Weisinger K, Atkins MB, Keogan MT, Kruskal JB (2001) Multiphase contrast-enhanced helical CT of liver metastases from renal cell carcinoma. Eur Radiol 11:2504–2509

Ravi R, Tongaonkar HB, Kulkarni JN, Kamat MR (1992) Synchronous bilateral parotid metastases from renal cell carcinoma. A case report. Indian J Cancer 29:40–42

Raviv S, Eggener SE, Williams DH, Garnett JE, Pins MR, Smith ND (2002) Long-term survival after "drop metastases" of renal cell carcinoma to the bladder. Urology 60:697

Ritchie AW, Layfield LJ, deKernion JB (1988) Spontaneous regression of liver metastasis from renal carcinoma. J Urol 140:596–597

Rivoire M, Voiglio EJ (1996) Late pancreatic metastases from renal cell carcinoma. Surgery 119:240

Robertson GS, Gertler SL (1990) Late presentation of metastatic renal cell carcinoma as a bleeding ampullary mass. Gastrointest Endosc 36:304–306

Russo P (2003) Seeking the solution to the problem of metastatic renal carcinoma. Cancer 97:2941–2944

Rypens F, Van Gansbeke D, Lambilliotte JP, Van Regemorter G, Verhest A, Struyven J (1992) Pancreatic metastasis from renal cell carcinoma. Br J Radiol 65:547–548

Safi AM, Rachko M, Sadeghinia S, Zineldin A, Dong J, Stein RA (2003) Left ventricular intracavitary mass and pericarditis secondary to metastatic renal cell carcinoma: a case report. Angiology 54:495–498

Sagalowsky AI, Molberg K (1999) Solitary metastasis of renal cell carcinoma to the contralateral adrenal gland 22 years after nephrectomy. Urology 54:162

Saidi JA, Newhouse JH, Sawczuk IS (1998) Radiologic follow-up of patients with T1-3a,b,c or T4N+M0 renal cell carcinoma after radical nephrectomy. Urology 52:1000–1003

Saitoh H, Nakayama M, Nakamura K, Satoh T (1982) Distant metastasis of renal adenocarcinoma in nephrectomized cases. J Urol 127:1092–1095

Sanchez-Ortiz RF, Tannir N, Ahrar K, Wood CG (2003) Spontaneous regression of pulmonary metastases from renal cell carcinoma after radio frequency ablation of primary tumor: an in situ tumor vaccine? J Urol 170:178–179

Santo-Tomas M, Mahr NC, Robinson MJ, Agatston AS (1998) Metastatic renal cell carcinoma invading right ventricular myocardium without caval involvement. J Cardiovasc Surg (Torino) 39:811–812

Savas MC, Celik I, Benekli M, Gullu IH, Tekuzman G (1998) Renal cell carcinoma presenting as solitary cervical node metastasis compressing the brachial plexus. Nephron 79:107–108

Scatarige JC, Sheth S, Corl FM, Fishman EK (2001a) Patterns of recurrence in renal cell carcinoma: manifestations on helical CT. Am J Roentgenol 177:653–658

Scatarige JC, Horton KM, Sheth S, Fishman EK (2001b) Pancreatic parenchymal metastases: observations on helical CT. Am J Roentgenol 176:695–699

Schatteman P, Willemsen P, Vanderveken M, Lockefeer F, Vandebroek A (2002) Skeletal muscle metastasis from a conventional renal cell carcinoma, two years after nephrectomy: a case report. Acta Chir Belg 102:351–352

Schijns OE, Kurt E, Wessels P, Luijckx GJ, Beuls EA (2000) Intramedullary spinal cord metastasis as a first manifestation of a renal cell carcinoma: report of a case and review of the literature. Clin Neurol Neurosurg 102:249–254

Schmidt M, Schmidt T, Ugi I (1994) Orbital metastasis of kidney carcinoma. Klin Monatsbl Augenheilkd 205:40–43

Seaman EK, Ross S, Sawczuk IS (1995) High incidence of asymptomatic brain lesions in metastatic renal cell carcinoma. J Neurooncol 23:253–256

Selli C, Carini M, Barbanti G, Barbagli G, Turini D (1987) Simultaneous bilateral adrenal involvement by renal cell carcinoma: experience with 3 cases. J Urol 137:480–482

Shiono S, Yoshida J, Nishimura M, Nitadori J, Ishii G, Nishiwaki Y, Nagai K (2004) Late pulmonary metastasis of renal cell carcinoma resected 25 years after nephrectomy. Jpn J Clin Oncol 34:46–49

Shiraishi K, Mohri J, Inoue R, Kamiryo Y (2003) Metastatic renal cell carcinoma to the bladder 12 years after radical nephrectomy. Int J Urol 10:453–455

Siemer S, Lehmann J, Kamradt J, Loch T, Remberger K, Humke U, Ziegler M, Stockle M (2004) Adrenal metastases in 1635 patients with renal cell carcinoma: outcome and indication for adrenalectomy. J Urol 171:2155–2159

Simo R, Sykes AJ, Hargreaves SP, Axon PR, Birzgalis AR, Slevin NJ, Farrington WT (2000) Metastatic renal cell carcinoma to the nose and paranasal sinuses. Head Neck 22:722–727

Slamovits TL, Burde RM (1988) Bumpy muscles. Surv Ophthalmol 33:189–199

Som PM, Norton KI, Shugar JM, Reede DL, Norton L, Biller HF, Som ML (1987) Metastatic hypernephroma to the head and neck. Am J Neuroradiol 8:1103–1106

Srinivasan S, Gray DG (2003) Images in clinical medicine. Choroidal metastasis from renal-cell carcinoma. N Engl J Med 349:e22

Stattaus J, Mertens H, Mackowski JM, Hacklander T, Cramer BM (1999) Metastases of renal cell carcinoma to the pancreas and gallbladder: possibilities and limits of MRI diagnosis. Rofo Fortschr Geb Rontgenstr Neuen Bildgeb Verfahr 170:598–600

Strijk SP (1989) Pancreatic metastases of renal cell carcinoma: report of two cases. Gastrointest Radiol 14:123–126

Studer UE, Scherz S, Scheidegger J, Kraft R, Sonntag R, Ackermann D, Zingg EJ (1990) Enlargement of regional lymph nodes in renal cell carcinoma is often not due to metastases. J Urol 144:243–245

Suzuki M, Machida T, Masuda F, Yanagisawa M, Tashiro K, Onishi T, Kishimoto K, Ishikawa E (1982) A case of renal cell carcinoma invading the spleen. Nippon Hinyokika Gakkai Zasshi 73:1333–1337

Szymanski M, Szymanska A, Morshed K, Siwiec H (2004) Renal cell carcinoma metastases to nose and paranasal sinuses presenting as recurrent epistaxis. Wiad Lek 57:94–96

Takada T, Doita M, Nishida K, Miura J, Yoshiya S, Kurosaka M (2003) Unusual metastasis to the cauda equina from renal cell carcinoma. Spine 28:E114–E117

Tapper H, Klein H, Rubenstein W, Intriere L, Choi Y, Kazam E (1997) Recurrent renal cell carcinoma after 45 years. Clin Imaging 21:273–275

Tartar VM, Heiken JP, McClennan BL (1991) Renal cell carcinoma presenting with diffuse peritoneal metastases: CT findings. J Comput Assist Tomogr 15:450–453

Tatsuta M, Shiozaki K, Masutani S, Hashimoto K, Imamura H, Ikeda M, Miya A, Ishida H, Kawasaki T, Furukawa H, Satomi T, Hoshida Y (2001) Splenic and pulmonary metastases from renal cell carcinoma: report of a case. Surg Today 31:463–465

Tharakan J, Iasacs P, Morris EA (1995) Renal carcinoma metastases presenting as duodenal obstruction. Am J Gastroenterol 90:683–684

Thoroddsen A, Gudbjartsson T, Geirsson G, Agnarsson BA, Magnusson K (2002) Spontaneous regression of pleural metastases after nephrectomy for renal cell carcinoma: a histologically verified case with nine-year follow-up. Scand J Urol Nephrol 36:396–398

Thrasher JB, Paulson DF (1993) Prognostic factors in renal cancer. Urol Clin North Am 20:247–262

Tomita T, Inouye T, Shinden S, Ogawa K, Mukai M (1998) Palliative radiotherapy for lingual metastasis of renal cell carcinoma. Auris Nasus Larynx 25:209–214

Toye R, Jones DK, Armstrong P, Richman PI (1990) Numerous pulmonary metastases from renal cell carcinoma confined to the middle lobe. Clin Radiol 42:443–444

Trufflandier N, Gille O, Palussiere J, Prie L, Pointillart V, Ravaud A (2002) Symptomatic neurological epidural metastasis with interleukin-2 therapy in metastatic renal cell carcinoma. Tumori 88:338–340

Uchino A, Hasuo K, Mizushima A, Matsumoto S, Mihara F, Jimi M, Takahashi M, Masuda K (1996) Intracranial metastasis of renal cell carcinoma: MR imaging. Radiat Med 14:71–76

Vassalli L, Ferrari VD, Simoncini E, Rangoni G, Montini E, Marpicati P, Mambrini A, Pagani M, Agazzi C, Marini G (2001) Solitary breast metastases from a renal cell carcinoma. Breast Cancer Res Treat 68:29–31

Vespasiani G, Porena M, Virgili G, Costantini E, Bonacina R, Mearini E, Rosi P, Micali F (1990) Renal cell carcinoma with synchronous adrenal metastases. Acta Urol Belg 58:197–203

Vleeming R, Dabhoiwala NF, Bosch DA (1994) Ten years survival after recurrent intracranial metastases from a renal cell carcinoma. Br J Neurosurg 8:229–231

Ware GT, Haik BG, Morris WR (1999) Renal cell carcinoma with involvement of iris and conjunctiva. Am J Ophthalmol 127:460–461

Wyczolkowski M, Klima W, Bieda W, Walas K (2001) Spontaneous regression of hepatic metastases after nephrectomy and metastasectomy of renal cell carcinoma. Urol Int 66:119–120

Yamashita K, Yamamoto M, Nishimura H, Akiyama H, Tsuchiya E, Tanaka S (2000) Hilar lymph node metastasis in renal cell carcinoma. Jpn J Thorac Cardiovasc Surg 48:194–197

Yavascaoglu I, Korun N, Oktay B, Simsek U, Ozyurt M (1999) Renal cell carcinoma with solitary synchronous pancreati-

coduodenal and metachronous periprostatic metastases: report of a case. Surg Today 29:364–366
Yokoyama Y, Sato S, Kawaguchi T, Saito Y (1998) A case of concurrent uterine cervical adenocarcinoma and renal-cell carcinoma, and subsequent vaginal metastasis from the renal-cell carcinoma. J Obstet Gynaecol Res 24:37–43
Yu CC, Huang JK, Tzeng WS, Wu JD, Lee YH, Jiaan BP (1992) Simultaneous bilateral adrenal metastases from renal cell carcinoma. Surgical implications and review of the literature. Eur Urol 22:335–338
Zhao B, Kimura W, Futakawa N, Muto T, Haida K (1997) Renal cell carcinoma of the spindle cell type with metastasis to the pancreas: a case report. Jpn J Clin Oncol 27:58–61